GALACTIC X-RAYS OBSERVED WITH X-RAY ASTRONOMY SATELLITE 'HAKUCHO'

S. HAYAKAWA

Department of Astrophysics, Nagoya University, Nagoya, Japan

(Received 23 June, 1981)

Abstract. Highlights of the results obtained with Japanese X-ray astronomy satellite '*Hakucho*' are reviewed. After a brief account of instrumentation (Section 2), some new features of non-bursting, non-pulsating objects are presented (Sections 3–5). The main part of the present review is devoted for X-ray bursts which are found more complex than one might have thought (Sections 6–11). The observation of X-ray pulsar, including a change of spin rate of Vela X-1, is described (Section 12). The main results obtained in the first two years are summarized in Section 13.

Contents

1. Introduction

A small X-ray astronomy satellite was launched on 21 February 1979 from Kagoshima Space Center (31° N, 131° E) and named *Hakucho* after constellation Cygnus. Since then Hakucho has continuously observed various cosmic X-ray sources and revealed several novel features of astrophysical interest. The present paper reviews highlights of these results.

Hakucho is a spin stabilized satellite with a spin period of about 10 s. A set of detectors looking perpendicular to the spin axis are capable of monitoring X-ray sources, both steady and transient, located in a belt covered by the fields of view. Another set of detectors whose view axes are parallel and nearly parallel to the spin axis can observe selected sources almost continuously. Among them a pair of detectors have rather large fields of view and are equipped with modulation collimators, so that they are suitable for finding X-ray bursts. Other detectors locate the source positions more accurately, measure the X-ray flux with low background, and obtain the spectra over wider energy ranges. *Hakucho* was purposely designed

Space Science Reviews **29** (1981) 221–290. 0038–6308/81/0293–0221 $10.50.

as an X-ray burst monitor, and has been proved powerful in the observation of X-ray bursts. Taking this advantage for granted, we have watched a number of burst sources simultaneously in a fixed field of view.

Hakucho are, therefore, dedicated mainly to observe selected X-ray sources with particular attention to their variabilities of various time scales. Since few X-ray observatories are available for this purpose during the active period of *Hakucho*, it is playing a role in keeping a record of recurrent activities of several X-ray sources and of pulsations of X-ray pulsars.

Hakucho was constructed and operated by the joint effort of many scientists belonging to several institutions under the responsibility of the Institute of Space and Aeronautical Science (ISAS), University of Tokyo (now reformed as Institute of Space and Astronautical Science, a joint interuniversity organization).

The fabrication of detectors, the operation of the satellite and the data analysis were taken part by twenty scientists under the direction of Prof. M. Oda. They made all the results, most of which are yet unpublished, available for the author. The present paper would have to be written by the authorships of these twenty scientists, but is written by a single author who was responsible for the planning of *Hakucho*. Most papers reporting the results of *Hakucho* were published under the coauthorships and are here referred to as the first author and *Hakucho* team. These authors are listed in the alphabetical order of names for individual affiliations which are ordered from east to west: Inoue, H., Koyama, K., Makishima, K., Matsuoka, M., Murakami, T., Oda, M., Ogawara, Y., Ohashi, T., Shibazaki, N., and Tanaka, Y. (Institute of Space and Astronautical Science); Kondo, I. (Institute of Cosmic Ray Research, University of Tokyo); Hayakawa, S., Kunieda, H., Makino, F., Masai, K., Nagase, F., and Tawara, Y. (Department of Astrophysics, Nagoya University); Miyamoto, S., Tsunemi, H., and Yamashita, K. (Department of Physics, Osaka University).

The present paper is an extension of earlier papers which reviewed the results available by that time. They can be found in a series of papers presented at the 16th IUPAP Cosmic Ray Conference (Inoue *et al.*, 1979) and papers given at symposia (Tanaka, 1979; Oda, 1980; Ogawara, 1980; Matsuoka, 1980).

2. X-ray Detectors and Their Performance

Instrumentation and initial performance of *Hakucho* have been given by Kondo *et al.* (1981). Only those necessary for understanding observed results are reproduced here.

Eleven X-ray counters and attitude sensors are arranged as shown in Figure 1. Proportional counters with thin plastic windows are sensitive to very soft X-rays of energies between 0.1 and 2 keV and named VSX, while those with beryllium windows are sensitive to soft X-rays of energies between 1.5 and 30 keV and named SFX. An NaI(Tl) scintillation counter sensitive to hard X-rays of energies between 10 and 100 keV is named HDX and is also used as a particle monitor for protecting

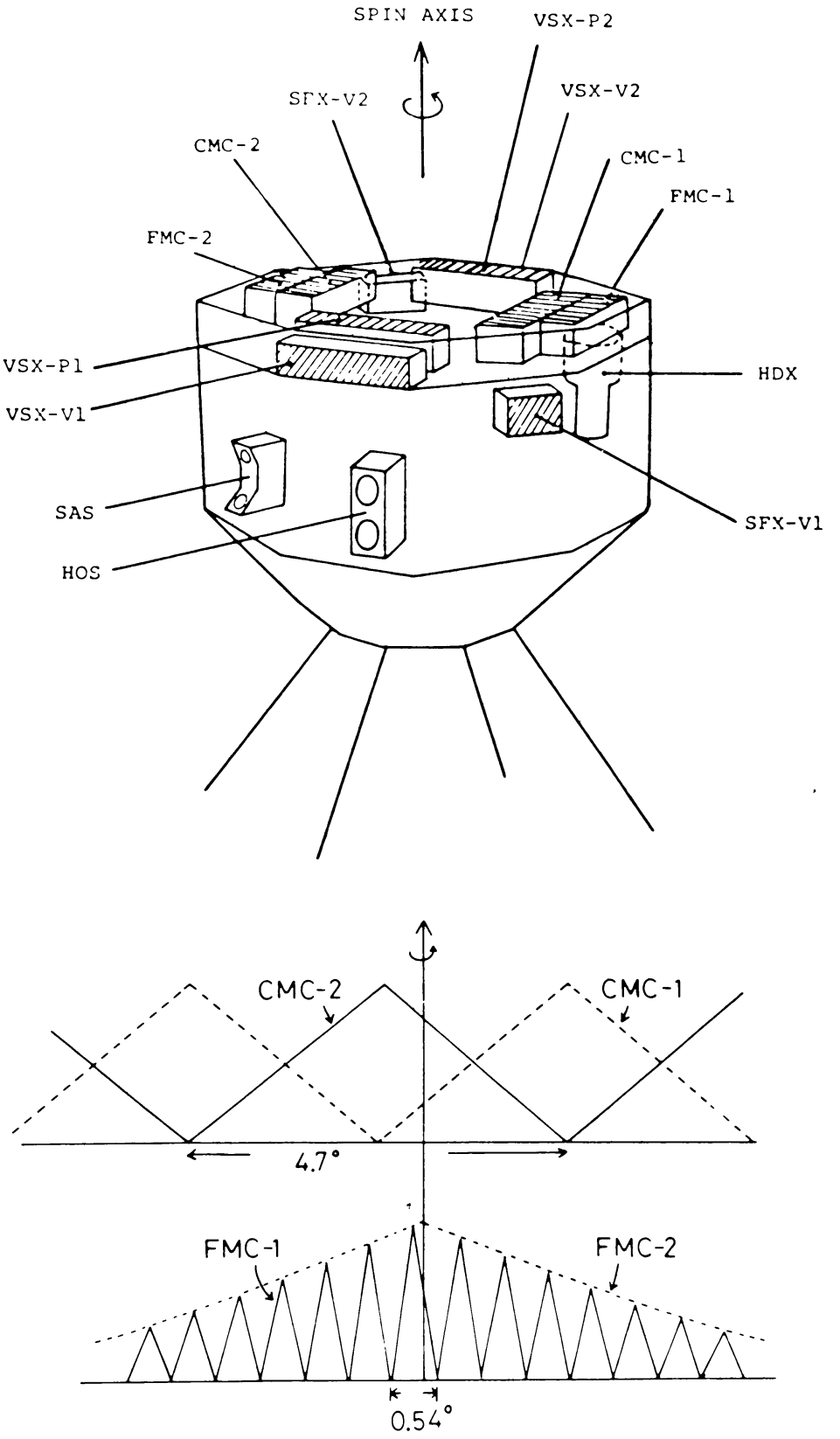

Fig. 1. The arrangement of X-ray counters and attitude sensors on the Hakucho satellite. The bottom figures represent the modulation patterns due to two pairs of counters, CMC-1 and -2 and FMC-1 and -2.

the counters from the hazard due to radiation belt particles. Their counting efficiencies for X-ray photons are shown in Figure 2. The counters with their view axes parallel and nearly parallel to the spin axis are indicated by *P*, whereas those vertical

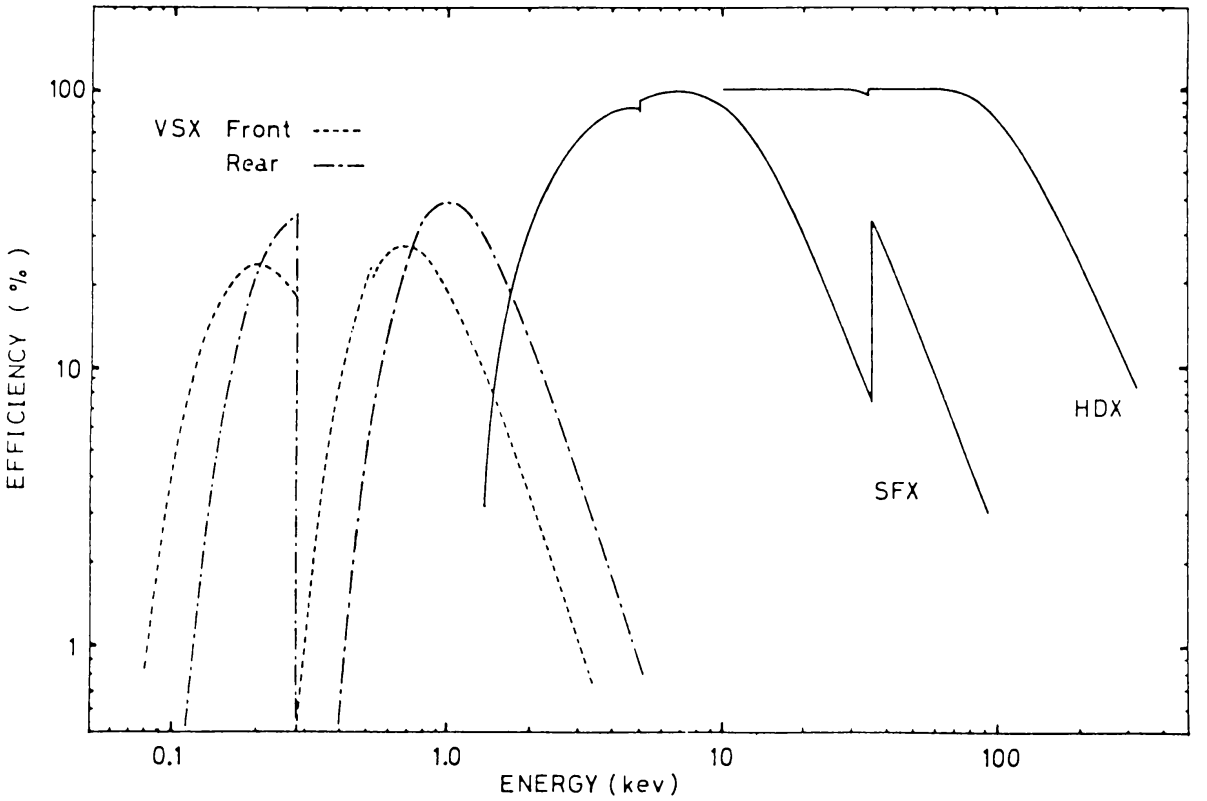

Fig. 2. The photon detection efficiencies of X-ray counters VSX (front and rear sections), SFX and HDX, versus photon energy.

to the spin axis are indicated by *V*. Two proportional counters with coarse modulation collimators are named CMC, whereas the one with a fine modulation collimator is named FMC-1. The same counter as FMC-1 but without modulation collimator is called FMC-2. The fields of view of these counters are shown in Figure 3. Further details of the counters are given in Table I.

Four V-counters scan rather wide sky belts to watch bright sources. If a transient is discovered thereby, the satellite is ready to direct the spin axis to this for detailed study.

A pair of VSX-P counters observe soft X-ray sources with sky chopping. Four SFX-P counters are suitable for the observation of X-ray bursts. Two CMC's have modulation phases opposite to one another, so that the sum of their counts shows an unmodulated burst profile and the difference thereof gives a doubly modulated profile free from background. Hence this device allows us to locate a burst source in a wide sky region and obtain the time profile of the burst. The position accuracy thus achieved is typically 0.5°. A more accurate position with typical uncertainty

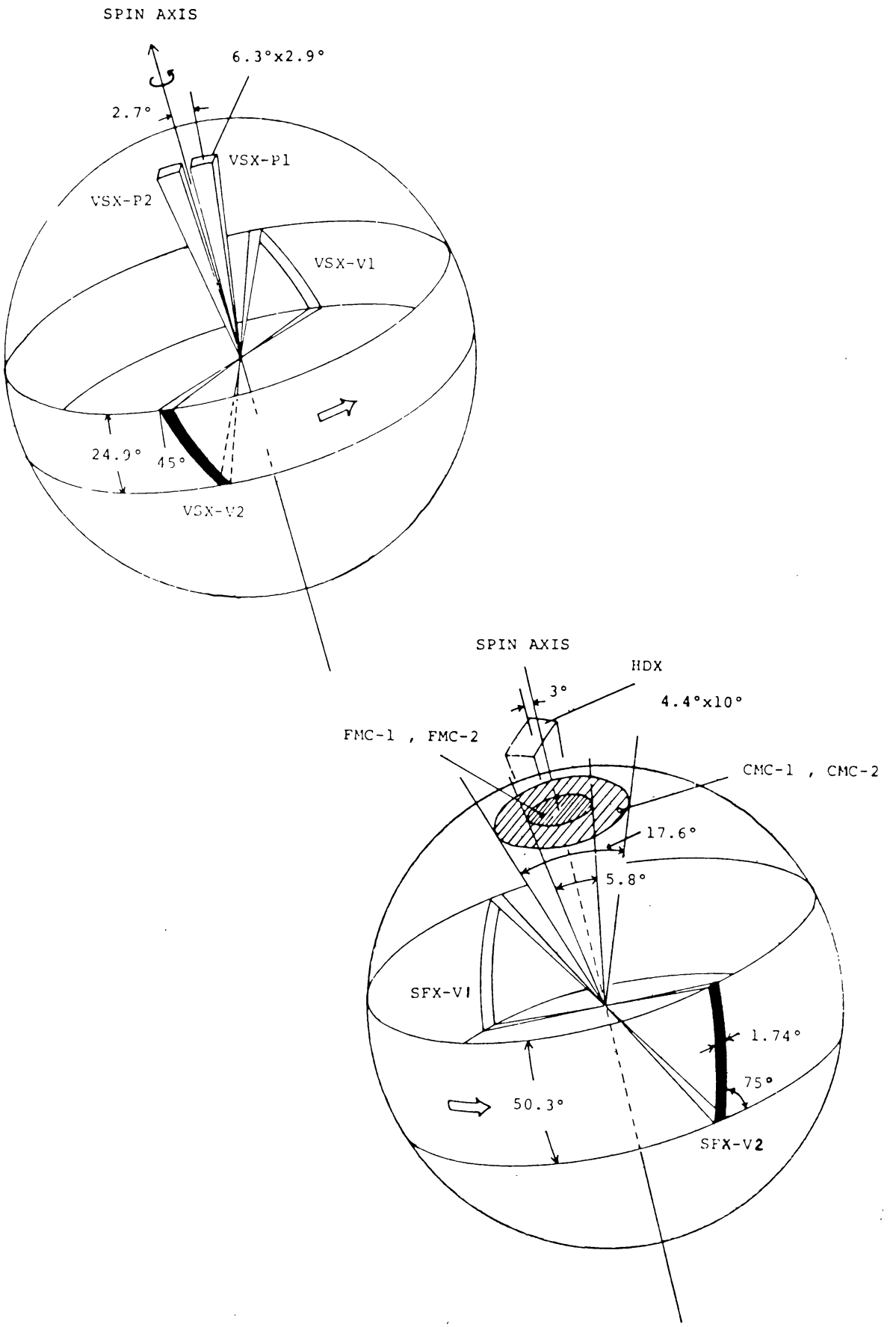

Fig. 3. The fields of view of X-ray counters; (a) for VSX and (b) for SFX and HDX.

TABLE I

Properties of X-ray counters

Energy range and counter	Viewing direction	Field of view (FWHM)	Pitch angle of modulation collimator	Area (cm^2)
VSX-P3	*P*, 2.7° offset	6.3°×2.9°*		78
VSX-P4	*P*, 2.7° offset	6.3°×2.9°*		78
VSX-V1	*V*, +45° tilted	24.9°×2.9°*		77
VSX-V2	*V*, −45° tilted	24.9°×2.9°*		77
SFX: CMC-1	*P*	17.4°**	4.72° pitch	69#
SFX: CMC-2	*P*	17.4°**	4.72° pitch	69#
SFX: FMC-1	*P*	5.8°**	0.54° pitch	40#
SFX: FMX-2	*P*	5.8°**		82
SFX-V1	*V*, +15° tilted	50.3°×1.7°*		32
SFX-V2	*V*, −15° tilted	50.3°×1.7°*		32
HDX	*P*, 3° offset	4.4°×10.0°		45

* A shorter side is perpendicular to the spin axis. For tilted fields of view, see Figure 3.

** FWHM of hexagonal field of view averaged over one spin.

\# The area takes into account a part masked by the modulation collimator.

of 0.1° is obtained with FMC-1, while a pulse profile with lower background is observed with FMC-2. Figure 4 gives an example of burst profiles observed with these counters.

The source position is thus obtained with respect to the spin axis. The direction of the spin axis and the modulation phase are determined by means of attitude sensors, a pair of horizon sensors (HOS) and a pair of sun sensors (SAS).

There are two modes of data acquisition. In the pulse count (PC) mode two energy channels are available for each counter, whereas in the pulse height (PH) mode 15 pulse height channels are available in the selected energy range. Since the bit rate is 8 times higher for the real time transmission than for the transmission of play-back data, the PH mode is selected usually only for the former, whereas the PC mode is used in most observation time both for real time and play-back data.

Since transmitted data are received only at Kagoshima Space Center, about 5 orbits out of about 15 orbits per day are available for data transmission. Even in good orbits the observation is interrupted by the South Atlantic Anomaly and by the earth occultation of a source. Hence the net observation time of a source is only several hours a day. The use of VSX counters is still more restricted, since they are affected by precipitating particles which are rather strong over a large fraction of orbit. Moreover, they were sometimes subjected to hazardous discharge. Hence VSX counters were operated only at night during the acquisition of the satellite except in the first few weeks after launch.

On 19 March 1979 VSX P-4 bursted. In the spring of 1980 VSX P-3 and V-1 which share a common high voltage supply became noisy, and all VSX counters stopped working in August 1980. Shortly thereafter, the counting rate of SFX V-1

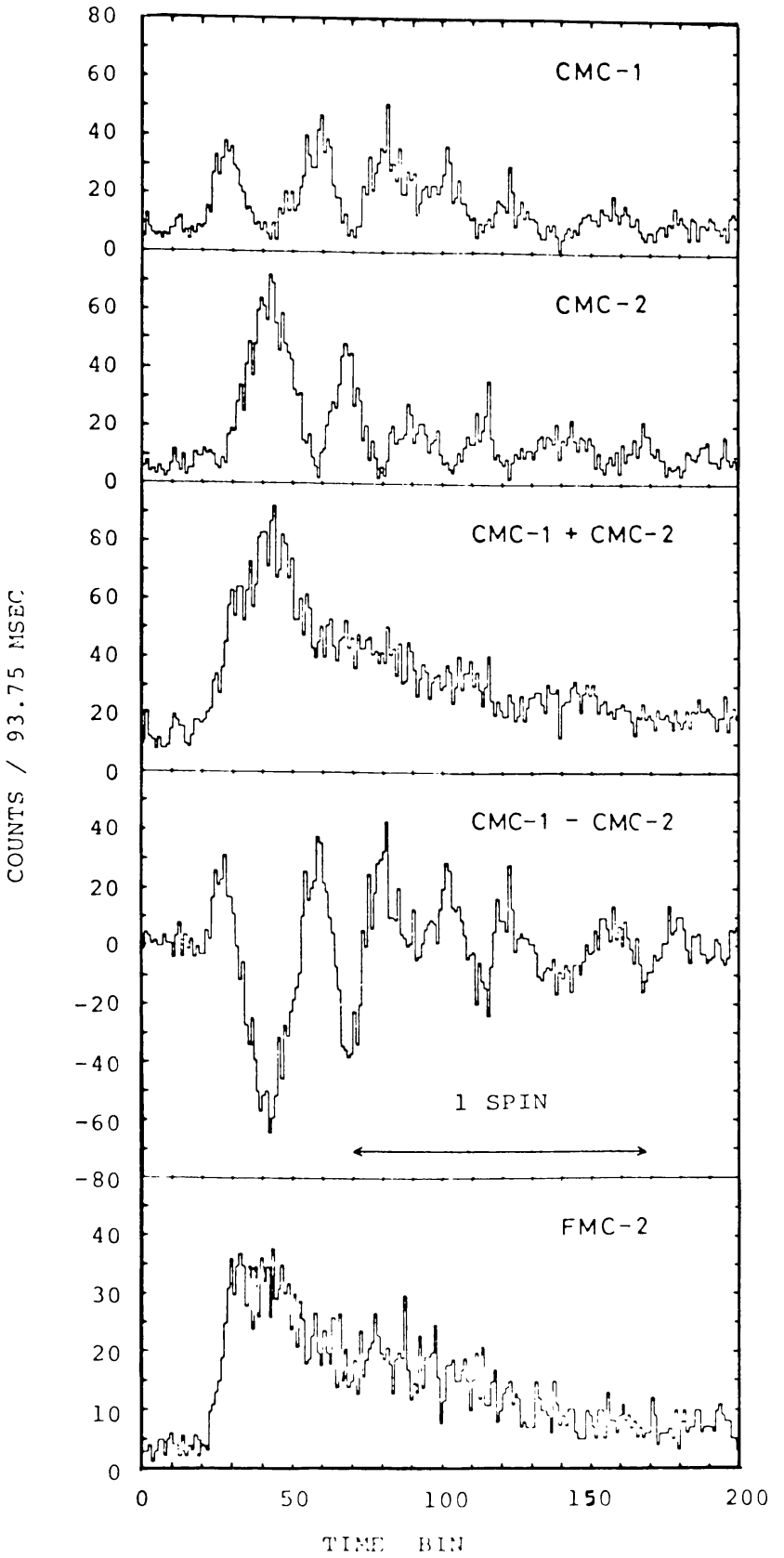

Fig. 4. The observed profiles of an X-ray burst from 1608–522, 1 time bin = 93.75 ms.

was found to increase too much during it was exposed to sun light. Hence the exposure of SFX counters to sun light has been thereafter avoided. Except for the above malfunctioning, *Hakucho* has functioned properly over two years.

The position of targets observable is restricted by the sun angle to 80°–150° with respect to the spin axis because of power requirement. In order that the counters are not exposed to strong sun light, the sun angle is further restricted to 125° to 150°. In addition, the observation was discontinued during the launch and initial operations of other satellites. Under these restrictions we have observed tens of objects during the last two years.

3. Intensity Variations of Cyg X-1

Cyg X-1 is a bright binary source with the orbital period of 5.6 days. A rather high orbital velocity of the optical companion, a supergiant, indicates that the X-ray source is as massive as (10–20) $M_{\odot}$. Since this exceeds the upper limit of neutron star mass, a few solar masses, the X-ray source is likely to be a black hole. A hard X-ray spectrum extending beyond 100 keV and rapid variabilities are in favor of the black-hole nature, since they may be associated with the accretion disk which forms a hot bulge close to the black hole. This source has also shown long-term variabilities. In the high state soft X-rays of energies lower than 10 keV are considerably enhanced, whereas hard X-rays are somewhat weaker than in the low state. These features of Cyg X-1 were summarized in a review by Oda (1977).

After the last high state terminated in January 1976, no transition to the high state had been reported until May 1980. On 12 June 1980 Cyg X-1 was found by SFX-V counters to be in the high state, and the X-ray flux in the L-band (1–12 keV)

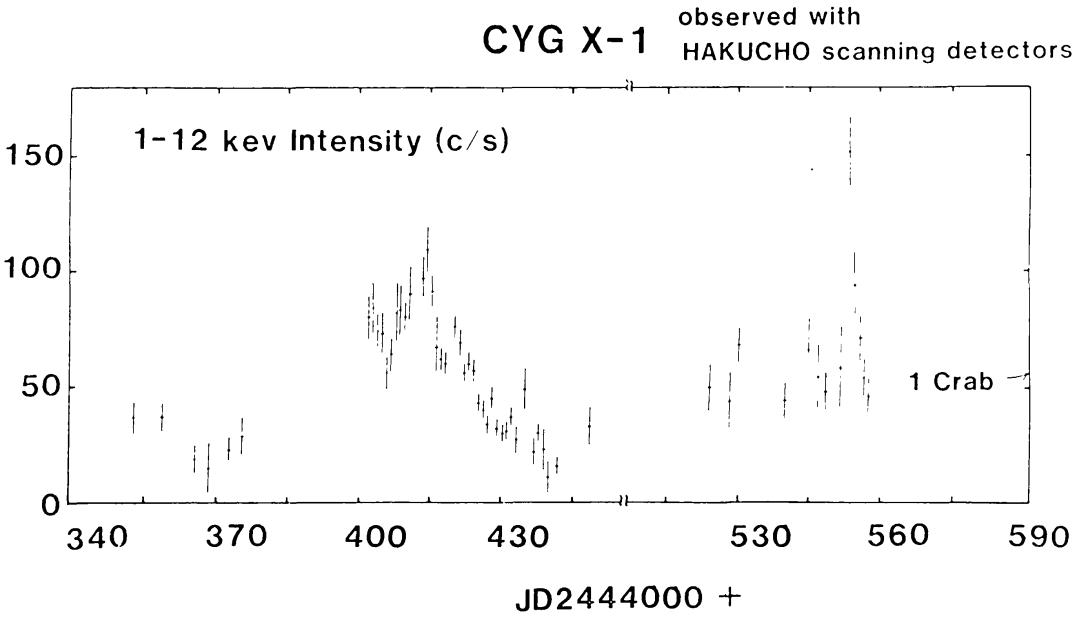

Fig. 5. The light curve of Cyg X-1 between the end of April and middle of November 1980.

increased to a peak around 20 June and then declined to the low state value towards the end of July, while the flux in the H-band (12–30 keV) was somewhat lower than that in the low state. A short flare was observed on 10 November. Except in these two high state periods, the flux varied by a factor of three or less. The light curve of Cyg X-1 in the L band is shown in Figure 5. No radio enhancement has been reported in these high states, whereas optical emission is somewhat correlated (Kemp *et al.*, 1981).

It was reported by Holt *et al.* (1976, 1979) that the X-ray intensity is modulated with the 5.6 day period of binary motion. Intensity dips were found at the superior

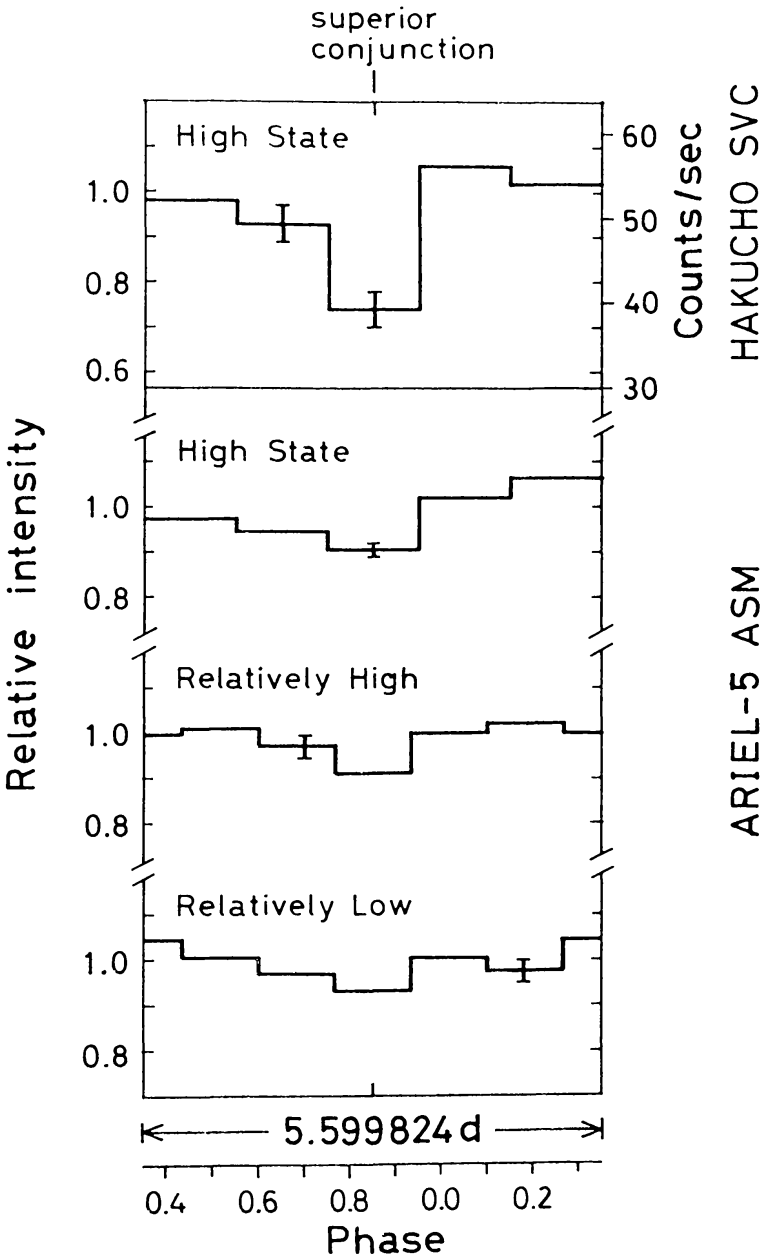

Fig. 6. A periodic X-ray variation of Cyg X-1 observed by *Hakucho* in comparison with that by Ariel-5.

conjunction of the optical companion HDE 226868 in the low and high states, though their statistical significance is not too high. A similar periodic variation is obtained in Figure 6, if data in 12 June through 20 July are folded modulo 5.599824 days. The minimum found at superior conjunction is about 20% lower than the average intensity, which is compared with the dip about 10% lower than the average in the earlier observation. It may be interesting to note that optical emission also shows a periodicity which can be interpreted in terms of the effect of gas stream in the binary system (Kemp *et al.*, 1981).

4. Irregular Variabilities of Cir X-1, GX 349+2 and GX 5-1

Striking X-ray flares were observed from Cir X-1 and GX 349+2 (4U 1702–363) on 23 April 1980 and 14 July 1980, respectively. However, these two sources are different in many respects. A strong source GX 5-1 showed a bimodal behavior.

4.1. Cir X-1

Cir X-1 is a non-pulsating binary source and is suspected to be a black hole on a weaker basis than Cyg X-1. Large variations have been observed, and the intensity at the peak may be higher than that of the Crab-nebula. A transition has been suspected to occur around a given phase of the binary period of 16.6 days.

During 21 April through 11 May 1980 we took part in the coordinated observation of Cir X-1 simultaneously with infrared and radio observations. Over the time span somewhat longer than the binary period, X-rays from Cir X-1 were mostly below the detection limit of FMC-2. At about 10 hr on 23 April Cir X-1 started to flare up, and the intensity increased more than ten times at the peak. The intensity decreased to the pre-flare value on 26 April, as shown in Figure 7. The spectrum was found much softer at the peak than in other periods. Infrared flares were observed on 21 March and 9 May, two periods before and approximately one period after the X-ray flare, and an apparent radio flare was detected on 10–13 May, one period after the X-ray flare. However, no X-rays were detected during 9–11 May.

At the peak of the X-ray flare a rapid variation of X-rays was observed, as also shown in Figure 7. The periodicity of this variation is not confirmed.

4.2. GX 349+2

GX 349+2 is supposed to be a binary whose companion is suspected to be a Mira variable. The X-ray intensity varies by a factor of three and is comparable at its peak to that of the Crab nebula.

The source was in the field of view of CMC continually during burst hunting periods, in April–May 1979 and in April–August 1980. In most of these periods X-ray emission was quiescent in the sense that the intensity stayed nearly constant over several days. In the rest the source was active in such a way that the intensity

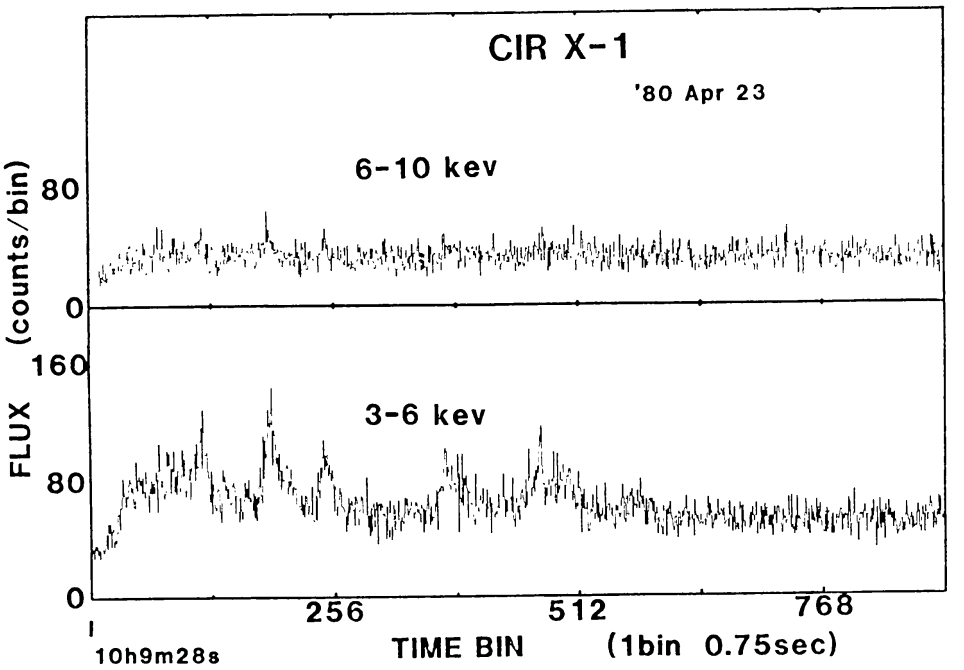

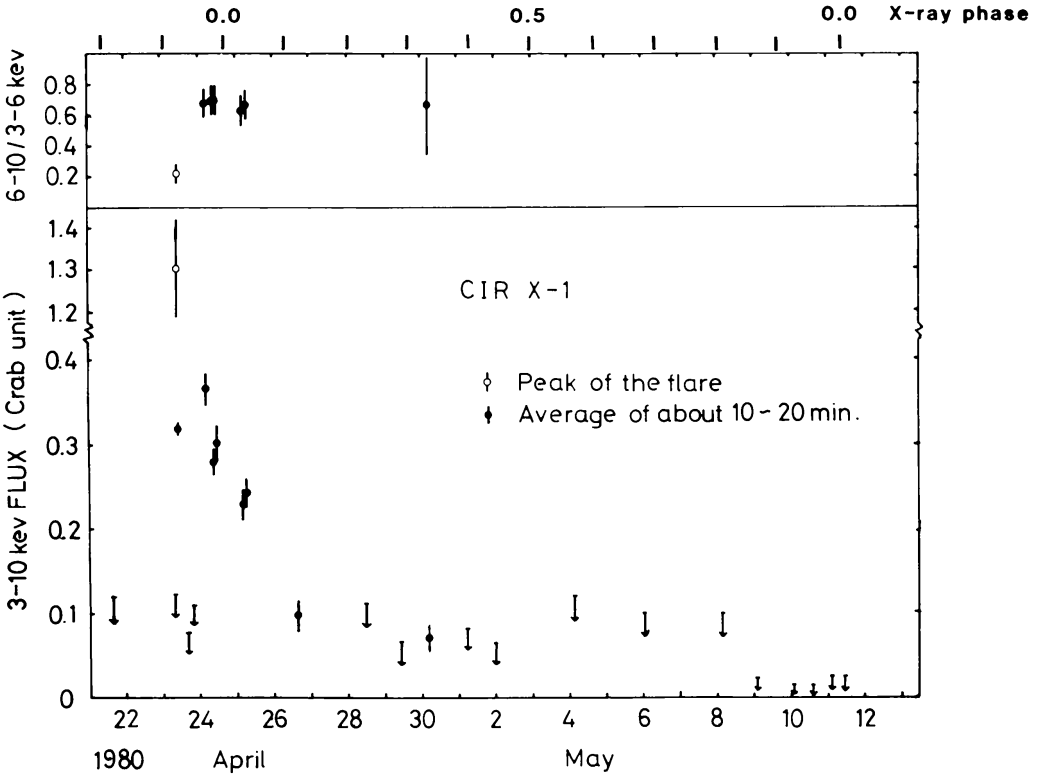

Fig. 7. The light curve of Cir X-1 in April–May 1980 together with the hardness ratios (bottom), and the short-term variations in two energy bands at the peak (top).

varied as large as by a factor of two for a few contiguous days. A number of flares occurred during an active period, and each flare persisted as long as 30 to 50 min. The above bimodal behavior can be observed from the data on 13 through 19 April 1980, as shown in Figure 8. In the active state on 16–19 April 1980, the

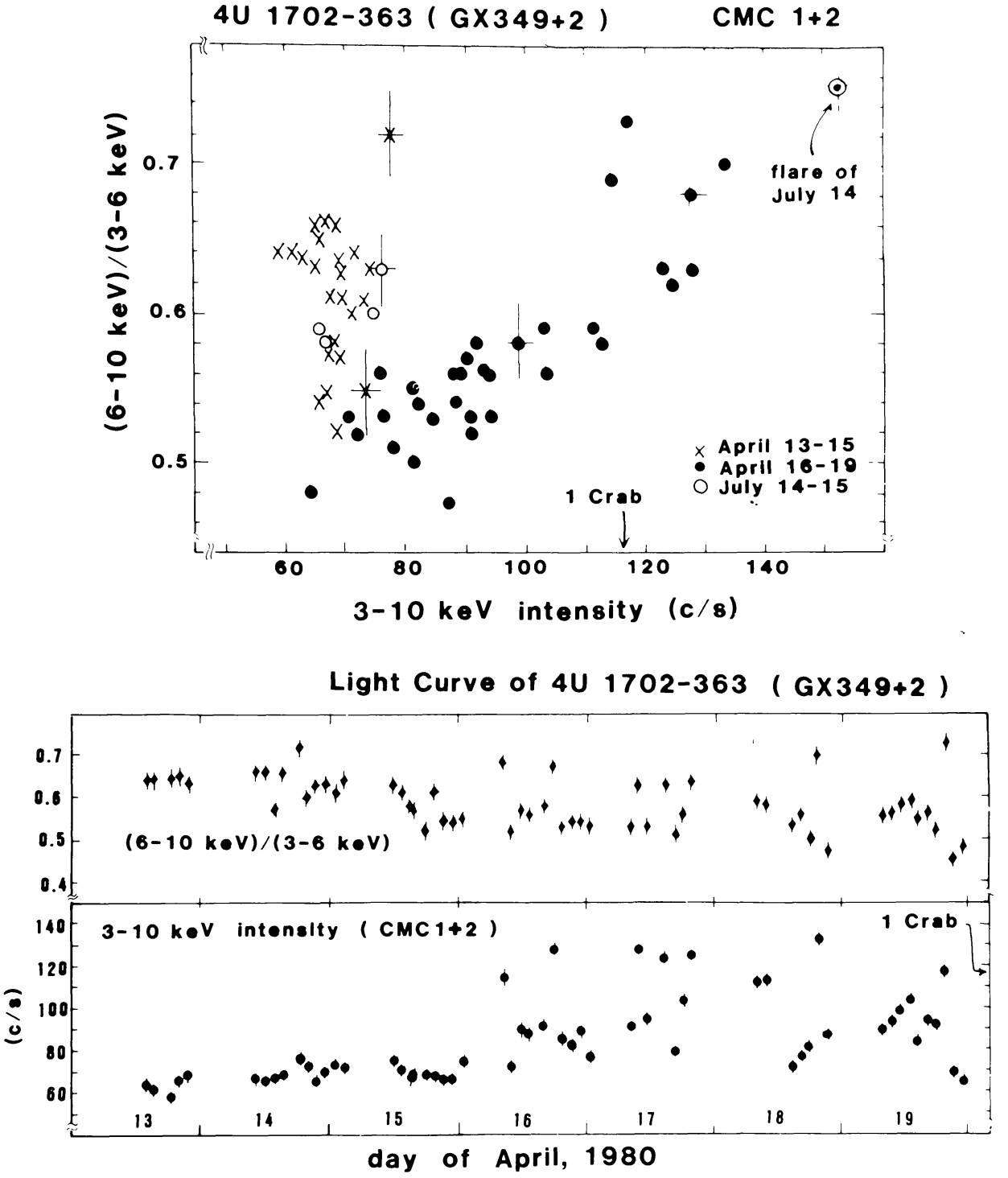

Fig. 8. Bimodal behavior of GX 349+2. The bottom figure shows a change from the quiescent state to the active state in April 1980. The top figure shows the hardness ratio against the intensity, which exhibits a bimodal behavior.

intensity was found proportional to the hardness ratio, as also shown in Figure 8.

The largest flare as strong as 1.3 times the Crab nebula intensity was observed on 14 July 1980. Unfortunately this occurred when the data recorder was not continuously on during a long loss of the satellite. Hence the complete light curve of the flare was not obtainable, but the intensity at the peak was observed for 20 minutes. Throughout this period the X-ray intensity was found pulsating with a period of 153 s or 306 s and with a modulation amplitude of about 20% (Makishima, private communication). A similar pulsation was detected also for a flare on 17 April 1980, but no appreciable pulsation was observable for other flares.

4.3. GX 5-1

GX 5-1 (4U 1758–250) is the brightest source in the galactic center region. Its optical counterpart is not yet found, while a radio counterpart is suspected. The X-ray luminosity fluctuates by a factor of three.

Hakucho observed GX 5-1 in the energy range 3–10 keV in July–August 1980. During this period the source showed a bimodal behaviour; in the high state the spectrum is softer, and the hardness ratio positively correlates with the intensity, whereas in the low state the spectrum is harder, and the correlation between the intensity and hardness ratio is weak. The transition between these two states takes place within a short time, shorter than 2.5 hr for a low-high transition and about 4.5 hr for a high-low transition. An apparent periodicity of 1.55 days was observed in the high state, though the conclusion will have to be waited for further observation (Mitsuda, 1981).

5. Soft X-Ray Emission from GX 339-4 and NGC 6624

No X-ray sources in and near the galactic bulge had been detected in the energy range below 1 keV, whereas some bright sources located far from the galactic center showed spectra extending to the soft X-ray region. *Hakucho* observed the soft X-ray emission from GX 339-4 and NGC 6624 in their high states with a VSX-P counter. Owing to its view axis slightly inclined with the spin axis, the components from these sources were discriminated against the diffuse component by sky chopping. Their spectra in a higher energy part are observable with SFX-P counters. This was indeed the case for NGC 6624, whereas GX 339-4 was somewhat confused by nearby sources.

5.1. GX 339-4

A highly variable source GX 339-4 (1659–487) was suspected to be a black hole candidate because of a harder spectrum in the low state (Markert *et al.*, 1973) and a rapid variability in 40 ms (Samimi *et al.*, 1979), as observed for Cyg X-1. However, its optical properties are similar to those of ordinary X-ray sources with dwarf companions. Although the optical companion was suggested to be a BV star on the basis of blue color and emission lines of ions observed in the high state (Grindlay,

1979), a low luminosity of $m_v \geq 19.5$ observed on 6–9 March 1981 (Ilovaisky, 1981) would give a distance farther than 20 kpc. Moreover, the ratio of X-ray to optical luminosities of about 250 and the emission lines to be excited by X-rays are similar to those observed for X-ray sources with dwarf companions such as Cen X-4 and A 0620–003. Shortly after the source was optically undetectable, *Hakucho* was also unable to detect X-rays with an upper limit of 30 Uhuru units on 7–9 April 1981 (Matsuoka, private communication).

In the high state *Hakucho* observed GX 339-4 between 24 June and 7 July 1979. The intensity in the energy range 0.7–1.8 keV changed by a factor less than two during this period. The spectra obtained with the front and rear parts of VSX-P are shown in Figure 9. The spectrum corrected for the counter efficiency is subject to an ambiguity at high energies because of a low efficiency, but is harder than that obtained by OSO-7. Markert *et al.* (1973) obtained the thermal bremsstrahlung

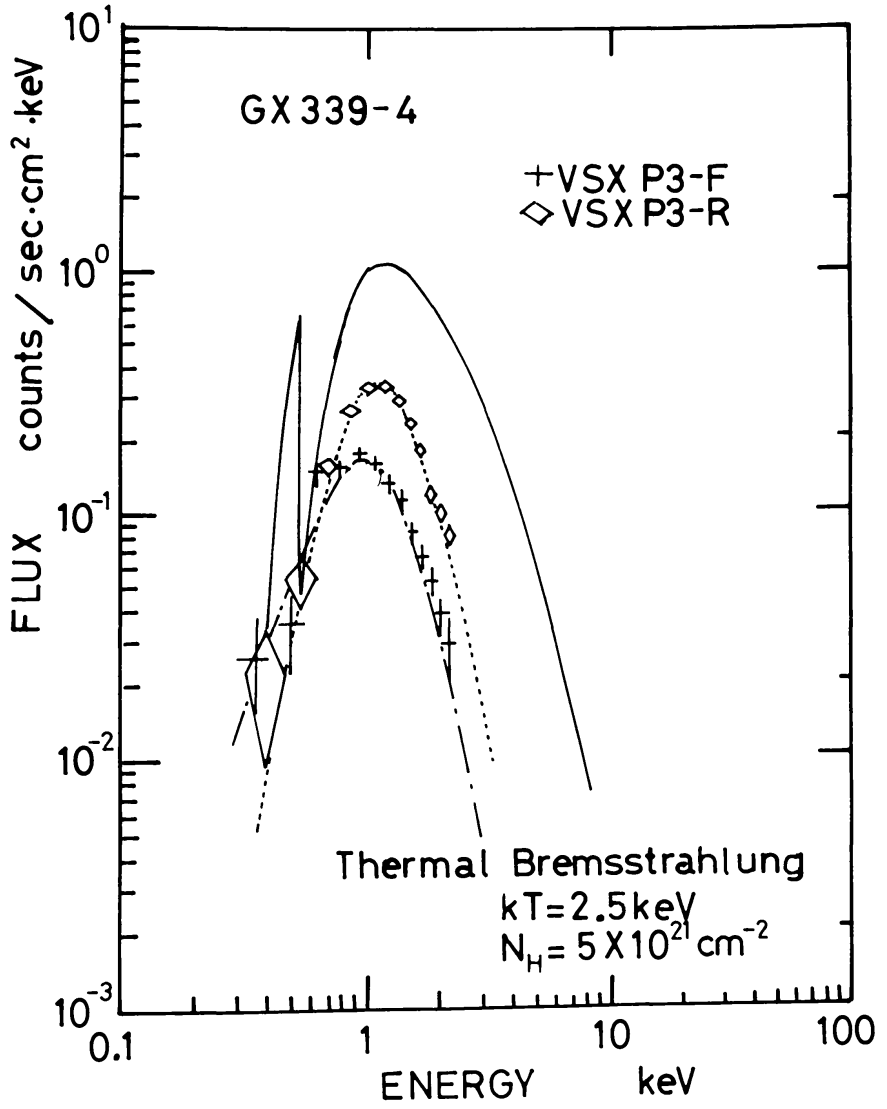

Fig. 9. X-ray spectrum of GX 339–4. The solid curve represents the thermal bremsstrahlung spectrum subject to interstellar absorption, and the dot-dashed and the dotted curves are the spectra observed by the front and rear parts of the counter, respectively.

temperature of 1.7 keV, whereas our spectrum gives a temperature higher than 2.5 keV. In Figure 9 we give the incident spectrum of $kT = 2.5$ keV and the interstellar absorption of $N_H = 5 \times 10^{21}$ H atoms cm^{-2} as well as the spectra to be observed in the front and rear parts of the counter. A power law spectrum with a power index $\alpha = 1.1$–2.2 and the same absorption measure is also consistent with the observed spectra.

Although the spectral parameters are not precisely obtainable, a strong flux of soft X-rays is undoubtedly present in the high state. The spectrum falling towards low energy, such as the blackbody spectrum is ruled out.

5.2. NGC 6624

At the center of globular cluster NGC 6624 is located an X-ray source 1820–303. This is known to be the first identified X-ray burster (Grindlay *et al.*, 1976), though

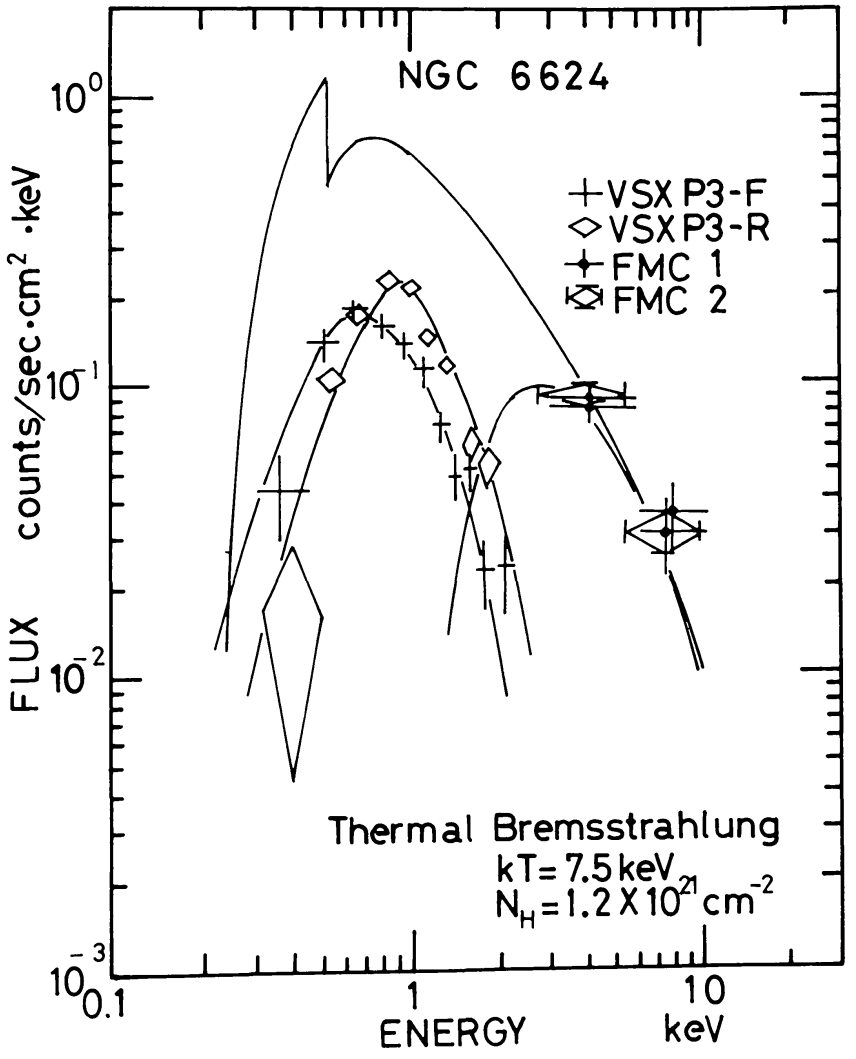

Fig. 10. X-ray spectrum of 4U 1820–303 (NGC 6624). The solid curve represents the thermal bremsstrahlung spectrum subject to interstellar absorption, and the lines connecting observed points represent the spectra observed by respective counters.

no bursts from this source have yet been observed by *Hakucho*. The spectrum was found to be rather hard (Canizares and Neighbours, 1975), fitted with a thermal bremsstrahlung spectrum of $kT \simeq 10$ keV or with a power law spectrum of $\alpha = 1.5$–2.0. Extension of the spectrum to low energy, as inferred from the model spectra, had not been confirmed.

NGC 6624 was in the fields of view of VSX-P and FMC on 15–24 August 1979. During this period the X-ray flux from 1820–303 was essentially constant, corresponding to 260 Uhuru units. The energy spectrum was observed by the pulse height mode on 19 August, as shown in Figure 10.

The observed spectrum is fitted with model spectra (Kamiya, 1981):

$$\text{thermal bremsstrahlung: } kT = 7.5^{+4.5}_{-2.3}\ \text{keV},\ N_{\mathrm{H}} = (1.2 \pm 0.3) \times 10^{21}\ \text{cm}^{-2},$$

$$\text{power law: } \alpha = 2.1 \pm 0.3, \qquad N_{\mathrm{H}} = (2.1 \pm 0.7) \times 10^{21}\ \text{cm}^{-2}.$$

The lines in Figure 10 represent the spectra for the thermal bremsstrahlung type of $kT = 7.5$ keV and $N_{\mathrm{H}} = 1.2 \times 10^{21}$ cm^{-2} taking into account the efficiencies and energy resolutions of respective counters. The spectral parameters thus obtained are consistent with those in earlier observations for the intensities of 50–400 Uhuru units, but are more precise owing to the data of soft X-rays.

6. Observation of X-ray Bursts

Before *Hakucho* were reported about thirty X-ray bursters. Lewin and Clark (1979) listed 27 sources which include 2 new bursters discovered by *Hakucho*, XB 1455–31 (Cen X-4) and XB 1608–52 and the one with only one burst-like event, 1535–29. The positions of 5 sources were poorly known, since only one burst from each was observed. XB 1702-42 was also questioned, since the coincidence of a suspected burster MXB 1706–43 was not confirmed. One near the galactic center had a large error box of size 4° centered at G4–4, and the position of Aql MXB was either one of two possible positions with an error box of size 1.4° each. Thus 16 sources are regarded as established.

We have newly established 8 bursters as listed in Table II. Among them three were listed by Lewin and Clark (1979) as XB sources. They were actually found by *Hakucho* as bursters; a transient source XB 1608–522 was burst active in April–July 1979 and in April–July 1980, XB 1455–31 (Cen X-4) emitted the largest burst ever observed on 31 May 1979 in the declining phase of its nova activity, and XB 1702–42 giving 21 bursts in April–July 1980 was identified with a steady source 4U 1702–429. Aql X-1 (4U 1908+005), which was excluded by Lewin and Clark (1979) from Aql MXB, emitted two bursts on 23 and 24 May 1980 also in the declining phase of nova activity. Then Cominsky *et al.* (private communication in 1980) reexamined the position of a single burst from Aql MXB on 20 July 1976 and found that this burst could well have been from Aql X-1 with a corrected collimator response function. A transient source MX 1715–32 which had shown a

TABLE II

X-ray bursters observed by Hakucho

Name	Observed days	Steady flux (CMC c/s)	No. of bursts	Burst peak (CMC c/s)	Burst size (10^3 cts)	Remark
1455–314* (Cen X-4)	22	150–5	1	4000	30	Nova
1608–522*	119	20–70	48	300–800	2–7	Fast-slow modes
		<10		180–250	2–6	in 1979
1636–536	117	≲15	89	150–300	0.8–2.5	Steadily
				80–120	0.8–2.5	bursting
1702–429*	98	≲20	21	120–210	1.1–3.2	Variable
1715–322*	67	<15	3	170–200	1.8–3.0	Transient
1728–337 (Slow burster)	70	≲15	32	160–190	1.2–18	Steadily bursting
1730–335 (Rapid burster)	60	~10	~500	50–150	0.5–20	Globular cluster
1732–303*† (Terzan-1)	60	<5	2	135–140	~2	Globular cluster
1735–444	89	15–40	3	140-150	0.6–0.9	Short bursts
1742–29 (GCX)	30	<15	12	50–130	0.6–1.5	Three sources not resolved
1744–265* (GX3+1)	26	60–200	18	150–300	1.0–1.5	
1745–248*† (Terzan-5)	24	<5	12	180–300	1.0–1.8	Globular cluster
1905+000	34	<5	6	120–150	1.2–1.8	
1908+005*	15	<5–40	2	~120	~1.4	Nova
1916+053	31	~5	2	~50	~0.6	Weak

* Established as bursters by *Hakucho*.
† Discovered as X-ray sources by *Hakucho*.

strong flare lasting 10 min was found to emit 3 bursts (Makishima *et al.*, 1981a). A bright bulge source GX 3+1 (4U 1744–265) gave 18 bursts in July–August 1980. In addition, we discovered 2 bursts from XB 1732–303 and 12 bursts from XB 1745–248 (Makishima *et al.*, 1981b), which had never been observed even as steady sources but are possibly identified with globular clusters Terzan-1 and Terzan-5, respectively. These newly established sources are now included in the burster list by Lewin and Joss (1981).

Instead, we have not observed any bursts from the following established bursters despite long exposure days; they are MXB 1658–298 which bursted in October 1976 and June 1977 with stable intervals, XB 1724–30 in a globular cluster Terzan-2, 1746–370 in a globular cluster NGC 6441, 1820–303 in a globular cluster NGC 6624, 1837+049 known as Ser X-1, and 1850–087 in a globular cluster NGC 6712. Three burst sources in the very vicinity of the galactic center were not resolved. It is not surprising that no bursts have been observed from these catalogued bursters, since some bursters active in one year were found inactive in the other

year. Only two sources have been found to emit bursts steadily; they are 1636–536 and 1728–337 (slow burster).

The burst sources observed by *Hakucho* in its first two years are listed in Table II. The positions of these sources along with those of other known bursters are shown in Figure 11, excluding those farther than 40° from the galactic center. In

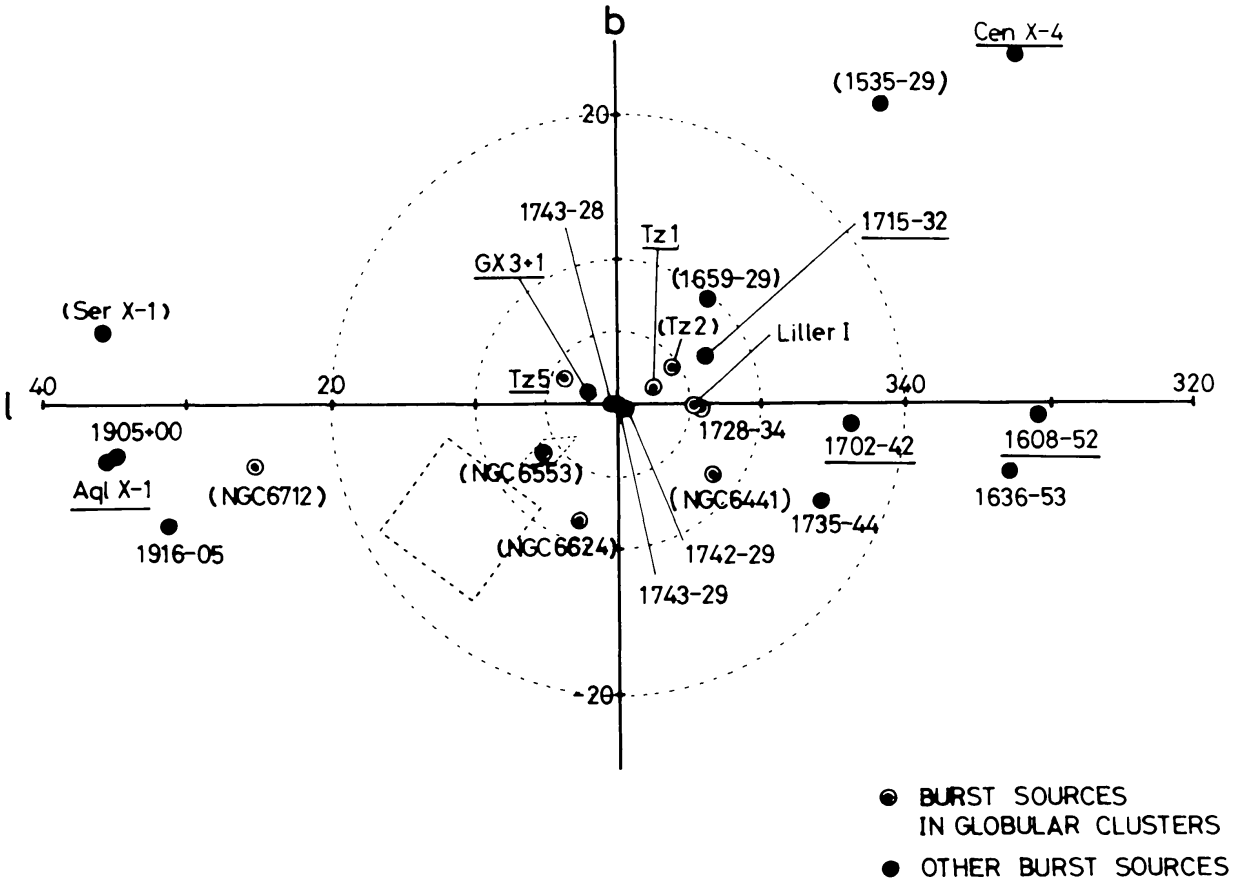

Fig. 11. The distribution of X-ray bursters near the galactic center. The bursters established by Hakucho are underlined, whereas the established bursters which did not emit bursts during the Hakucho observation are parenthesized.

addition to 15 bursters listed in Table II, there are 6 established bursters within 40° from the galactic center, and a GCX burster in Table II should be resolved into three. Hence the total of 23 bursters are located within 40° from the galactic center. Lewin and Joss (1981) listed three more burst sources in this region; 1535–29? gave only one burst-like event, and XB 180?–2? and XB 183?–2? are located in rather large error boxes.

Among the above 23 bursters, 13 sources are located within 10° from the galactic center. The strong concentration of bursters towards the galactic center is remarkable in comparison with the distribution of general galactic X-ray sources. It is also worth noticing that 7 out of 23 sources are associated with globular clusters. Another

burster 0512–401 is located in a globular cluster NGC 1851. Only a few other X-ray sources associated with globular clusters have not yet been found bursting. It is remarkable that about 10% of globular clusters in the Galaxy contain X-ray sources, and most of them have been found to be bursters.

Lewin and Joss (1981) listed five more bursters outside the 40° circle centered at the galactic center. Except for 0512–401 in NGC 1851, the positions of four sources were poorly determined, and only one burst has been observed from each of three. *Hakucho* has not spent time to watch bursters in the region far from the galactic center, since its spin axis has been directed towards the center region from April to September. In the rest of time, the spin axis pointed the Vela region for about two months, the Cygnus and Taurus region for about two months, and other scattered regions for about one month. We have spent the total of about one month for maneuvering the spin axis and stopped observation for about two months for the launch operation of other satellites and other reasons. The sky coverage by CMC shown in Figure 12 gives the idea how burst hunting has been performed.

Thanks to a wide field of view of CMC, we have been able to watch a number of bursters simultaneously and to determine their positions when bursting. Hence

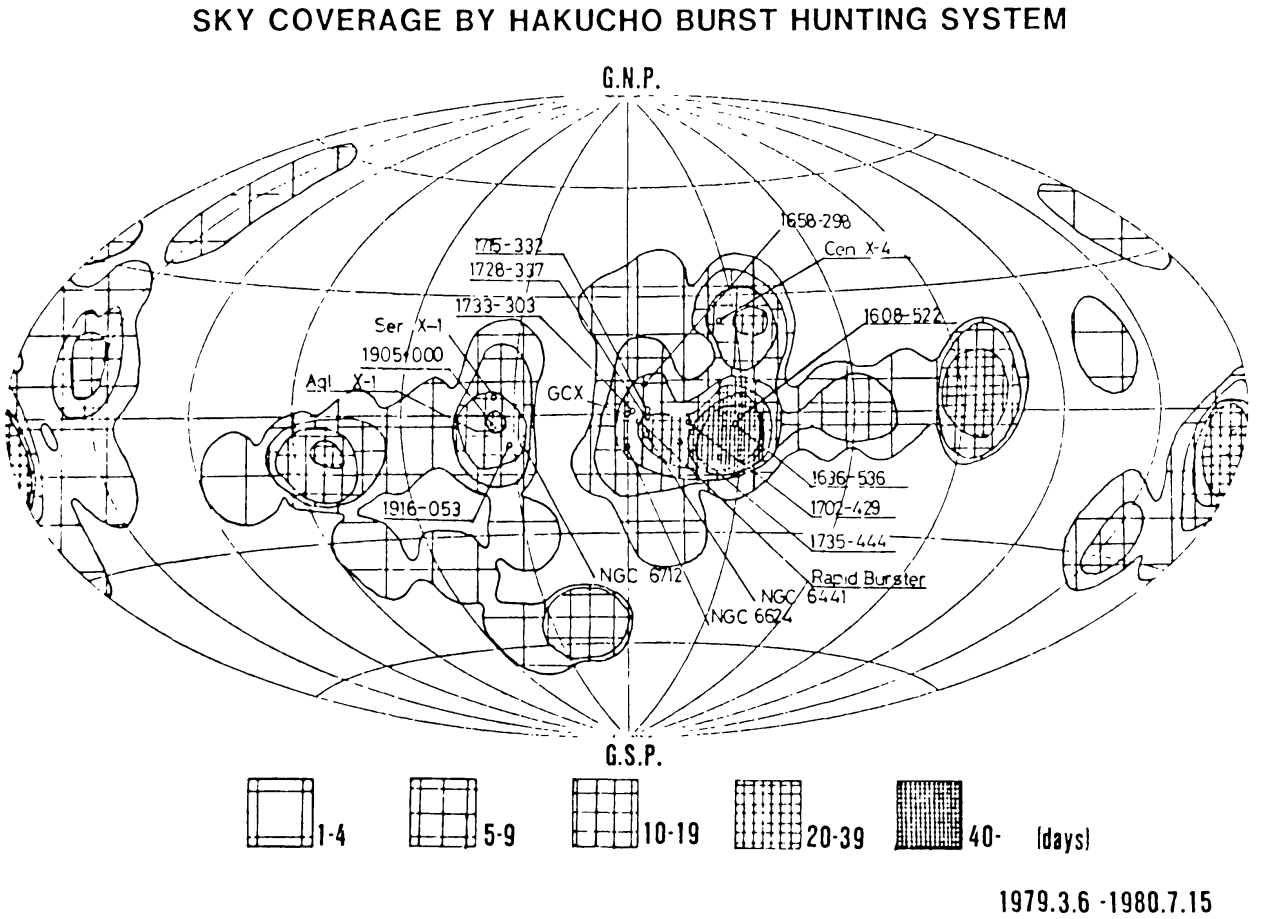

Fig. 12. The sky coverage by CMC between 6 March 1979 and 15 July 1980. Bursters from which bursts were observed are underlined.

we have thus far detected about 230 bursts, excluding about 470 bursts from the Rapid Burster. Several novel features of selected bursters will be described in the following sections.

Since general properties of X-ray bursts have been described by Lewin and Joss (1981), we have only to introduce some terminologies to characterize individual bursts. According to Hoffman *et al.* (1978), there are two types of bursts, type I and type II. Since bursts of type II have been observed only from the Rapid Burster, we will not specifically mention the burst types, particularly because no type I burst was observed from the Rapid Burster in August 1979. All bursts from the other sources should be understood as type I which is characterized by the spectral softning in the decay phase.

Bursts from sources other than the Rapid Burster have characteristic time profiles. The time profile consists of a rising part, a rather flat top, if exists, sometimes showing a complex structure, and a gradual decay part. The time profile of a burst is represented by the counting rate versus time, $I(t)$, after correcting for the counter background, dead time and aspect. This consists of the steady and burst components, $I(t) = I_s(t) + I_b(t)$. The time for the burst component to reach a half of the peak value is defined as the rise time t_r, whereas the e-folding time in the decay part is defined as the decay time t_d. We call fast/slow rise and fast/slow decay according to

$$\begin{aligned} &\text{fast rise: } t_r \simeq 1.5 \text{ s}\,, \text{ slow rise: } t_r \simeq 3 \text{ s}\,, \\ &\text{fast decay: } t_d \simeq 10 \text{ s}\,, \text{ slow decay: } t_d \simeq 15 \text{ s}\,. \end{aligned} \tag{6.1}$$

The decay time is energy dependent, and we define t_d for the energy range below 10 keV.

In the PC mode two energy channels are available. Two sets of channels have been alternately used, 3–6 keV/6–10 keV and 1–9 keV/9–22 keV. The ratio of counting rates in the high and low energy channels is called the hardness ratio. Assuming the black-body spectrum, we derive the color temperature from the hardness ratio. Assuming further the black-body temperature to be equal to the color temperature, we make the bolometric correction to obtain the energy flux $F_b(t)$. Likewise we can obtain the energy flux of the steady component F_s. Integrating F_b and F_s over a burst duration and a burst interval, respectively, we obtain the integrated energies of respective components,

$$\varepsilon_b = \int F_b(t)\,\mathrm{d}t\,, \qquad \varepsilon_s = \int F_s(t)\,\mathrm{d}t\,. \tag{6.2}$$

An important parameter, the energy ratio, is introduced by

$$\alpha \equiv \bar{\varepsilon}_s / \varepsilon_b\,, \tag{6.3}$$

where the bar represents the average over many bursts or burst intervals. Another

parameter sometimes used is

$$\gamma \equiv F_s/F_{b,\max}\,, \tag{6.4}$$

where $F_{b,\max}$ is the maximum burst flux.

These quantities are transformed to the quantities for burst sources. For simplicity, we assume spherical emission. The source luminosity is therefore given by

$$L_{s/b} = 4\pi D^2 F_{s/b} \tag{6.5}$$

for the assumed distance D. Since the maximum burst luminosity is often close to the Eddington limit, the maximum possible luminosity for spherical radiation,

$$L_E = 4\pi cGM/\kappa = 1.25(M/M_\odot)2(1+X)^{-1}\,(\kappa_{\rm Th}/\kappa)\times 10^{38}\ \mathrm{erg\ s^{-1}}\,, \tag{6.6}$$

where M is the mass of the source, X is the mass fraction of hydrogen, κ is the opacity, and $\kappa_{\rm Th}$ is the opacity for hydrogen by Thomson scattering. If X-rays are black-body radiation, the source area or the source radius R is given by

$$L = 4\pi R^2 \sigma T^4\,, \tag{6.7}$$

where σ is the Stefan-Boltzmann constant. The integrated energy is also converted for sources as

$$E_{s/b} = 4\pi D^2 \varepsilon_{s/b}\,. \tag{6.8}$$

The quantities introduced above are repeatedly referred to in the following sections. Among them, the distance D is obtained with the least reliability, but the ratios α and γ are free from this ambiguity.

7. X-ray Bursts Associated with Recurrent Novae, Cen X-4 and Aql X-1

One of the most striking discoveries by *Hakucho* is the occurrence of X-ray bursts during the active periods of recurrent novae, Cen X-4 and Aql X-1. They are two of several optical/X-ray novae. In past observations the light curves in the optical and X-ray bands had been found nearly parallel, but no burst had been observed. During their declining phases, one burst from Cen X-4 on 31 May 1979 and two from Aql X-1 on 23 and 24 May 1980 were detected. Results of these discoveries are reported by Matsuoka *et al.* (1980) and by Koyama *et al.* (1981), respectively.

The light curves of these outbursts together with the profiles of three bursts are shown in Figure 13. Characteristic properties of these objects are summarized in Table III.

These three bursts are similar to each other in many respects. They show fast rises and fast decays with extended tails due to the soft component. The spectra are rather soft, and the color temperatures for the black-body spectrum are 2–2.5 keV. The γ values, the ratios of steady flux to burst flux, are about 0.02. The burst frequency is approximately given by $\gamma/\alpha t_b$, where t_b is the burst duration. For $\alpha = 100$ and $t_b = 10$ s, this gives one burst in 14 hr. This is comparable to the

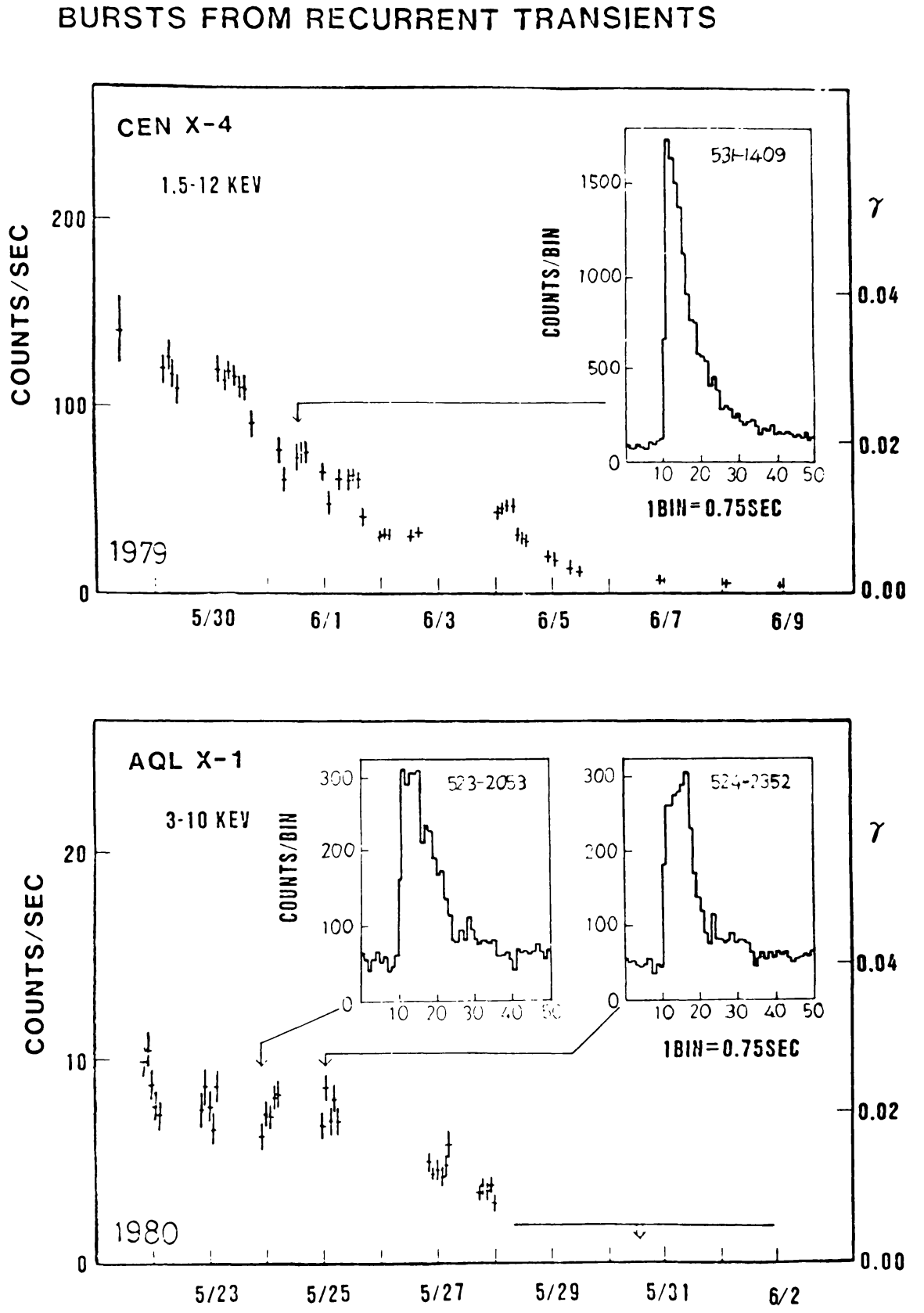

Fig. 13. X-ray bursts associated with recurrent X-ray novae, Cen X-4 and Aql X-1. The X-ray light curves and burst profiles are shown.

TABLE III

Cen X-4 and Aql X-1

	Cen X-4 (1455–314)	Aql X-1 (1908+005)
Recurrence period	~10 yr	~1 yr
Optical object	K3–K7	G7–K3
Periodicity	8.2±0.2 hr	~1.3 days
Outburst		
Onset	11–13 May 1979	<16 May 1980
Maximum	17 May (4 Crab, $V\sim 13$ m)	<16 May ($V\simeq 17$ m)
Decay time	3.5 days	6 days
Hakucho obs. (effective exposure)	28 May–16 June (67 hr)	20 May–9 June (80 hr)
L_x/L_{opt}	2×10^3	6×10^3
Burst	31 May	23, 24 May
Burst peak int.	25 Crab	5 Crab
temperature	~2 keV	2.5 keV
γ	0.018	0.025
Distance*	1.3 kpc	4 kpc
Radius*	11 km	7 km

* Based on the Eddington limit argument.

average burst interval estimated for three bursts during the total net exposure time of about 40 hr for $\gamma \geqslant 0.01$.

If we assume that the peak intensity corresponds to the spherical Eddington limit, the distances to Cen X-4 and Aql X-1 are obtained to be 1.3 kpc and 4 kpc, respectively, which lie within the limits estimated from optical features. Then their radii are 11 km and 7 km, respectively, consistent with the size of neutron star. The values of L_x/L_{opt} observed are also in rough agreement with those of X-ray sources which do not pulsate and have faint optical companions.

These observations indicate that recurrent X-ray novae are not essentially different from other X-ray sources concentrated in the galactic center region, though Cen X-4 and Aql X-1 are located far from the galactic center. Hence all of them may belong to the same population, not always confined in the galactic bulge, though they are often called the galactic bulge sources. Since these recurrent novae are binary systems consisting of neutron stars and dwarf stars, all the bursters may be considered to belong to such binary systems. Their X-ray emission is triggered by an increase of the accretion rate, and the optical emission arises from the accretion flow irradiated by X-rays. Bursts take place during enhanced accretion by the same mechanism in all bursters but the Rapid Burster.

8. Varieties of X-Ray Burst Profiles: 1636–536, 1608–522 and Others

It was suggested before *Hakucho* that type I bursts would be similar to each other in their time profiles and luminosities. The theory of helium flash to explain such

bursts was motivated in part by the similarity of profiles and luminosities (Joss, 1977). This led van Paradijs (1978) to propose the standard candle hypothesis that the peak luminosities would be essentially equal to the Eddington luminosity given by Equation (6.6). As the number of observed bursts increased, however, a complexity of profiles and luminosities have become apparent. Indeed, Lewin *et al.* (1980) have demonstrated on the basis of 56 bursts from 1735–444 that the maximum flux varies by a factor of seven and with the standard deviation of 37%. Murakami *et al.* (1980a) have found a remarkable feature that 22 bursts from 1608–522 observed by *Hakucho* in April–July 1979 form two distinct groups, one consisting of bursts of fast rises and high peak luminosities, and the other of slow rises and low peak luminosities. In April–July 1980, however, the same burster emits 26 bursts of intermediate profiles, some of which show double peaks. The appearance of such different modes seems to be correlated with the flux of persistent emission, as will be discussed shortly. On the other hand, 1636–536 emits a variety of bursts without any correlation with the persistent flux. We begin with the description of bursts from 1636–536.

8.1. 1636–536

This is one of a few bursters which emit X-ray bursts rather steadily. The persistent flux varies by a factor of about three. Optical emission is due probably to the accretion disk irradiated by X-rays because of a lack of absorption lines and of large red and blue shifts of emission lines to be interpreted in terms of the Kepler motion of the disk of large inclination. The total of 89 bursts were observed in April–July 1979 and April–August 1980.

Burst profiles in two energy ranges as observed in June–July 1979 are shown in Figure 14 (Ohashi *et al.*, 1981). All show spectral softening in the decay phase independently of profile. Their profiles are of great variety, fast rise-fast decay, fast rise-slow decay, and slow rise-slow decay. They came in a random way, although bursts arriving after short intervals, say about 100 min, appear to be of small sizes. Oda (private communication) has remarked that intervals shorter than 84 min have never been observed, all bursts after intervals of 90–120 min are small, and those after 165–225 min are large. Besides, the burst profile does not seem to correlate with any other quantities. Four bursts in Figure 14 occurred in one day, on 28 June 1979, but none of them looks similar to each other. The frequency of bursts was also found irregular. Figure 15 shows epochs of bursts along with sizes for selected periods. The distribution of size is also irregular. However, there is a rather good correlation between the size and peak flux, as shown in Figure 16. This implies that the burst duration does not vary too much, 5–12 s except for one smallest event, despite that the size and peak flux vary by a factor of eight. Bursts in 1979 show a saturation of the peak flux, that is, the profiles of high peak bursts appear to have a flat top. For bursts in 1980, however, higher peaks without flat top were observed.

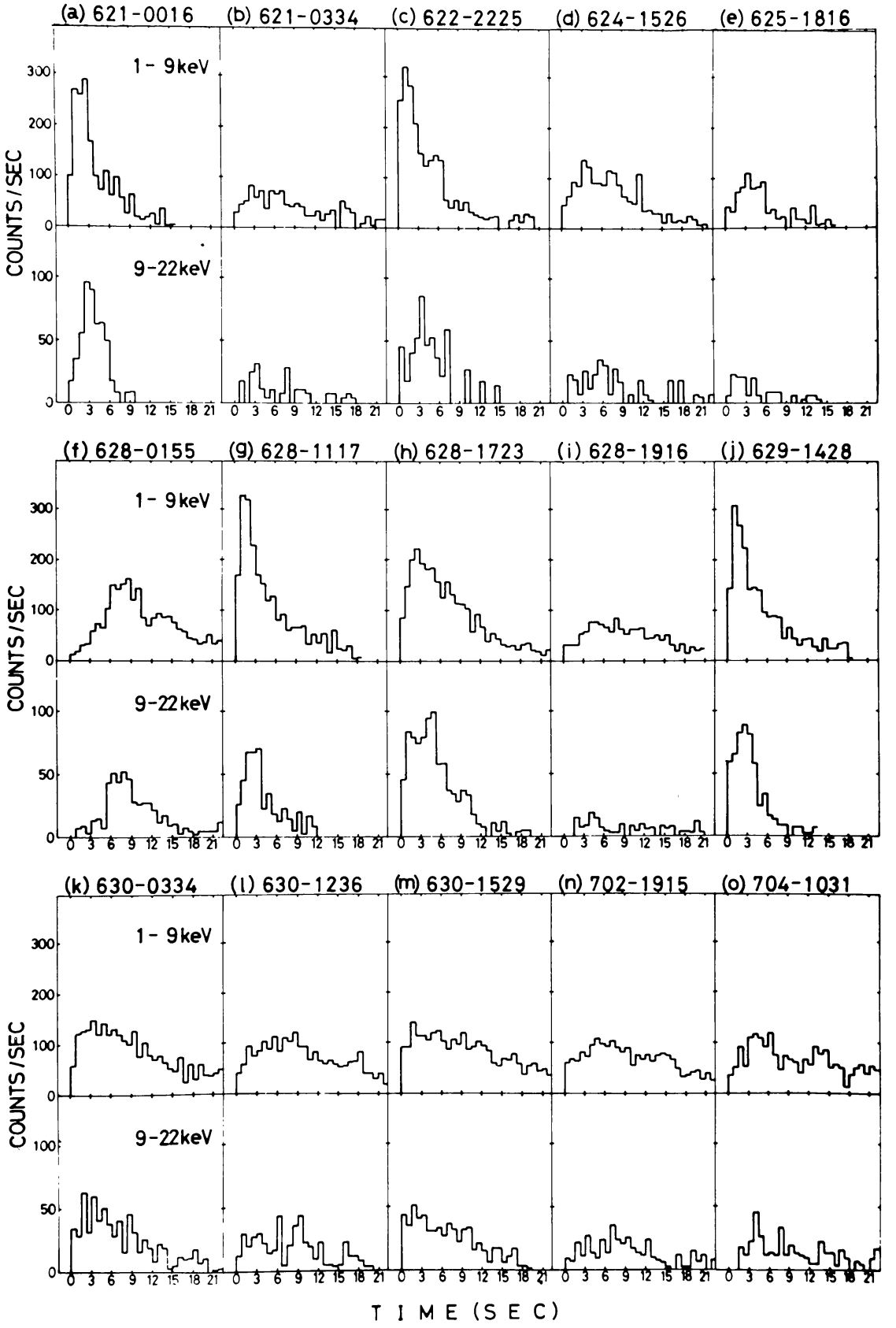

Fig. 14. Various profiles of X-ray bursts from 1636–536 in two energy bands observed in June–July 1979.

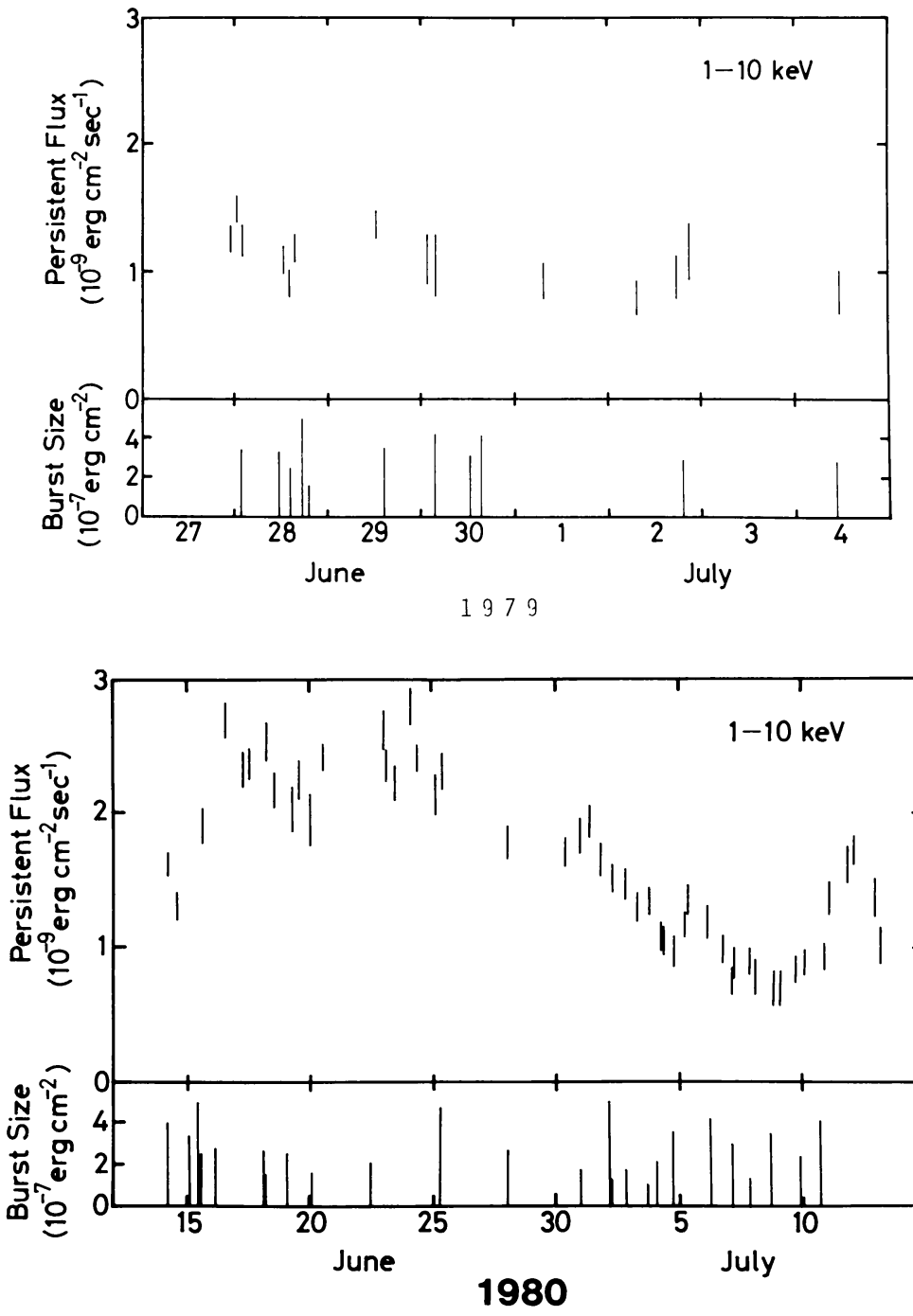

Fig. 15. The persistent flux and the size of burst from 1636–536 in June–July 1979 (a) and in June–July 1980 (b).

In 1980 an appreciable change of the persistent flux was observed, as shown in Figure 15. A glance at Figure 15 indicates that the persistent flux correlates neither with burst size nor with burst frequency. This implies that the properties of bursts does not appreciably depend on the α-value. If we compare the data in 16–25 June 1980 and in 4–10 July 1980, the values of the persistent flux and of the time averaged burst energy flux in units of erg cm^{-2} s^{-1} are 2.4×10^{-9} and $(1.3\pm0.5)\times$

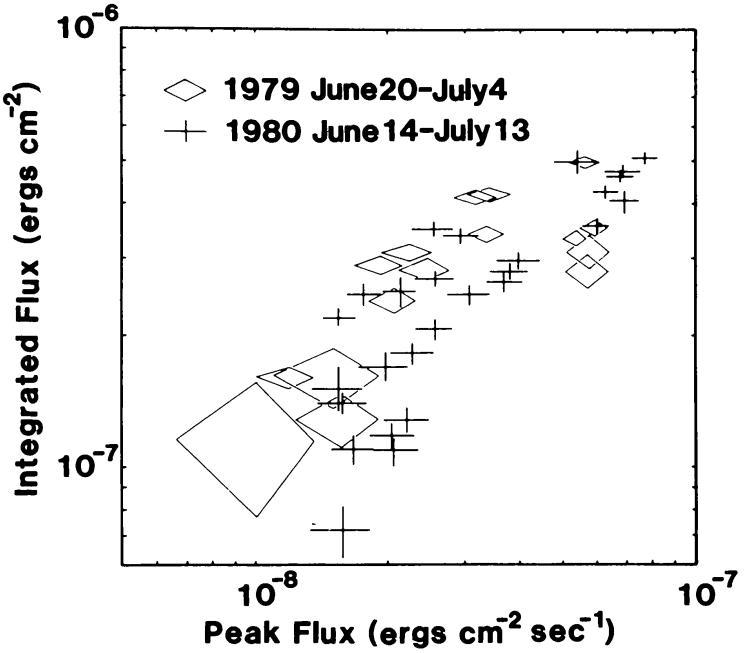

Fig. 16. The relation between the peak flux and the integrated flux for bursts from 1636–536. The diamonds and crosses represent events in 1979 and 1980, respectively.

10^{-11} in the former period and 1.0×10^{-9} and $(2.0\pm0.7)\times10^{-11}$ in the latter period, respectively (Ohashi, 1981). Hence the α-values are about 180 and 50, respectively, due mainly to the change of persistent flux. This implies that both the amount of energy spent for bursts and the mode of spending energy for bursts are independent of the persistent flux or the accretion rate. This provides a strong constraint to the burst mechanism.

8.2. Bursts of very short intervals

An even stronger constraint is given by bursts of very short intervals. On 14 August 1980 two bursts from Terzan-5 occurred with an interval of 8 min (Inoue 1980, private communication). As shown in Figure 17, neither their profiles nor their sizes are different from one another and from those of other bursts. Short intervals of 17 min and 4 min were observed for three bursts from MXB 1743–28, one of GCX bursters (Lewin *et al.*, 1976b), but no other bursts have been observed therefrom. An interval of 10 min was observed for two bursts on 6 July 1979 among a series of bursts from 1608–522 (Murakami *et al.*, 1980b).

One might think that bursts of short intervals could be due to partial burning of nuclear fuel, and a variety of bursts independent of the accretion rate could also be attributed to partial burning, so that the amount of fuel for each burst would fluctuate. If this were the case, the burst emitting area would fluctuate depending on the size and profile. In Figure 18 we give the radii of emitting area for bursts of different profiles (Ohashi *et al.*, 1981). The radii derived with the method described in Section 6 are constant in time except in the rising phase and are

BURSTS AT VERY SHORT INTERVAL

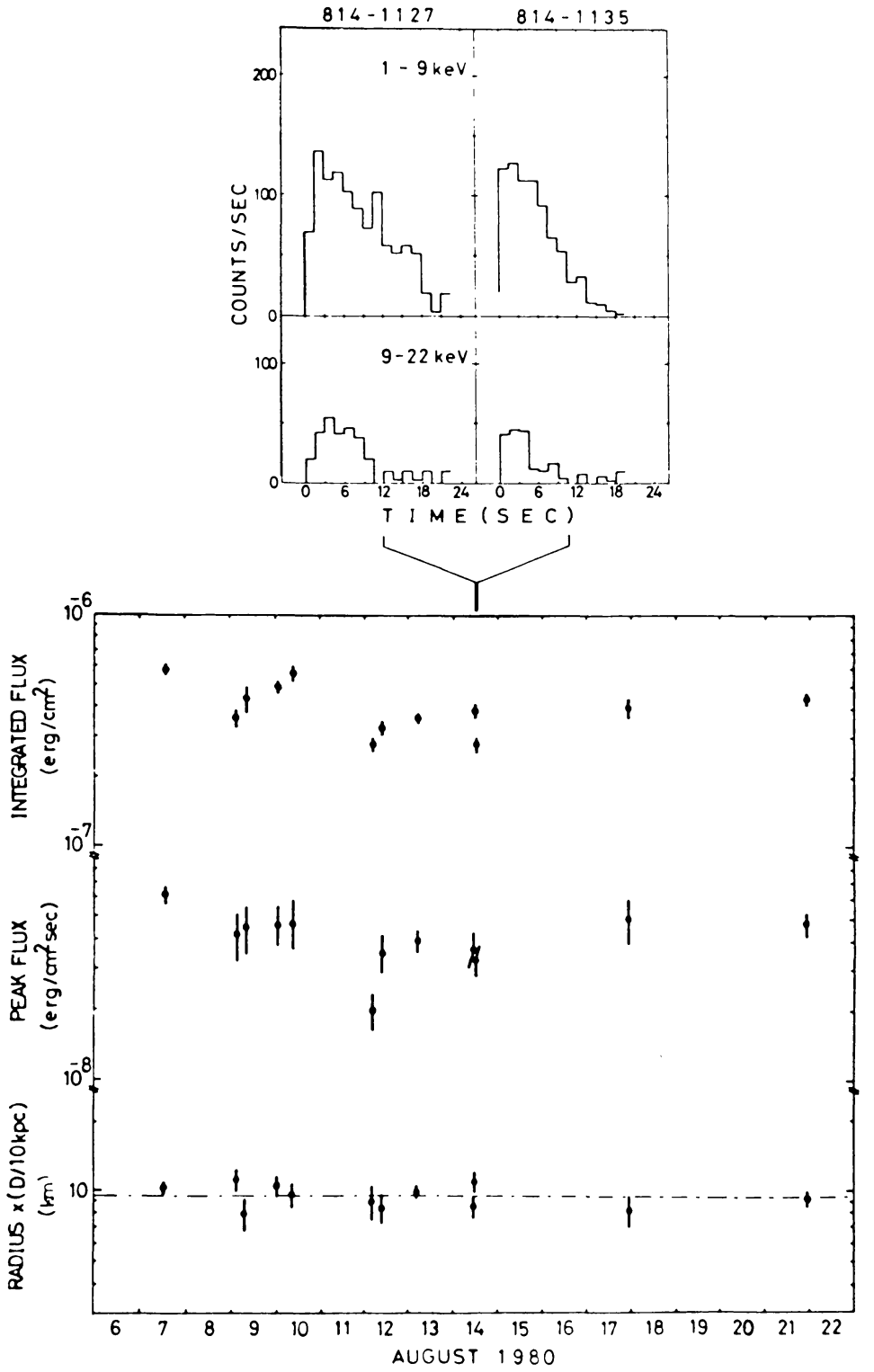

Fig. 17. Profiles of two bursts from Terzan-5 with an interval of 8 minutes. The values of integrated flux, peak flux and the radius of emitting area for these two bursts are compared with those of other bursts from Terzan-5 in the bottom figure.

essentially the same, 10 km, for all bursts. The same radii are obtained for the two bursts of 8 min interval (Inoue *et al.*, 1981b).

The absolute value of 10 km implies that practically the whole surface of a neutron star is responsible for burst emission. This remains to hold if the maximum luminosity exceeds the Eddington limit, as will be discussed later. If the area were smaller than the total area, bursts with the maximum luminosity appreciably smaller than the Eddington limit would be due to the partial burning. However, it is very difficult to understand why the area is constant despite that all other features change.

8.3. 1608–522

A transient X-ray source 1608–522 was found to emit 22 bursts in April–July 1979 and 26 bursts in April–July 1980. Two distinct modes in correlation with the persistent flux were observed in 1979 (Murakami *et al.*, 1980a).

Figure 19 shows the counting rates at burst peaks and of the persistent flux observed in 1979. The persistent flux was high in April–May, while it was below the detection limit in June–July. In the former period the bursts were of fast rise and nearly constant duration, whereas in the latter the bursts were of slow rise and nearly of constant peak flux. These events form two distinct groups in the F_b–ε_b plane, as shown in Figure 20. The α-values are about 500 and smaller than 70 for respective groups.

In 1980 the persistent flux was weak, though detectable with FMC. No correlation was found between the persistent flux and the burst profile. The events in 1980 fill the gap between two groups in 1979, as shown in Figure 20. The α-value is as small as or smaller than 25.

It is remarkable that a single burst source shows such different faces. Earlier 1608–522 had not emitted bursts. In 1979 and 1980 this was as active as 1636–536 and showed different burst features in three different periods.

8.4. Double peak bursts

Another prominent feature of 1608–522 is the emission of double peak bursts. Bursts with multiple peaks had been observed from 1743–29, 1728–34, and 1850–08 with SAS-3 (Hoffman *et al.*, 1980) and from the burster in Terzan-2 with the Einstein observatory (Grindlay *et al.*, 1980). Similar bursts of double peaks were observed with *Hakucho* two from 1608–522, one from 1636–536, one from 1905+000, and one from 1728–337. Their profiles are shown in Figure 21. Some bursts from Terzan-5 also have double peaks, though not shown.

In all these bursts double peaks are more distinct in the high energy band than in the low energy band. This implies that the temperature shows double peaks, if the black body spectrum holds over the whole burst. This in turn results in a peak of emission area at the dip of temperature profile. If the emission region has a constant thickness and a varying linear size l, the constant luminosity gives $l^2T^4 = \text{const}$, while the adiabatic change gives $l^{2/3}T = \text{const}$. Although Grindlay *et al.* (1980) have found the latter, *Hakucho* data for five bursts do not give a common

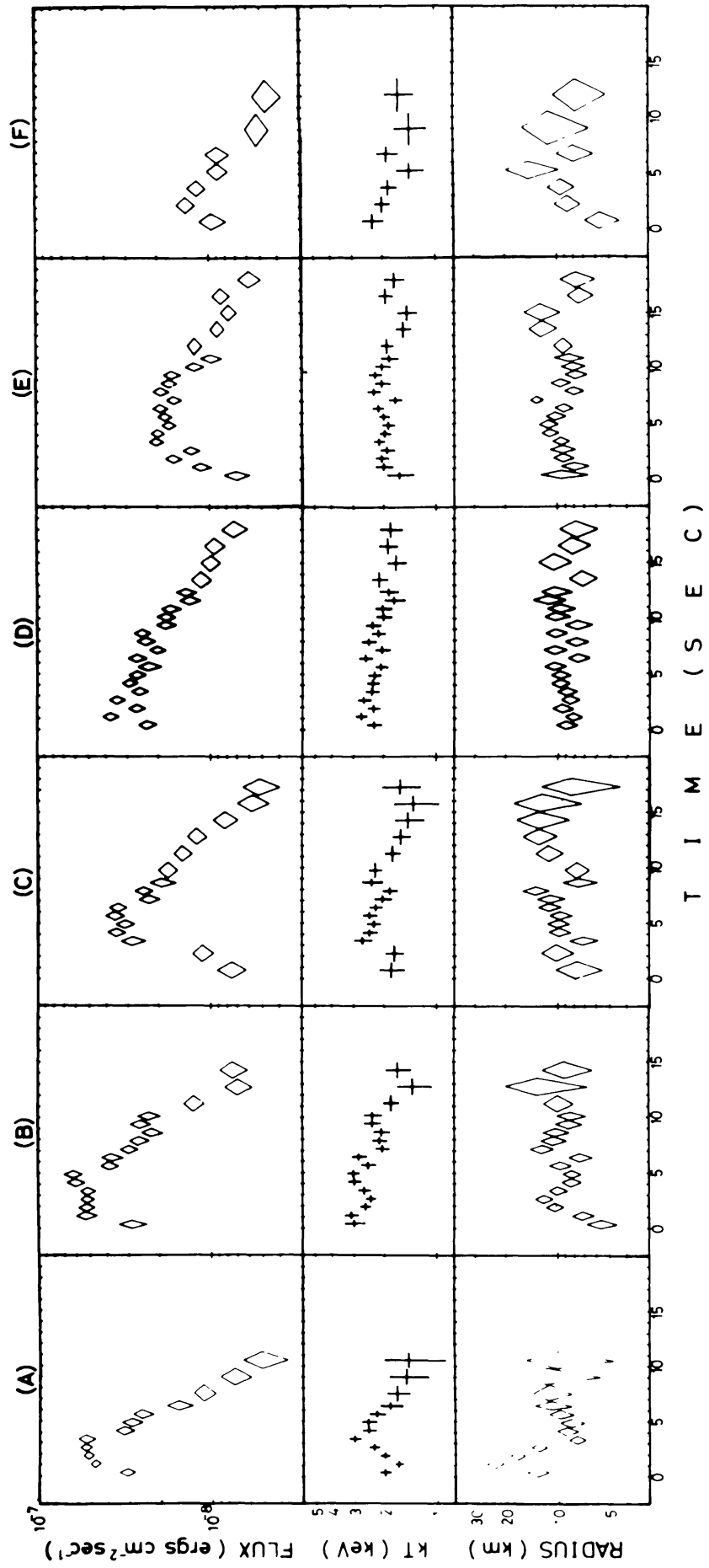

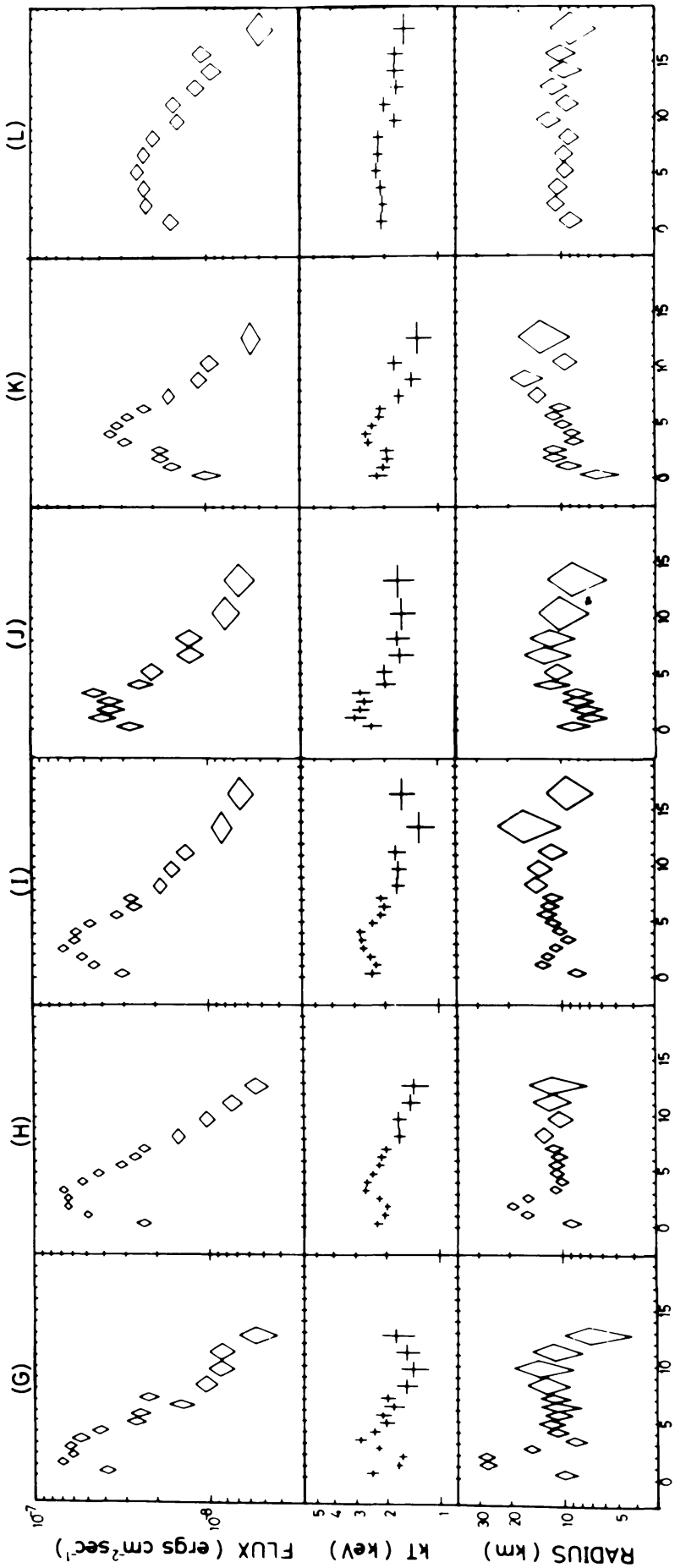

Fig. 18. The profiles, the temperatures and the radii of emitting area for different bursts from 1636–536.

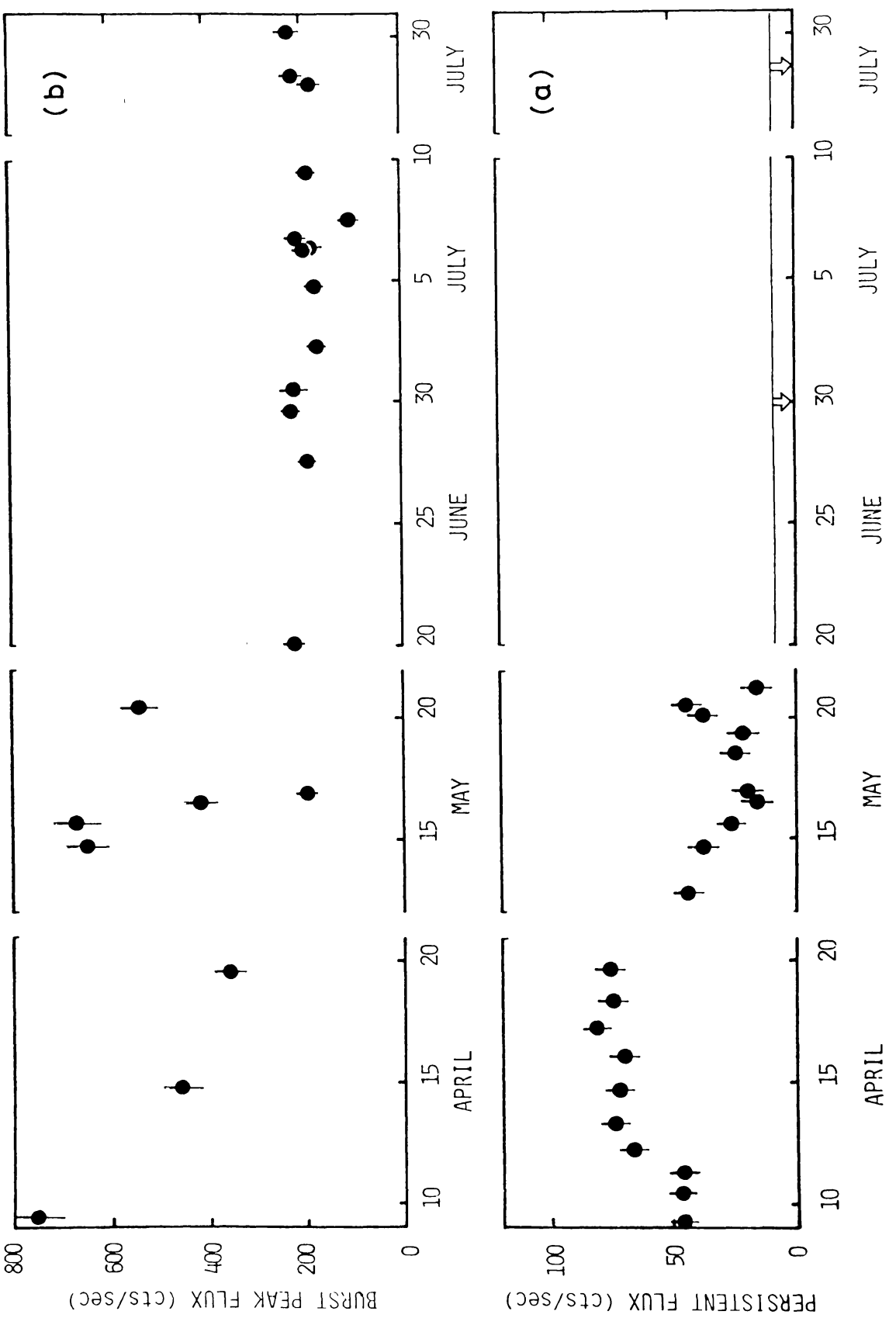

Fig. 19. Correlation between the burst peak flux and the persistent flux observed for 1608–522 in 1979.

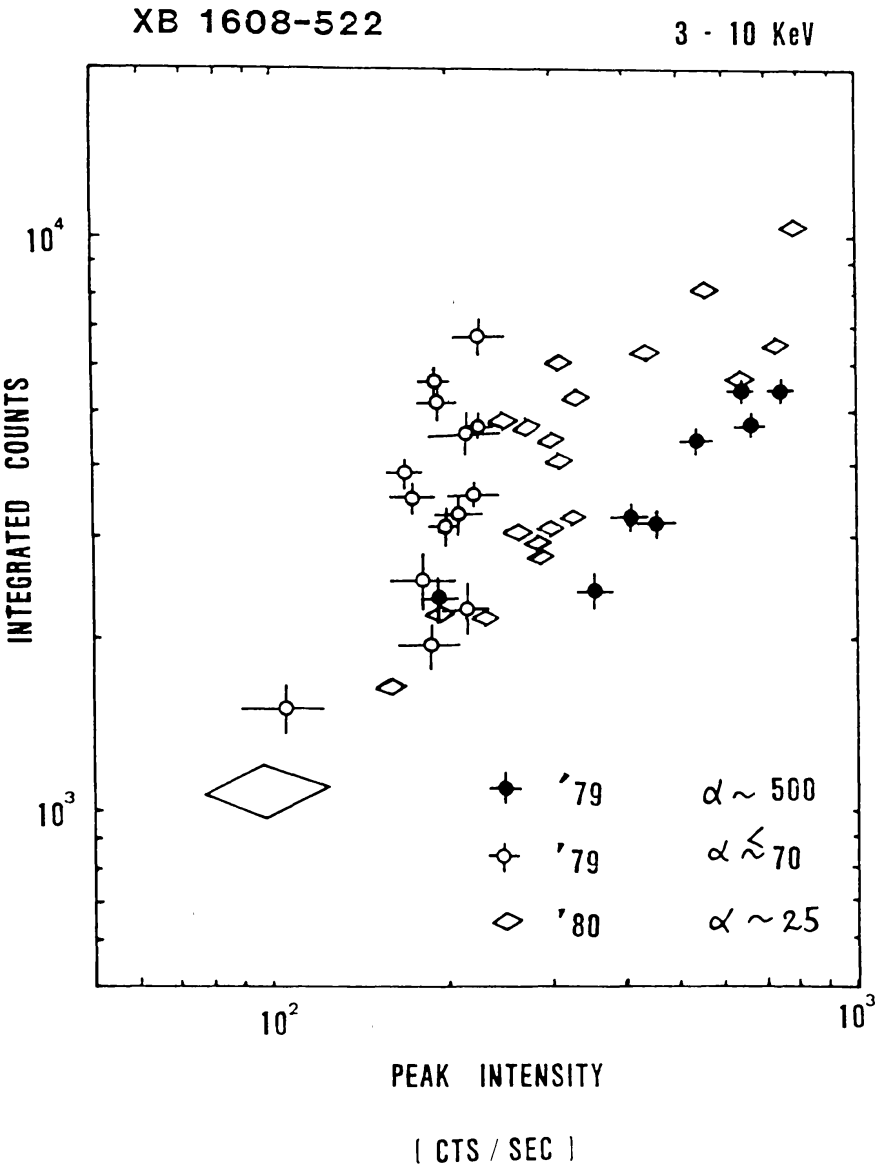

Fig. 20. Relation between the peak flux and the integrated flux observed for 1608–522 in three separate periods.

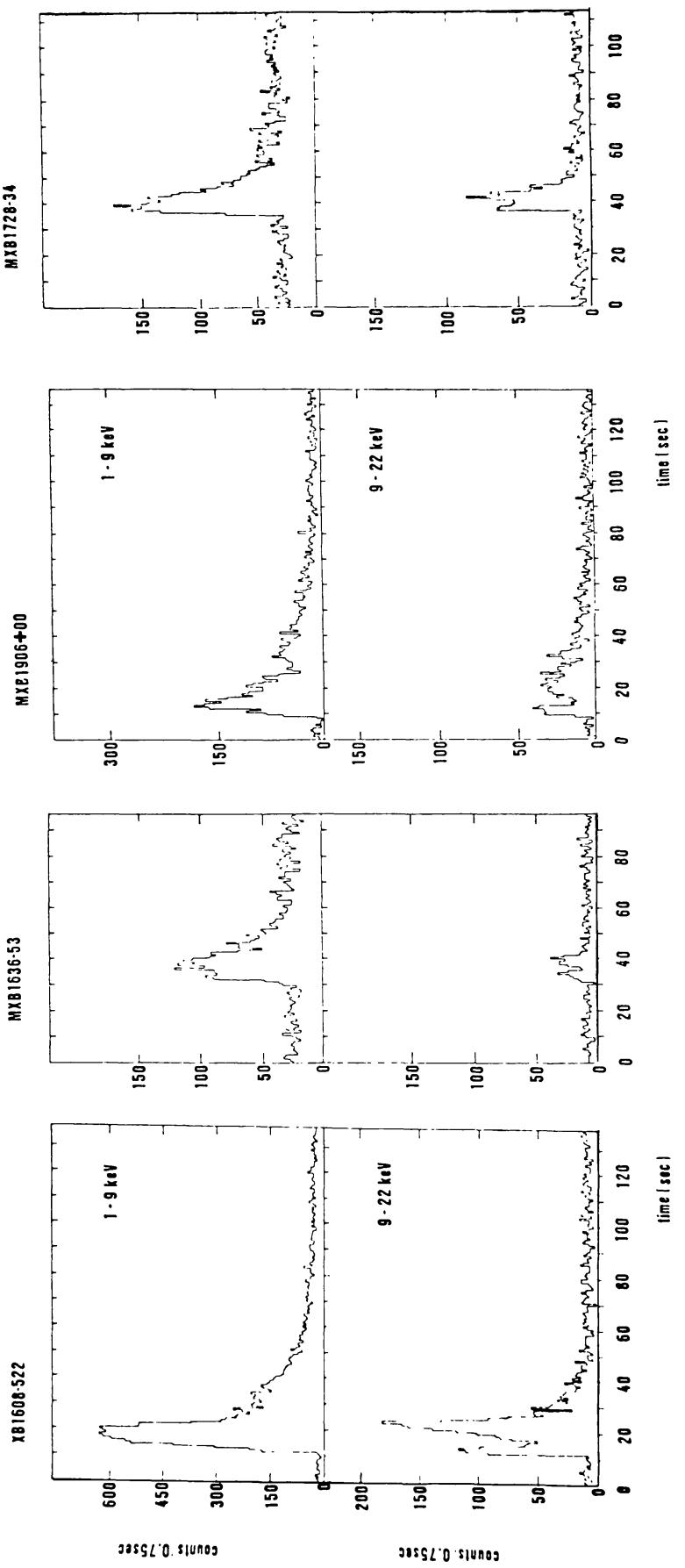

Fig. 21. Profiles of double peak bursts observed from four different bursters.

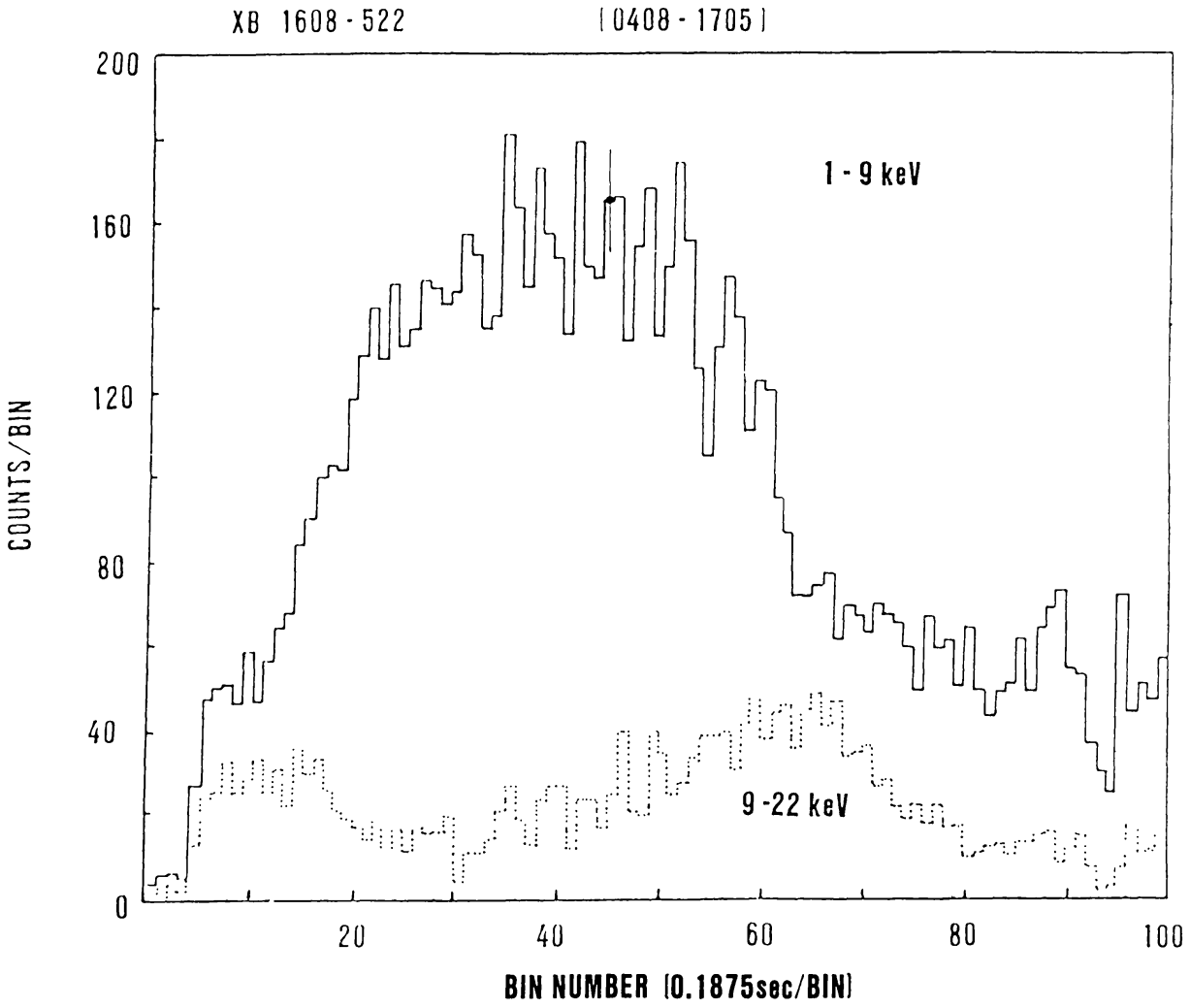

Fig. 22. Oscillation observed at the peak of double peak burst from 1608–522.

l–T relation (Matsuoka, 1980). The existence of double peak bursts can hardly be interpreted in terms of the nuclear flash model.

If we examine the peak structure in more detail, we find ringing with a period of about 0.6 s (Makishima and Murakami, private communication). This is observed for a burst from 1608–522 on 8 April 1980, as shown in Figure 22. Such a feature is not apparent for other bursts. The periodic variation could be relevant to triple peaks with an interval of 0.5 s as observed from 1728–337 (Hoffman *et al.*, 1980).

9. Bursts from the Galactic Center Region

As discussed in Section 6, X-ray bursters are strongly concentrated to the galactic center. Among them 7 bursters are located within 5° from the center, and three of them are associated with globular clusters, Terzan-1, -2 and -5. As we were unable to resolve three galactic center sources and observed no burst from Terzan-2,

we have observed bursts from four sources within 5° from the center, among which GX 3+1, Terzan-1 and -5 are newly discovered sources. To them we add 4U 1728–337 (Slow Burster) which is located at 6° from the center. These five bursters are likely to be located in the galactic bulge and emit bursts similar to those from others, such as 1636–536, as shown in Figure 23 (Inoue *et al.*, 1981).

For a superposed burst from each burster the black-body temperature and the radius of emission area are derived under the assumptions of distances to be $D = 10$ kpc and the hydrogen column densities of $N_H = 1 \times 10^{23}$ cm^{-3} for the galactic center sources and $N_H = 3 \times 10^{22}$ cm^{-2} for others. The black-body temperatures and the radii of emission area are found to be about 3 keV at the peak and about 10 km, respectively. The distributions of peak luminosity thus derived for respective bursters are shown in Figure 24. The peak luminosity scatters by a factor of 3 or more, and most of them are 2–6 times higher than the Eddington limit for the normal abundances and $1.4 M_\odot$. It is worth remarking that no burst is less luminous than 10^{38} erg s^{-1}, thus being unlikely that these sources lie closer to us.

The peak luminosities appreciably higher than the Eddington limit have been already noticed for bursts from NGC 6624 (Clark *et al.*, 1976), from 1728–337 (Hoffman *et al.*, 1977) and, from Terzan-2 (Grindlay *et al.*, 1980). The largest peak luminosity has been observed for 1728–337 to be 2×10^{39} $(D/10 \text{ kpc})^2$ erg s^{-1}, nearly 10 times the Eddington limit for 1.4 $M_\odot$.

All these results lead us to conclude without doubt that there exist X-ray bursts which are appreciably more intense than the Eddington limit. The conclusion is further strengthened by answering the following questions.

(1) *Distance to the galactic center.* Even if we accept that the burst sources lie within 1 kpc from the galactic center, the distance to the galactic center may be shorter than 10 kpc. Adopting the smallest value of distance, 8 kpc (Graham, 1979), we can reduce the absolute luminosity only by a factor of 1.6.

(2) *The neutron star mass.* One might attribute the large luminosity to the Eddington limit for more massive stars. Because of the gravitational effect, however, the Eddington limit has a maximum for a fixed stellar radius. Since the radius of a neutron star generally increases as the mass decreases, it is hardly possible to have the Eddington limit exceeding 2×10^{38} erg s^{-1} for the normal chemical composition.

(3) *Dynamical effects.* Since the Eddington limit is attained by the balance between the radiation pressure and the gravitational force, a super-Eddington luminosity is possible if X-rays are emitted while the surface is expanding. This may be the case in the initial phase of bursts, as seen from the variation of emission area shown in Figure 23. In the initial phase the assumption of black-body radiation would fail, so that the bolometric correction based on the black-body spectrum could bring about an overestimate of luminosity. After the peak, however, the emission area is essentially constant, and the derivation of luminosity is hardly in error. The post-peak luminosity is not weaker than a half of the peak luminosity, yet this exceeds the Eddington limit.

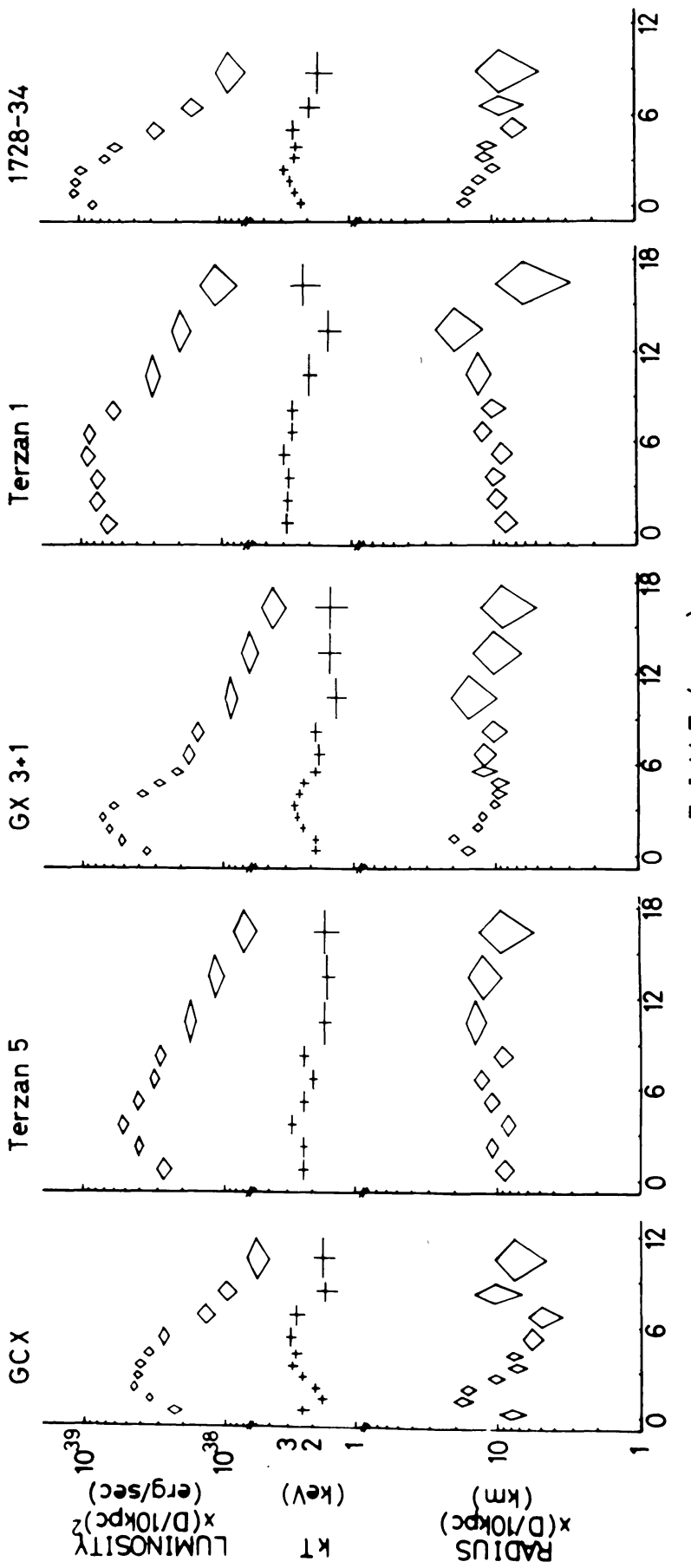

Fig. 23. The profiles, black-body temperature and radii of emission area of typical bursts from 5 bursters in the galactic center region, the galactic center sources (GCX), Terzan-5, GX 3+1, Terzan-1, and 1728–337.

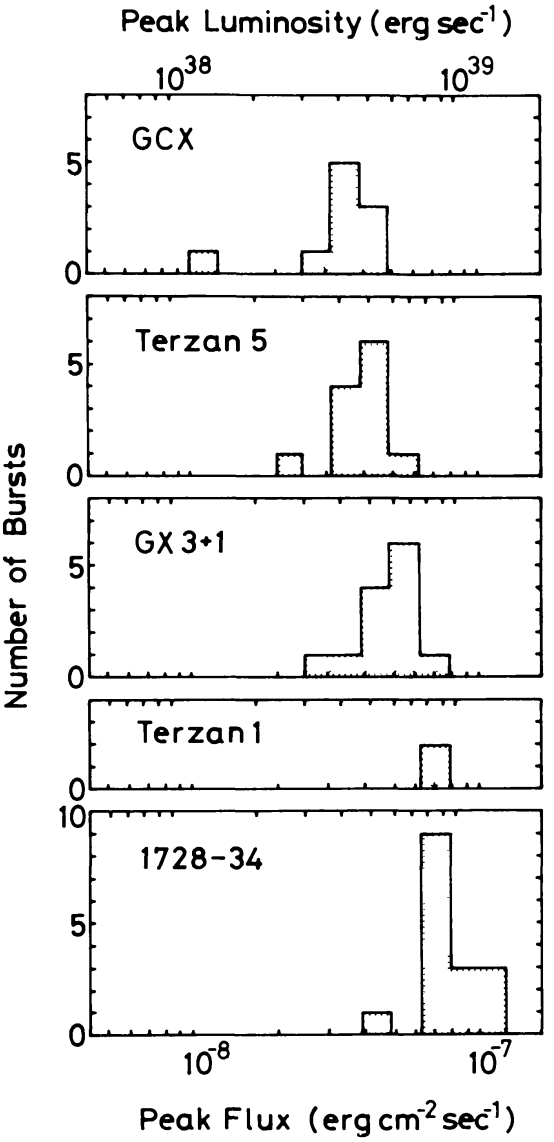

Fig. 24. The distributions of peak luminosity for 5 bursters in the galactic center region. The distance of 10 kpc is assumed.

Even if we take all the above effects into account, we cannot get rid of the luminosity at least 2–3 times the Eddington limit. We are therefore led to consider the reduction of opacity, as this is only a quantity left at our disposal in Equation (6.6). Assuming that the energy source lies at the bottom of accretion layer, as suggested by the nuclear flash model, we point out the following causes for the reduction of opacity.

(4) *Compton scattering.* In the burning region the photon energy is so high that the scattering cross section is appreciably smaller than the Thomson cross section. This causes the reduction of opacity, (D. Sugmimoto, private communication). For the black-body radiation of temperature T, the opacity is given by

$$\kappa = \frac{\kappa_{\mathrm{Th}}}{1+(T/T_c)}, \quad T_c \simeq 40\ \mathrm{keV}\,. \tag{9.1}$$

Hence the radiation more than twice the Eddington limit can be transported for $T > T_c$.

This effect is even greater, if we take into account the fact that the spectrum is harder than the Planck spectrum due to a plasma effect. Since the index of refraction is different from unity, the spectrum of radiation is modified to

$$B(\omega) = \left(1 - \frac{\omega_p^2}{\omega^2}\right) B_0(\omega), \qquad E_p = h\omega_p = 0.29\left(\frac{1+X}{2}\right)^{1/2} \rho^{1/2}\,\mathrm{keV}, \quad (9.2)$$

where $B_0(\omega)$ is the Planck spectrum. Since the spectrum is cut off at the plasma frequency ω_p, the average photon energy is higher than that for $\omega_p = 0$, thus decreasing T_c in equation (9.1). However, this effect is unimportant for $\rho < 10^3\ \mathrm{g\ cm^{-3}}$, which corresponds to $T < 20$ keV in the nuclear flash model.

(5) *Effect of electron correlation on Thomson scattering.* The Coulomb field of an electron is shielded in a plasma at distances greater than the Debye length $D = (kT/4\pi e^2 n)^{1/2}$. The cross section for Thomson scattering is therefore reduced for

$$2kD \sin(\theta/2) < 1,$$

where k is the photon wave number and θ the scattering angle. The differential cross section is expressed as (Fejer, 1960; Dougherty and Farley, 1960; Salpeter, 1960; Rosenbluth and Rostoker, 1962)

$$\frac{\mathrm{d}\sigma}{\mathrm{d}\cos\theta} = \pi\left(\frac{e^2}{mc^2}\right)^2 (1+\cos^2\theta)\frac{4k^2D^2\sin^2(\theta/2)+\frac{1}{2}}{4k^2D^2\sin^2(\theta/2)+1}. \quad (9.3)$$

The total cross section is approximately given by

$$\sigma = \sigma_{\mathrm{Th}}\left(\tfrac{3}{4} + \tfrac{3}{16}\cos\theta_0 + \tfrac{1}{16}\cos^3\theta_0\right) \quad (9.4)$$

with

$$\cos\theta_0 = 1 - \frac{1}{2k^2D^2}.$$

The numerical value of kD,

$$kD = 0.56\left(\frac{T^3_{\mathrm{keV}}}{\frac{1}{2}(1+X)\rho}\right)^{1/2}, \quad (9.5)$$

is not small enough to reduce the cross section by the maximum factor of two. Yet the reduction of a few tens of percent may take place.

(6) *Effect of magnetic field.* For photons propagating along the magnetic field, the opacity is reduced to

$$\kappa = \kappa_{\mathrm{Th}}/[1 + (E_c/E)^2], \quad (9.6)$$

where E is the photon energy and $E_c = 11.6\,B_{12}$ keV is the cyclotron energy in the magnetic field of strength B in units of 10^{12} G. For photons propagating in the perpendicular direction, the component of polarization perpendicular to the field

is reduced in the same way, whereas the other component is not affected by magnetic field. The opacity averaged over the dipole field for the spherical black-body emission is given by (Joss and Li, 1980)

$$\kappa = \frac{4\pi^2}{5} \kappa_{\mathrm{Th}} / [1 + (E_c / kT)] . \tag{9.7}$$

If the magnetic field is as strong as several times 10^{12} G, the reduction of opacity is appreciable in the region where the reduction of Compton scattering is unappreciable. Hence luminosities exceeding the conventional Eddington limit are attainable.

The above arguments show that luminosities higher than the Eddington limit are possible if the magnetic field is appreciably stronger than 10^{12} G. Other important consequences of a strong magnetic field are a variety of burst profiles. In the presence of magnetic field the accretion flow is channeled to the magnetic poles. In the polar region the internal temperature is lower than in other regions, because of a higher cooling rate due to a lower value of opacity, so that matter can accumulate on the surface without being subject to slow nuclear burning. Hence the nuclear flash may start more frequently in the pole region than in others, and the flash may be quenched without spreading over the whole surface because of rapid cooling, thus leaving some nuclear fuel unprocessed. The effect of magnetic field, further combined with pure helium flash (Joss, 1978) and hydrogen-helium flash (Fujimoto *et al.*, 1980), could explain a variety of burst profiles including double peaks, though detail would have to be worked out.

10. Simultaneous X-ray and Optical Bursts from 1636–536

Optical bursts simultaneous to X-ray bursts were observed from 1735–444 (Grindlay *et al.*, 1978; McClintock *et al.*, 1979) and from 1837+049 (Hackwell *et al.*, 1979). A collaboration between *Hakucho* and ESO has made it possible to observe five simultaneous bursts from 1636–536 in 1979 and five in 1980.

These three burst sources have common properties of X-ray and optical emission, as shown in Table IV. The ratio of optical to X-ray luminosities for bursts is several times smaller than that for steady emission, the optical burst delays with respect

TABLE IV

Simultaneous X-ray and optical bursts

Source	1735–444	1837+049	1636–536
$(L_{\mathrm{op}}/L_x)_{\mathrm{steady}}$	1×10^{-4}	2×10^{-5}	6×10^{-4}
$(E_{\mathrm{op}}/Ex)_{\mathrm{burst}}$ *	2×10^{-5}	3×10^{-6}	1×10^{-4}
Delay	~3 s	1–2 s	~2 s

* The integrated luminosity E is used because of better statistical accuracy.

to the X-ray burst by a few seconds, and their profiles are similar to one another except in the tail which is appreciably longer for optical bursts.

These sources persistently emit X-rays whose flux varies by a factor of three or so. They are associated with faint optical objects which are characterized by UV excess and emission lines. The absence of absorption lines indicates that companion stars, if any, are dwarfs which do not appreciably contribute to optical emission. Emission lines are those excited by X-rays. For 1636–536 the lines are blue and red shifted with velocities of about $\pm 1000\ \mathrm{km\ s^{-1}}$. These features suggest that optical emission arises from X-ray irradiated disks formed around the X-ray sources.

Under the coordination of the MIT X-ray astronomy group, *Hakucho* and ESO telescopes spent as much as possible time for the observation of simultaneous X-ray/optical bursts from 1636–536 (Oda, 1979; Ogawara, 1980). In 1979 five simultaneous bursts were recorded, one of which missed the onset of optical burst. In 1980 a longer time was allocated for the campaign, and 14 X-ray bursts and 23 optical bursts were recorded. Among them only five coincided, and the rest of them occurred out of the observation window of the other, except for one case. This optical burst occurred in the X-ray window, but a simultaneous X-ray burst would have been hardly observable, because this occurred at an epoch close to the entry to the radiation belt and the optical burst was very weak. It is interesting to note that two optical bursts on 6 July 1980 occurred with an interval of 6 min but outside of the X-ray window.

Thus we have, for the first time, succeeded in observing multiple simultaneous bursts from a single source. The time profiles of optical and X-ray bursts on 28 June 1979 and 16 June 1980 are shown in Figure 25 (Ohashi, 1981). Here the optical bursts were observed in the B band, while the X-ray bursts were observed in two energy channels of FMC-2.

The profiles of X-ray and optical bursts are related with each other as follows:

$$I_{\mathrm{op}}(t) \propto [I_x(t-\Delta)]^{\beta}, \tag{10.1}$$

where Δ is the delay time and β is a constant of about 0.3. For the burst on 28 June 1979, this relation is shown in Figure 26 for $\Delta = 2.3$ s. For all bursts the values of Δ and β are a few seconds and about 0.3, respectively. This indicates that the optical burst is emitted from a wall heated by the X-ray burst.

If the wall were a companion star, we would be looking in the direction nearly normal to the orbital plane, in order that Δ remains constant. Then the temperature would be

$$T = \left(\frac{L_x}{4\pi (c\Delta)^2 \sigma}\right)^{1/4} = 4\times 10^4 \left(\frac{L_x}{10^{37}\ \mathrm{erg\ s^{-1}}}\right)^{1/4} \left(\frac{6\times 10^{10}\ \mathrm{cm}}{c\Delta}\right)^{1/2} \mathrm{K} \tag{10.2}$$

for the delay of 2 s, where σ is the Stefan–Boltzmann constant. This would give β somewhat smaller than 0.3 but within a permissible range. However, the Doppler shift of emission lines does not result, since the disk plane has to be perpendicular

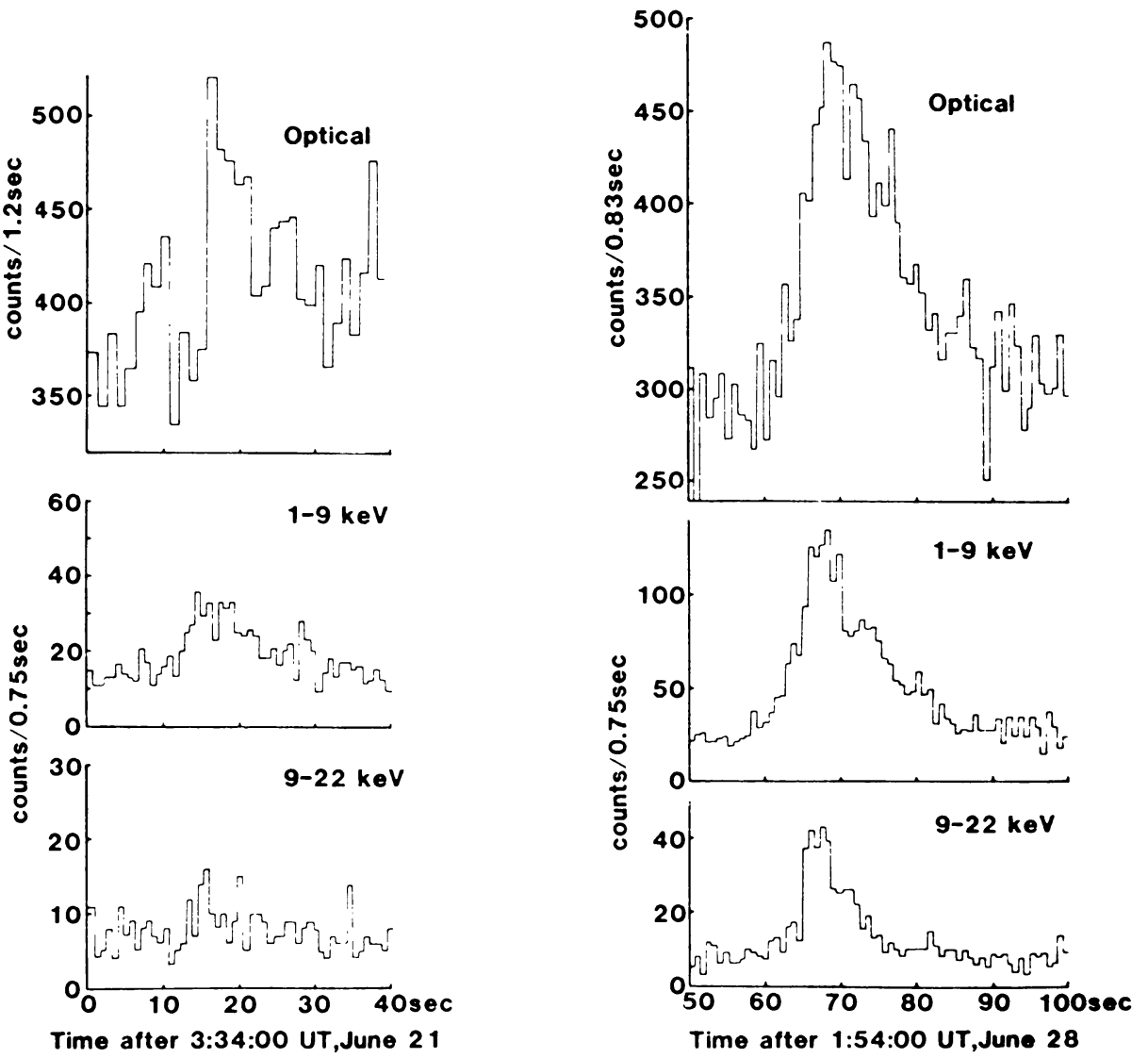

Fig. 25. Profiles of simultaneous optical and X-ray bursts from 1636–536.

to the line of sight. If the inclination angle is large, we should observe a variation of Δ according to the orbital phase, and the delay time Δ would correlate with I_{op}/I_x.

If the accretion disk is responsible for optical emission, the optical profile would have to be smeared, since emission would arise from a wide region of the disk plane. However, the disk irradiated by X-rays cannot maintain a flat structure. Beyond the distance of about one light second, the disk blows up to form a geometrically thick structure because of efficient X-ray heating. In the transition region is formed a wall which is optically thick for optical radiation but transparent for hard X-rays (Hayakawa, 1981). Hence the temperature is about 3×10^4 K for $\Delta \simeq 1$ s.

The above consideration demonstrates that simultaneous X-ray/optical bursts provide a means of investigating the disk structure, which is otherwise studied only theoretically.

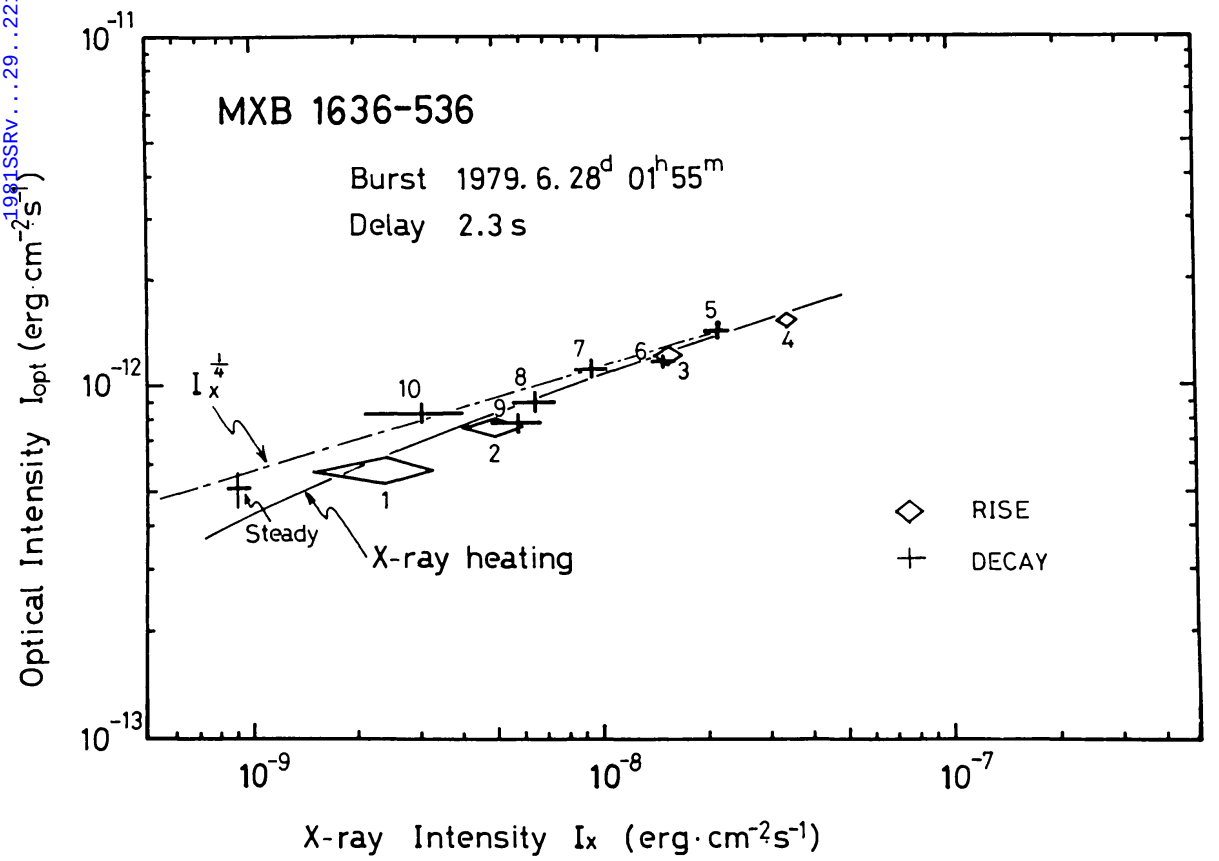

Fig. 26. Correlation between the X-ray and optical flux values for a burst on 28 June 1979. The X-ray burst is shifted backward by $\Delta = 2.3$ s. The lines represent equation (10.1) with $\beta = 0.25$ and the correlation based on the black-body spectrum with temperatures given by Equation (10.2).

11. Rapid Burster

Unlike other X-ray bursters, burst source 1730–335 was found unique in the sense that it emits bursts with short intervals, several seconds to several minutes. Because of this rapid repetitivity, the source is called the Rapid Burster (Lewin *et al.*, 1976a). Since its discovery in March 1976, the source has been active during two contiguous periods per year, and a recurrent interval of half a year is suggested by taking earlier data into account (Grindlay and Gursky, 1977). The burster became active on 8 August 1979 (Inoue *et al.*, 1980) a little earlier than expected from the 6 months interval and the previous activity in March 1979.

11.1. General behavior

Hakucho began to watch the Rapid Burster on 30 July 1979 and detected the first burst in this active period at $00^h\ 16^m$ on 8 August. About 110 bursts were recorded with FMC during the net exposure time of 31.5 hr until the source was lost out of the field of view because of the sun angle restriction. Thereafter about 360 bursts were recorded with CMC alone during the net exposure time of 41 hr. The source went away from the field of view on 22 August, when the burster was still active.

During this active period, the behavior of the Rapid Burster was quite different from that observed earlier. Immediately after the activity started, a long burst of trapezoidal profile with duration of 72 s was detected. Another similar burst with duration of 148 s was observed on the first day. These two look similar to 'very long' bursts observed with SAS-3 in March 1979 (Basinska *et al.*, 1980). Except for these two, 20 bursts during the exposure time of 88 min were of triangular profile, though no interval shorter than 40 s was found. After 7^h on 8 August, however, all bursts were trapezoidal and of high peak luminosities. During the exposure time of 30 hr by the end of 15 August, 87 such bursts were exclusively of such type. The longest duration was 12 min. Thereafter triangular bursts began to be mixed, and finally only such bursts were observed. Some of the observed data are shown for 7 separate periods in Figure 27.

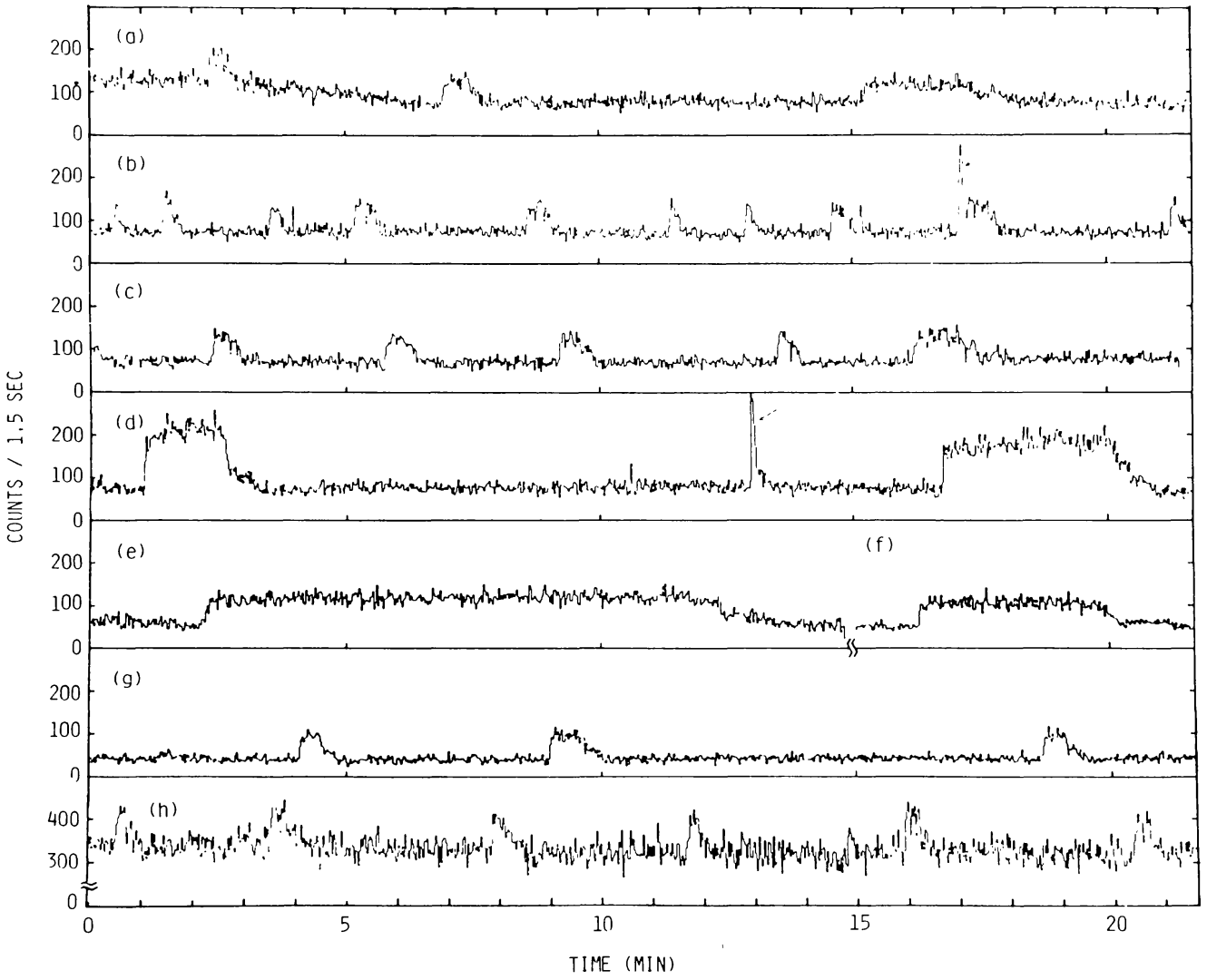

Fig. 27. Counting rate record of FMC-2 (a–d: 1–10 keV, e–g: 3–10 keV) and CMC (h: 3–10 keV) in selected periods. The segments start at (a) 8/8 1^h 55^m 19.25^s, (b) 8/8 3^h 37^m 39.8^s, (c) 8/8 5^h 19^m 45.3^s, (d) 8/8 19^h 48^m 00^s, (e) 8/11 19^h 19^m 54.3^s, (f) 8/12 16^h 08^m 24.1^s, (g) 8/14 17^h 22^m 58.2^s, and (h) 8/17 13^h 43^m 39.1^s. Two bursts indicated by arrows are from 1728–337.

In the expected active periods of 13–20 April 1980 and 14 July–25 September 1980, we watched the Rapid Burster for the exposure times of 31 hr and 293 hr, respectively. No burst was found during these periods above the detection limit of 0.1 times the Crab nebula intensity. The history of observation is summarized in Figure 28.

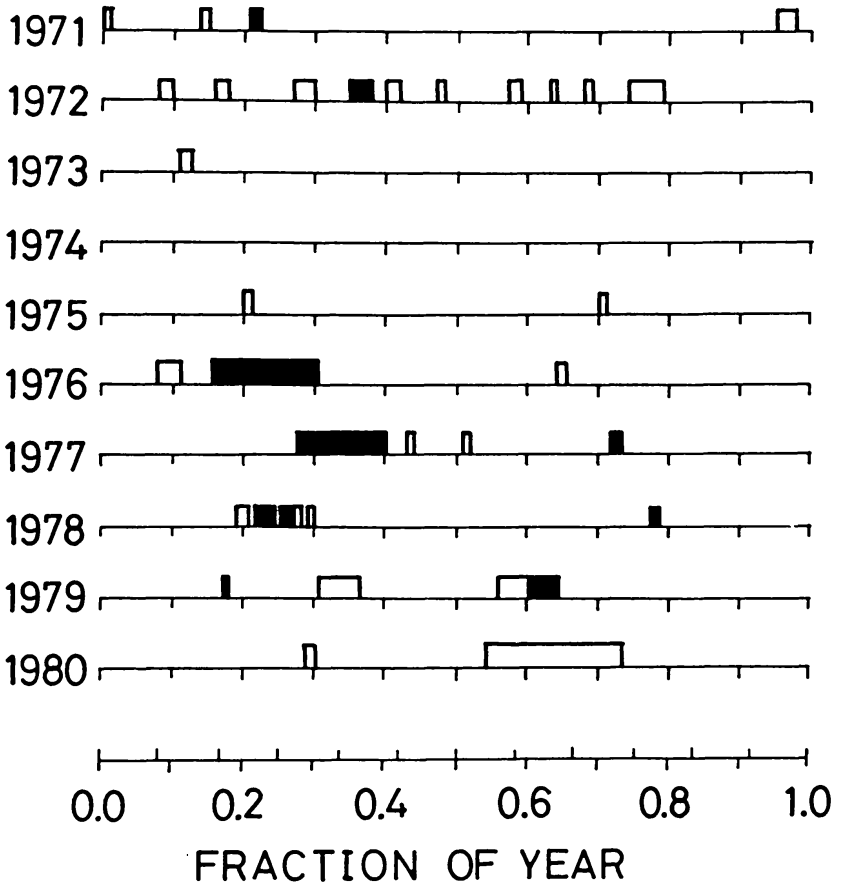

Fig. 28. Record of burst activity of the Rapid Burster. Rectangles show the observation windows. The active periods are blacked.

In order to elucidate the unique behaviour that the Rapid Burster showed in August 1979, we devide the whole period into three phases and summarize characteristic properties of activity in Table V (Kunieda *et al.*, 1981).

11.2. Correlations among observed quantities

Three quantities E, L_p and L_B characterize the activity of the Rapid Burster. They are small in phase I, steeply increase as time goes on, reach maxima in phase II, and are of intermediate values in phase III, as shown in Figure 29 (Oda, 1980; Tawara, 1981). These quantities would appear to change continuously from one phase to the next. However, the correlation diagrams of two quantities show rather clear separation of three phases.

TABLE V

Properties of the rapid burster in three phases

Phase	I	II	III
Date (Aug. 1979)	8.01–8.24	8.29–15.94	16.58–22.52
Number of bursts	22	87	360
Net exposure time	1.5^h	31^h	41^h
Burst profile	Triangular but 2	Mostly trapezoidal	Triangular
E^* (10^{39} erg)	3.2	32	4.6
L_p *(10^{38} erg s^{-1})	1.7	2.8	2.1
L_B * (10^{37} erg s^{-1})	1.6	3.3	1.7
L_s (10^{37} erg s^{-1})	<0.8	1.3–2.2	—

* L_p represents the peak luminosity. E represents the total energy contained in a burst.

$L_B = E/t_i$, where t_i is the time to the following burst, represents the averaged burst luminosity. L_s is the luminosity of persistent emission. The energy values are derived for the assumed distance of 10 kpc.

In these diagrams we use the time between the onset time of a burst and that of the next burst, t_i, instead of L_B, since L_B is derived from

$$L_B = E/t_i \,. \tag{11.1}$$

We also use the burst duration t_b which is defined by

$$E = L_p t_b \,. \tag{11.2}$$

Figure 30 shows the correlation diagrams of $E - t_i$, $L_p - E$ and $L_p - t_b$ (Kunieda *et al.*, 1981).

The $E - t_i$ diagram was first constructed for the activity in March 1976. On the basis of its linearity Lewin *et al.* (1976a) suggested a model that the energy stored in a reservoir is suddenly released to produce a burst, and the reservoir waits for the energy supply at a constant rate to fill up to the threshold value. Figure 30(a) would appear to show the linearity over a wider range. Closer examination shows that the overall $E - t_i$ relation is not linear but $E \propto t_i^{1.2}$. However, a linear relation holds separately for each phase. According to Equation (11.1), this is due to the correlation between E and L_B, as indicated in Figure 29. In the $E - t_i$ diagram the points belonging to phase I and phase II are separated by a gap, and those to phase III fill the gap. A jump from phase I to phase II justifies the introduction of phases, implying that the behavior abruptly changes at the transition from phase I to phase II. The recovery from phase II takes place gradually in phase III.

Similar gaps are also noticed for the $L_p - E$ and $L_p - t_b$ diagrams. These two are not independent because of the relation (11.2), but intuitively reveal important properties. In these diagrams two long bursts in phase I are distinctly separated from long bursts in phase II, because of low L_p of the former. In addition, the intensity fluctuations at the top are appreciably higher in the former than those in

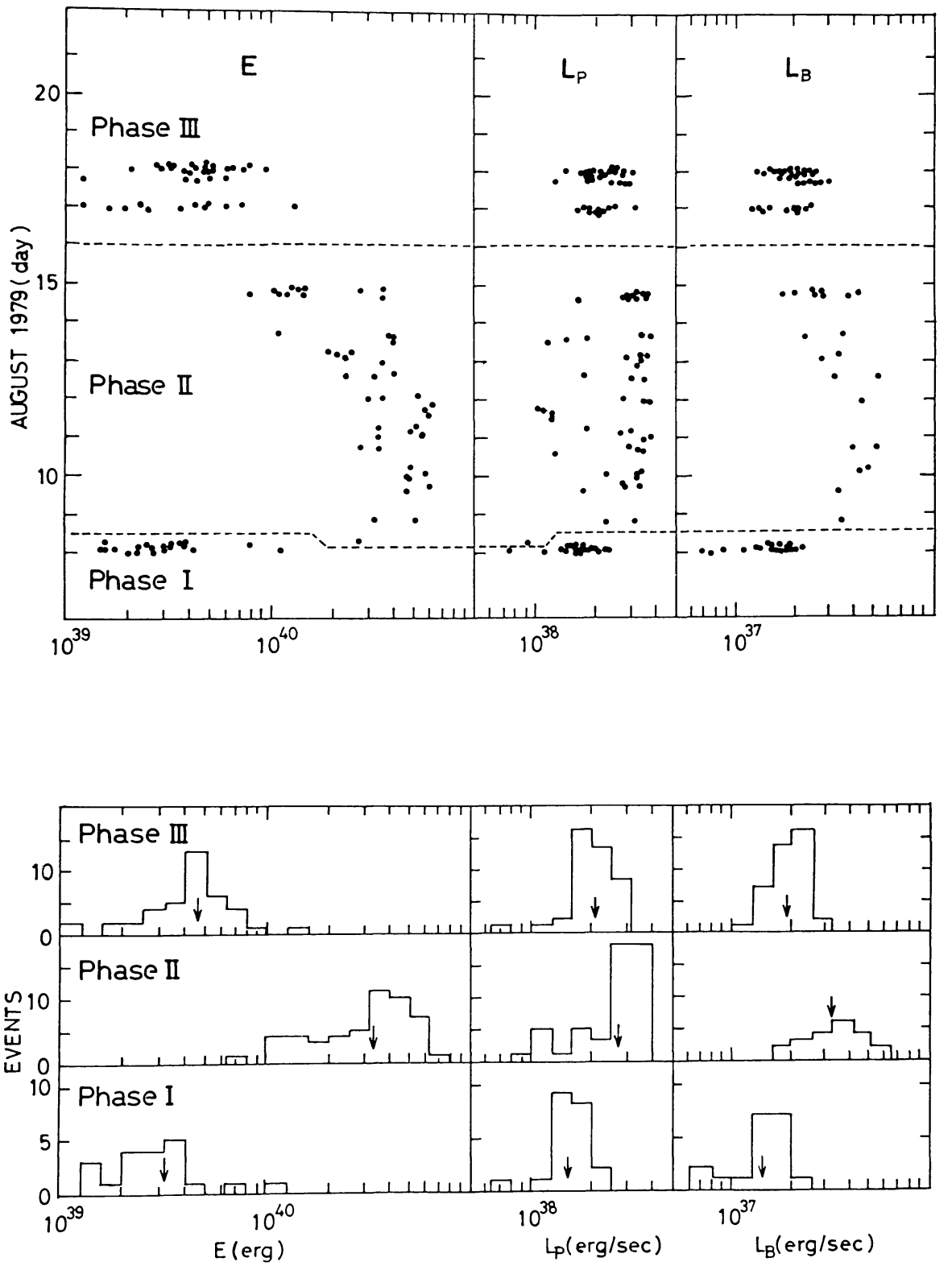

Fig. 29. Time variations of burst parameters, the total energy E, the peak luminosity L_p, and the average burst luminosity L_B. The frequency distributions and the average values (arrows) of these quantities are shown separately for three phases in the bottom figure. Phase I (8.01–8.24), phase II (8.29–15.94), and phase III (16.58–22.52) from the bottom to the top.

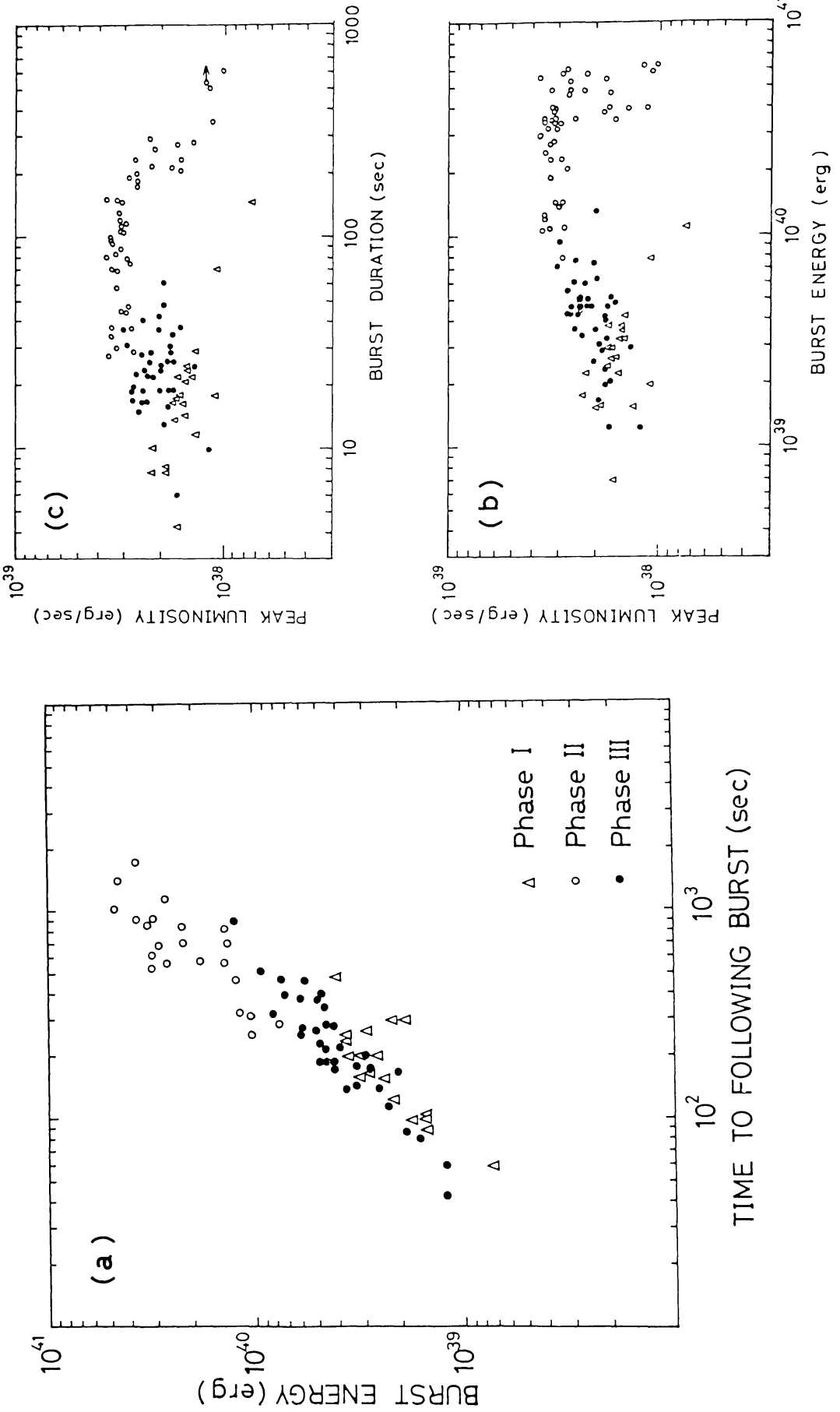

Fig. 30. Correlation diagrams for (a) the burst energy E vs the time to the following burst t_i, (b) the peak luminosity L_p vs the burst energy E, and (c) the peak luminosity vs the duration t_b. Data points in three phases are represented by △ (I), ○ (II), and ● (III).

the latter which show flat tops only subject to statistical fluctuations, except for two oscillatory events described later.

The reason for presenting two diagrams for $L_p - E$ and $L_p - t_b$ can be seen in their right ends, where L_p spreads over a range below its maximum value. In the $L_p - E$ diagram the decrease of L_p takes place when E reaches the maximum value, $E_{\max} \simeq 6 \times 10^{40}$ erg. In the $L_p - t_b$ diagram this begins when t_b exceeds 150 s, and the relation $L_p \propto t_b^{-1}$ is observed up to $t_b \simeq 700$ s. What causes the decrease of L_p, the decrease of emission area or that of temperature or both?

The spectra of trapezoidal bursts were observed for five events, when *Hakucho* was operated with the pulse height mode. If the spectra are fitted to thermal bremsstrahlung and power law spectra, large values of the column density of absorbing matter are required for cutting off the low energy part, particularly on account of that the bursts were not detected by VSX counters. They are too large to be compared to the interstellar column density, 2.4×10^{22} H atoms cm^{-2}, derived from the extinction of Liller I globular cluster (Liller, 1977; Kleinmann *et al.*, 1976), in which 1730–335 is located, unless a large value of circumstellar absorption is assumed. On the other hand, the blackbody spectra can fit the observed spectra with temperatures 1.7–2.0 keV and the absorption column density of about 3×10^{22} H atoms cm^{-2} (Kunieda *et al.*, 1981). Hence we assume black-body spectra and derive the radiation temperatures of all trapezoidal bursts from the hardness ratios observed. We then derive the emission areas assuming the spherical isotropy.

The relation between peak luminosity and temperature is shown in Figure 31. The temperature decreases as the luminosity decreases. In order to show that the decrease is also associated with a decrease of the emission area, equi-area lines expected for black-body emission are drawn. There is an apparent correlation between the temperature and the area. The correlation may be expressed as

$$A = 3.2 \times 10^{13} (T/1.8 \text{ keV})^4 \text{ cm}^2 . \tag{11.3}$$

as indicated in Figure 31.

11.3. Oscillation at the top of trapezoidal bursts

A rapid oscillation found for two trapezoidal bursts also shows an oscillatory change of the emission area but not of the energy spectrum. The power spectral analysis of trapezoidal bursts in phase II gives no indication of periodic variations except for two events (Tawara *et al.*, 1981). These two bursts show pulsating tops with amplitudes extending to about 30% and with periods of about 0.5 s. Other than the pulsations these two share the same properties with other bursts of the highest luminosities.

The pulsation is different from that of X-ray pulsars in view of that the periods of two differ by one per cent for the time lapse of about one day, and that the pulsation ceases in the initial and last phases of a burst. Moreover, the period drifts during a few minutes of a burst, as shown in Figure 32. These variations appear with the same relative amplitude in two energy channels.

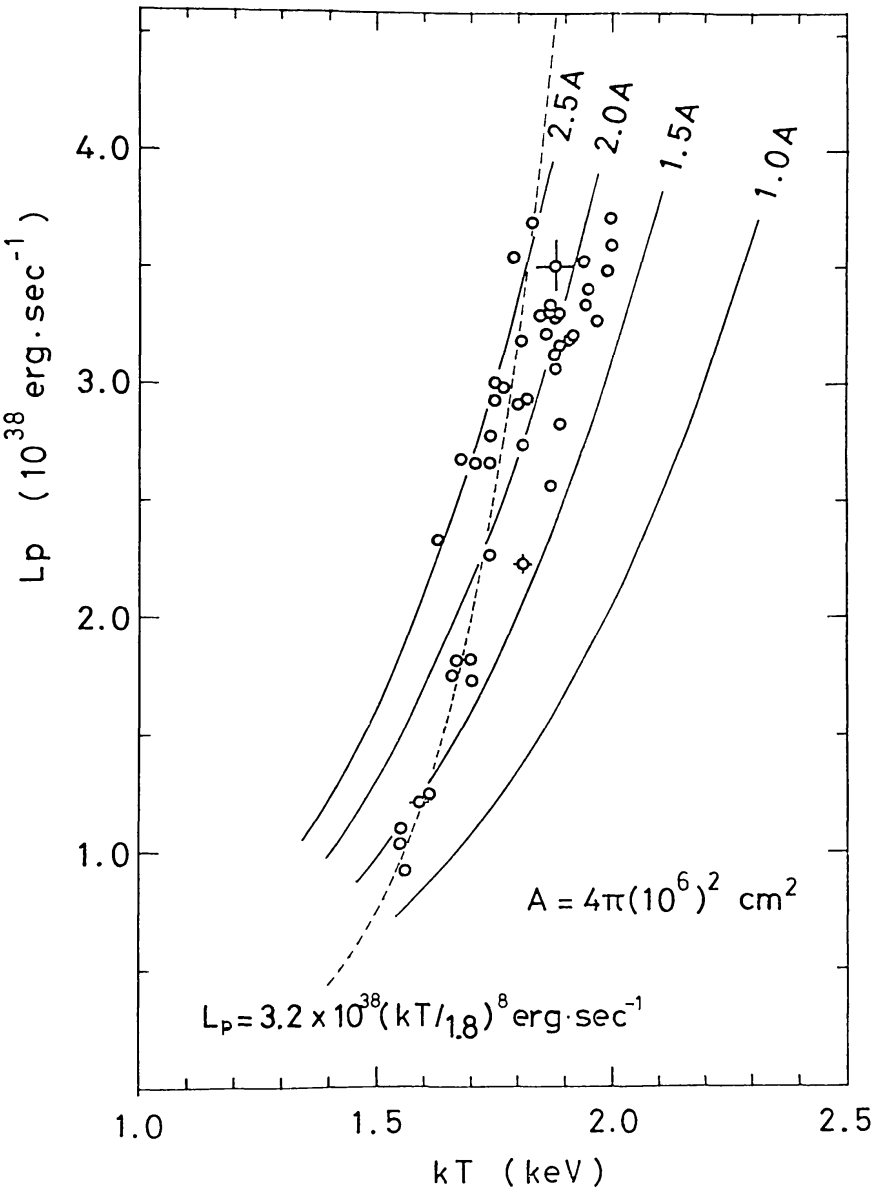

Fig. 31. Correlation between the peak luminosity L_p vs the radiation temperature T for trapezoidal bursts in phase II. The solid lines represent the relations for fixed areas, and the dashed line represents the correlated case, $A \propto T^4$ as given by Equation (11.3).

11.4. Burst profile and persistent emission

In addition to the gross structure of bursts, the fine structure of bursts also gives interesting information. Figure 33 shows the time profiles of a typical trapezoidal burst in two energy channels. This shows a drop as sharp as a rise, though the decays of some other bursts are gradual. The rise is always as fast as one second, but the profile of decay is variable, as seen from Figure 27. It is therefore difficult to define the decay time without ambiguity but with physical meaning. Roughly speaking, for trapezoidal bursts, the decay time varies from 10 s to 1 min with an apparent correlation with duration. A change of temperature in the decay part is

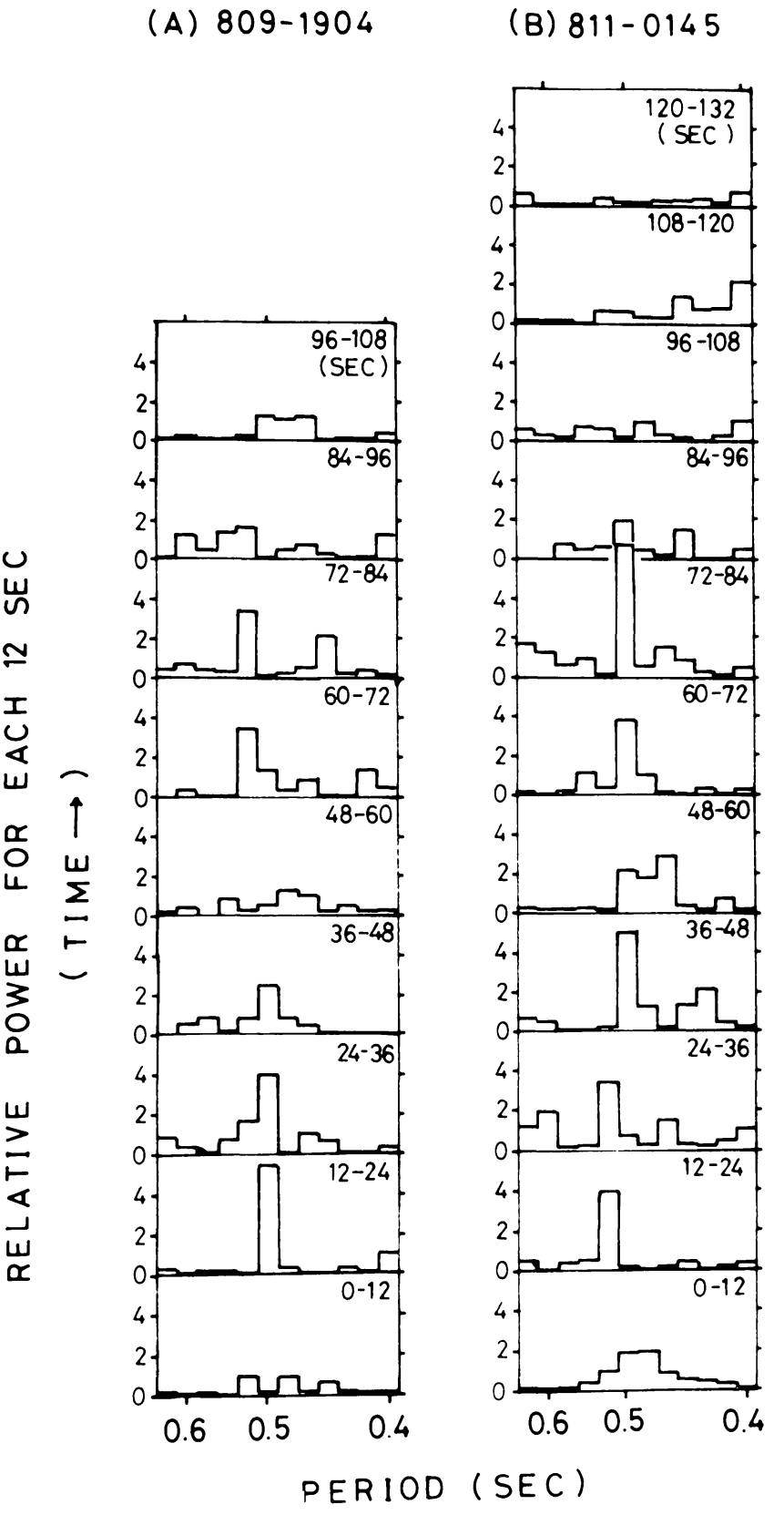

Fig. 32. The period of pulsation in every 12 s for two pulsating bursts. Each diagram shows the power spectrum in the given time segment.

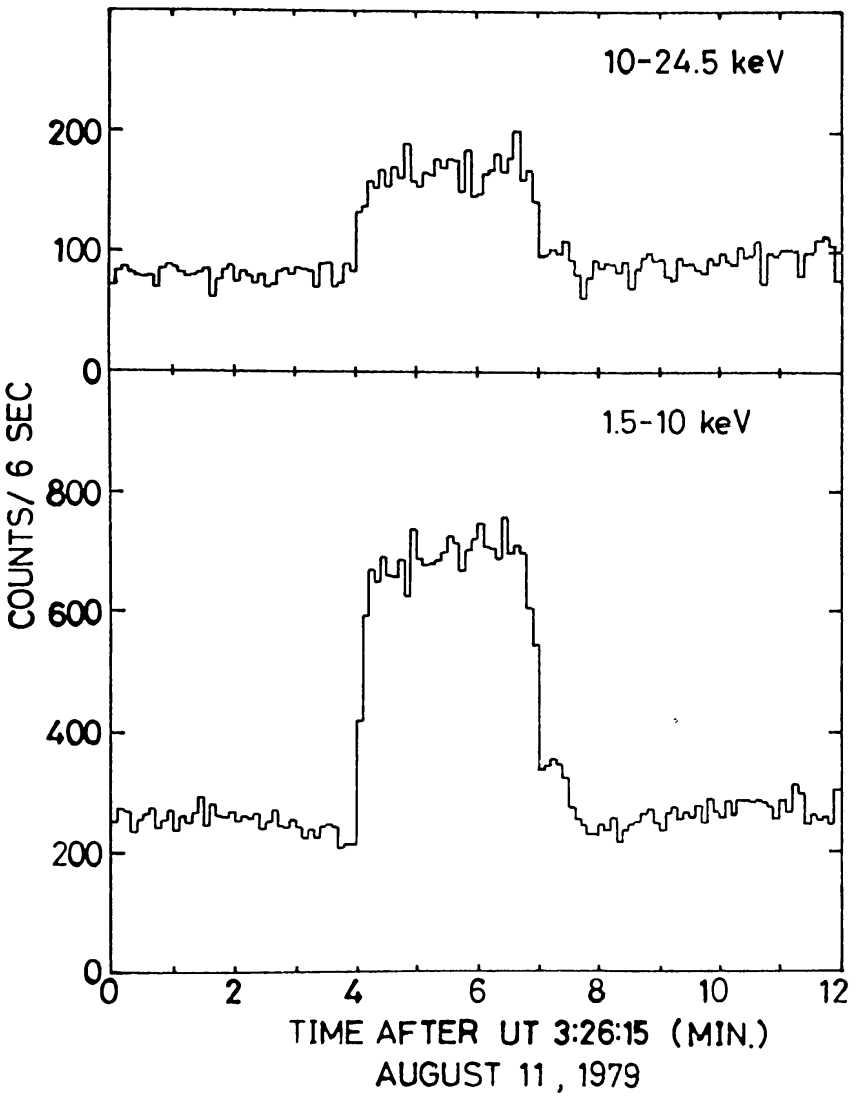

Fig. 33. The time profiles of a typical trapezoidal burst in two energy channels.

unappreciable, as was first noticed by Lewin *et al.* (1976a), but a slight decrease of temperature is suspected for gradual decays.

A striking phenomenon is the appearance of dips lasting about one minute each before and after a trapezoidal burst, as clearly seen in Figure 33 (Tawara, 1980). The depth of dips is about one-tenth of the peak luminosity. This seems similar to an increase of emission at the midst of triangular bursts with intervals longer than 1 min, as observed with SAS-3 (van Paradijs *et al.*, 1979), although the emission of 6×10^{36} erg s^{-1} they observed is too small to be detected with our instrument.

The dip is considered to indicate the turn-off of persistent emission from the Rapid Burster. In fact, the rate of persistent emission of $(1.3\text{–}2.2)\times10^{37}$ erg s^{-1} is observed with FMC during burst intervals in phase II. In phase I and prior to the burst activity, no persistent emission is detected, that is, the emission is weaker than 8×10^{36} erg s^{-1} which is our detection limit. In phase III the detection limit

is much worse, since the source was observed only with CMC. The persistent emission thus observed is just as strong as the dip mentioned above. The hardness ratio of persistent emission is not appreciably different from that of bursts.

It is interesting to note that the intensity of persistent emission is comparable to L_B. As L_B increases in phase II, the persistent emission also becomes strong. The Rapid Burster seems to have two channels of X-ray emission, the persistent and burst channels. There is a time interval of one minute between the switch off of one channel and the switch-on of another.

11.5. No evidence for simultaneous infrared and microwave bursts

A simultaneous observation was performed by Sato *et al.* (1980) at Mauna Kea Observatory in four infrared bands (I, H, K, and L) on 9, 11, and 12 August 1979. Although the observation windows of X-rays and infrared radiation rarely overlapped, no infrared burst as reported by Kulkarni *et al.* (1979) and by Jones *et al.* (1980) was detected. During the IR coverage only one X-ray burst of trapezoidal shape was observed, but no excess was detected in any band. The upper limit of IR luminosity is 10^{36} erg s^{-1}, which is weaker by two orders of magnitude than the peak luminosities of the infrared bursts during the absence of X-ray observation.

Microwave bursts from the Rapid Burster were reported by Calla *et al.* (1979, 1980). One of them on 20 August 1979 with a duration of 480 s occurred during our X-ray coverage. No enhancement of X-ray emission was detected during the microwave burst, whereas a triangular burst occurred 30 s after the microwave burst terminated.

11.6. Model

Since the linearity between E and t_i still holds in phase II, the relaxation oscillator model proposed by Lewin *et al.* (1976a) is essentially correct for the new burst mode as well. Namely, there is a reservoir which stores energy $E_{\max}$, and a part of the energy spills out to form a burst. The amount of energy spilling out is not always the same, though not entirely random, and the empty part of the reservoir is filled up by the supply at a constant rate to reach $E_{\max}$. The energy spilling out produces a burst at a radiator whose properties are almost independent of the total energy of a burst. The burst luminosity declines as the radiator size diminishes.

This model is elaborated by reference to our new findings.

(a) There are two channels of energy flow to bursts and persistent emission, which are switched from one to the other with a time lapse of about one minute. The flow rates in these channels are comparable to and correlated with one another.

(b) The mode of bursts depends on the rate of energy supply, which is $L_B + L_s$. An abrupt change of the energy supply rate from phase I to phase II gives rise to a large increase of E and an appreciable increase of L_p. As L_B decreases, both E and L_p decrease. The above behavior implies that the burst activity is controlled by the energy supply rate. There are a threshold of the energy supply rate to start the burst activity and another threshold for the mode change.

(c) There exists a maximum of E in phase II. For $E = E_{\max}$ L_p is scattered over a wide range. The value of L_p is determined at the onset of a burst and stays constant during the burst. A smaller value of L_p is associated with lower temperature and smaller emission area.

These are main features which should be incorporated with a model. We can readily rule out the nuclear flash model, since the value of $\alpha \simeq L_s/L_B$ is about unity, as already pointed out by Lewin *et al.* (1976a). Type I bursts which are considered to be due to nuclear flash are not observed during the active period in August 1979, though they were observed in an earlier active period (Hoffman *et al.*, 1978). Bursts standing high in Figure 27 are identified with those from 1728–337.

It is therefore natural to attribute the X-ray energy to the gravitational energy released by accreted matter. The luminosity of persistent emission and the area of emission region are comparable to those of X-ray sources which are considered to be accreting neutron stars. There is no compelling reason for excluding the black hole, particularly because the absence of regular pulsation does not favor the neutron star. However, the behavior of persistent emission is quite different from that of Cyg X-1, a most likely candidate of black hole. On the other hand, the magnetic field, which is considered to be accompanied with most neutron stars, may play a role in the generation of bursts probably through magnetic instabilities. The absence of regular pulsation can be understood if the magnetic axis is aligned with the rotation axis.

If we assume the neutron star nature of the Rapid Burster, the reservoir which stores infalling matter may be formed in some region of the magnetosphere, and the reservoir opens an outlet when it is filled up to a threshold level, so that a part of the matter falls on to the radiator on the star. The reservoir and the radiator are only weakly coupled, and the latter emits X-rays at a rate almost independent of the amount of matter released from the former. This general picture is now elaborated under the light of the new findings (a) through (c).

(A) Since two components, persistent emission and bursts, are switched from one to the other with a time lapse, it is likely that these two are once stored in one and the same reservoir. In most of time the reservoir is leaky for one component, but the leak is closed shortly before the reservoir is filled up so as to be prepared for a much greater rate of leak to produce a burst. When a significant fraction of matter stored leaks out, the reservoir is almost empty or left with the matter which can hardly leak. It takes some time for the reservoir to be mixed with leakable matter.

(B) In the burst inactive state the reservoir cannot store the matter enough to reach the threshold level. If the accretion rate increases, the amount of matter stored reaches the threshold level so as to trigger its outflow. If the accretion rate further increases, the capacity of the reservoir increases so as to store more matter. This increases the threshold for outflow and also to some extent the size of the radiator. These variations depend continuously on the accretion rate, as one sees in the transition from phase II to phase III. The abrupt transition from phase I to phase II is due to a steep rise of the accretion rate.

(C) Matter flowing out of the reservoir is poured into the radiator on the stellar surface. Since the surface area is variable, the radiator does not cover the whole stellar surface. The radiator may be an accretion column formed on the magnetic pole. The radiator may be connected with the reservoir through the stellar magnetic field. As the accretion rate increases, the reservoir is formed closer to the star, and the radiator size increases accordingly. The radiator area is controlled to be proportional to the infall rate which is chiefly dictated by the reservoir. If the leak rate is too high, the rate of infall to the radiator is controlled by radiation pressure, so that the value of L_p is kept nearly constant, as observed for trapezoidal bursts in phase II. When almost all amount of matter in the reservoir is thrown out, the rate of ejection varies, so that L_p varies by a factor of about three. For smaller L_p, the radiator becomes fatter, that is, the surface area becomes smaller for a fixed volume. This results in a lower surface temperature because of a larger optical depth, if the internal temperature is the same. The burst declines as the radiator collapses due to the loss of radiation pressure which supports the radiator. These properties may also be attainable for the accretion column.

The pulsations observed for two bursts may find their origin for the reservoir, since an oscillation without changing the temperature seems difficult to take place in the radiator. The period of half a second can result from a magnetic pulsation in the reservoir with size of 10^7 cm, magnetic field strength of 10^8 G and density of 10 g cm^{-3}.

12. X-ray Pulsars, Vela X-1 and A0535+262

Since most of the observation time has been spent for X-ray bursters, only two X-ray pulsars have been observed. Vela X-1 was observed in March 1979, March and December 1980, and January and March 1981, whereas A0535+262 was observed during its enhancement in October 1980.

Vela X-1 (4U 0900–403) is a binary X-ray pulsar with orbital period $P_{\rm orb} = 8.96$ days and pulse period $P = 283$ s. Its optical companion is a supergiant of B0.5 Ib type which is catalogued as HD 77581. Since the coverage was longer than that of any previous observation, more accurate data were obtained particularly for the pulse period variation.

12.1. Variations with orbital phase and pulse profile of Vela X-1

The intensity of Vela X-1 fluctuates by a factor of ten or so, but the intensity variation correlates primarily with the orbital phase. Variations not associated with the orbital phase are somewhat smaller, except for flaring which seems to occur rather frequently.

Figure 34 shows a light curve of Vela X-1 obtained in March 1980 (Nagase *et al.*, 1981b). The intensities in the energy ranges 1–9 keV and 9–22 keV, which are here called the soft and hard X-ray ranges, respectively, are separately plotted against modulo the binary period of 8.965 days. It is readily seen that the variation

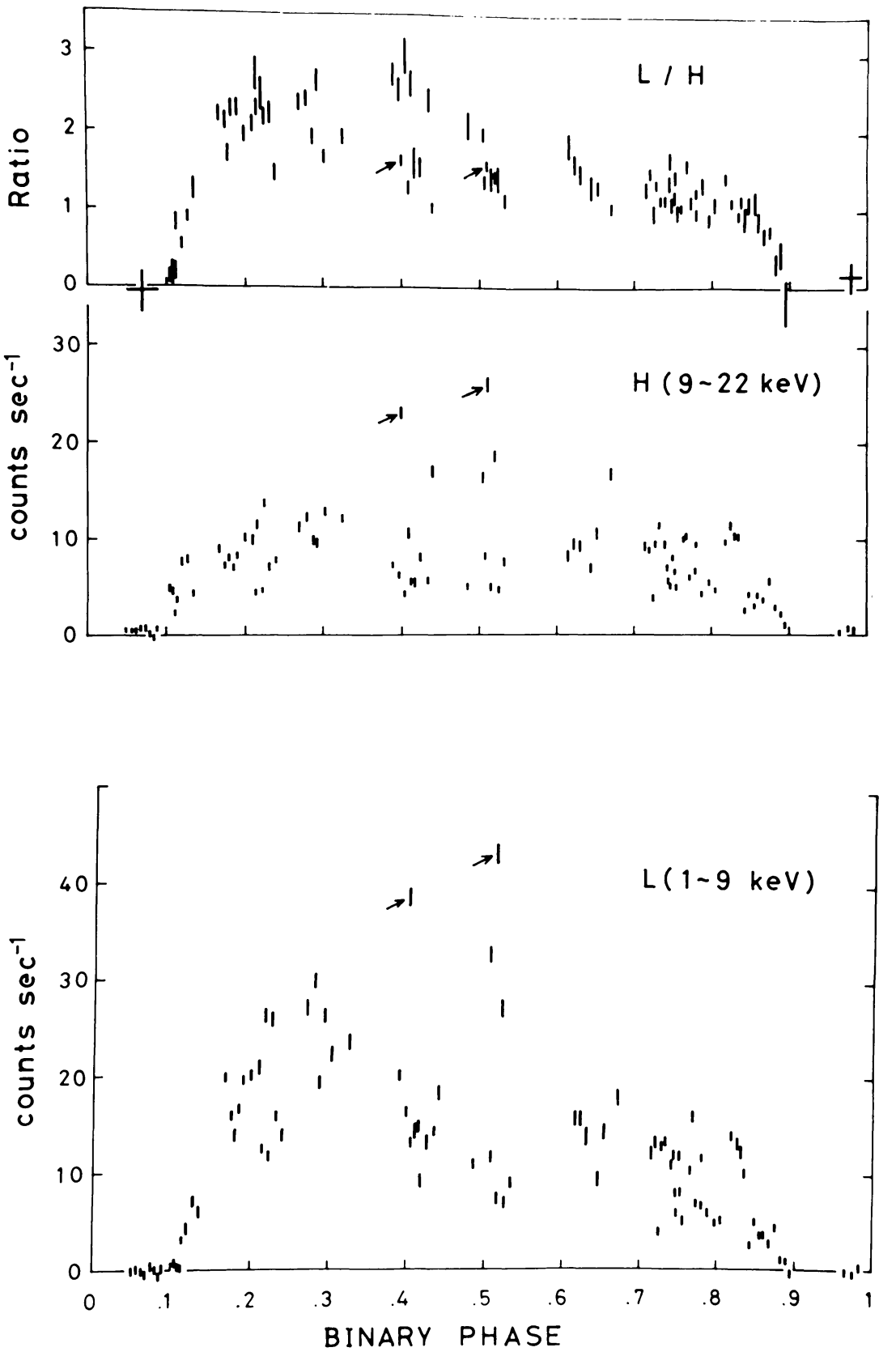

Fig. 34. The light curves of Vela X-1 against binary phase in two energy ranges, 1–9 keV (L) and 9–22 keV (H), and the variation of the softness ratio (L/H). Data during 5.2–24.0 March 1980 are folded modulo the binary period 8.965 days. The data points indicated by arrows show small flares.

of hard X-rays is rather small except for several high points. The variation of flux other than these high points is due mainly to soft X-rays as shown by the softness ratio, the ratio of intensity in the 1–9 keV range to that in the 9–22 keV; the light curve of the softness ratio is essentially parallel to that of soft X-rays.

This suggests that the absorption plays a main role in the variation. To prove this, the energy spectra in high, intermediate and low states are compared in Figure 35. The turn-over energy of the spectrum increases, as the intensity decreases, which is expected for the increase of absorption with decreasing energy. Expressing the differential energy spectrum as

$$f(E) = F_0 E^{-\alpha} \exp\left[-\sigma(E) N_{\mathrm{H}}\right], \tag{12.1}$$

where $\sigma(E)$ is the X-ray absorption cross section per hydrogen atom and N_{H} the hydrogen column density, we obtain the best-fit values of α and N_{H} for three states, as given in Figure 35. The change of spectral index α is insignificant, while the hydrogen column density N_{H} increases three times.

There are several points which show high intensities in both energy ranges, as indicated by arrows in Figure 34. These points are due to enhancements over a wide energy range without subject to the modulation by absorption, and even the hardening of spectrum is observed. A flare lasting longer than 30 min but shorter than 90 min, as observed on 25 July 1979 (Tsunemi *et al.*, 1980), is regarded as an enhancement similar to but three times larger than the enhancements shown in Figure 34. Flares observed previously by Uhuru (Forman *et al.*, 1973), by Copernicus (Charles *et al.*, 1978) and by Ariel-5 (Watson and Griffiths, 1977) were as high as the flare we observed in July 1979 but appreciably longer than ours.

The effect of absorption can also be seen from pulse profiles. Figure 36 shows pulse profiles in the high and low states. The structure of soft X-ray pulse is smeared out in the low state, while the profile of hard X-rays shows little difference between the high and low states. The profile of softness ratio also in Figure 36 gives the absorption effect more intuitively.

Comparing the profiles of soft and hard X-rays, we notice that the difference between them may also be attributable to the absorption effect. For hard X-rays there are two broad peaks at nearly symmetric phases, whereas for soft X-rays there are five narrow peaks, and two of the troughs correspond to the peak tops of hard X-rays. The profile of softness ratio shows these two troughs more clearly between structureless parts, suggesting that they are due to absorption. Such a feature of the pulse profile persists all over the binary period, although the modulation of soft X-rays in the low state is weak. We therefore conclude that this feature is intrinsic to the pulsar, independent of the binary phase.

The above analysis shows that there are two sources of circumstellar absorption. One is associated with the binary phase and is probably caused by the accretion flow towards the X-ray source. A pattern of accretion flow is suggested by Bessell *et al.* (1975), from the variation of optical features with binary phase. Varying spectral features are considered to be due to the irradiation of accretion flow by

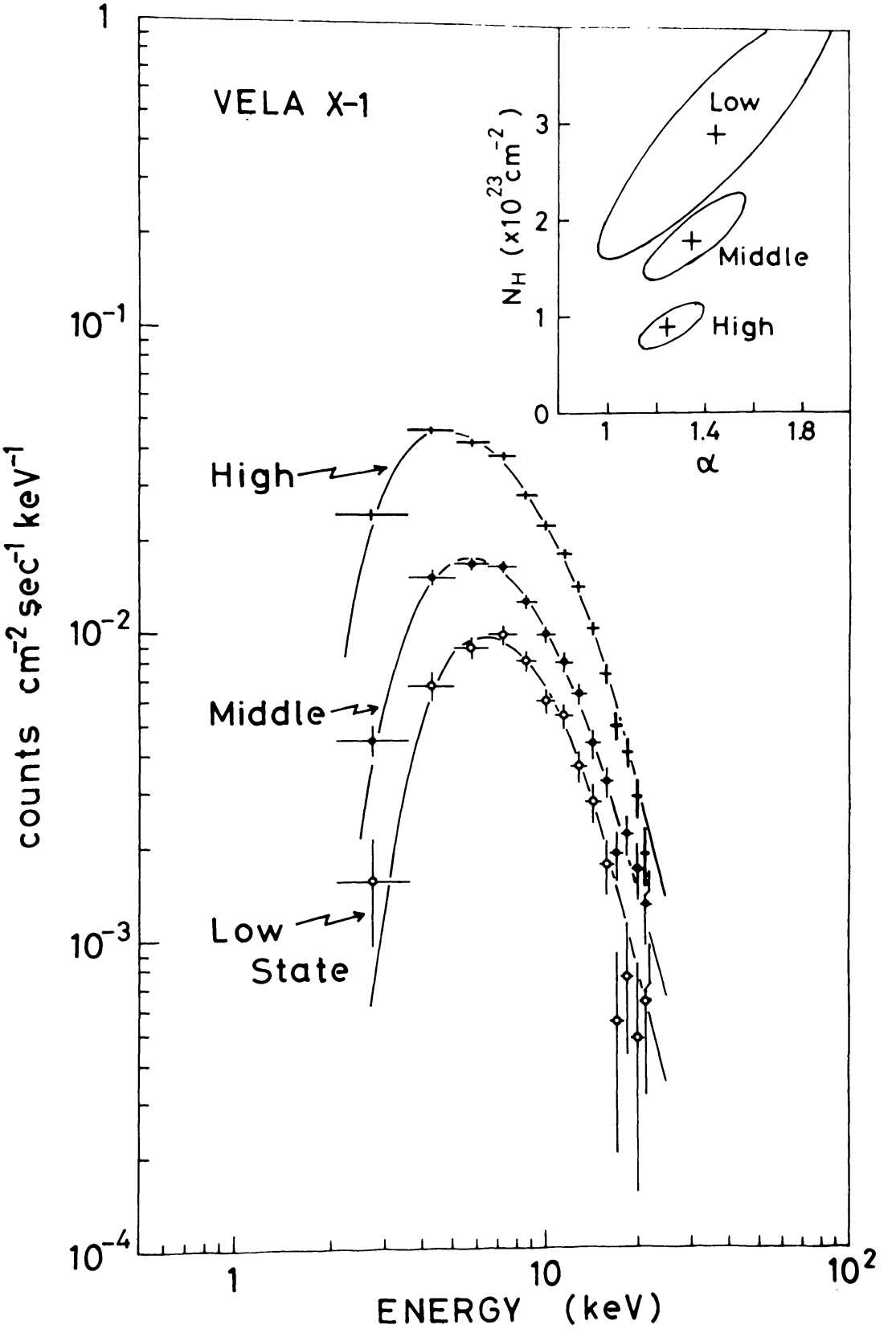

Fig. 35. The energy spectra of Vela X-1 in the high, intermediate and low states. The solid lines represent the spectra given by Equation (12.1) with the best fit values of α and N_H. The insert shows the 90% confidence contours in respective states.

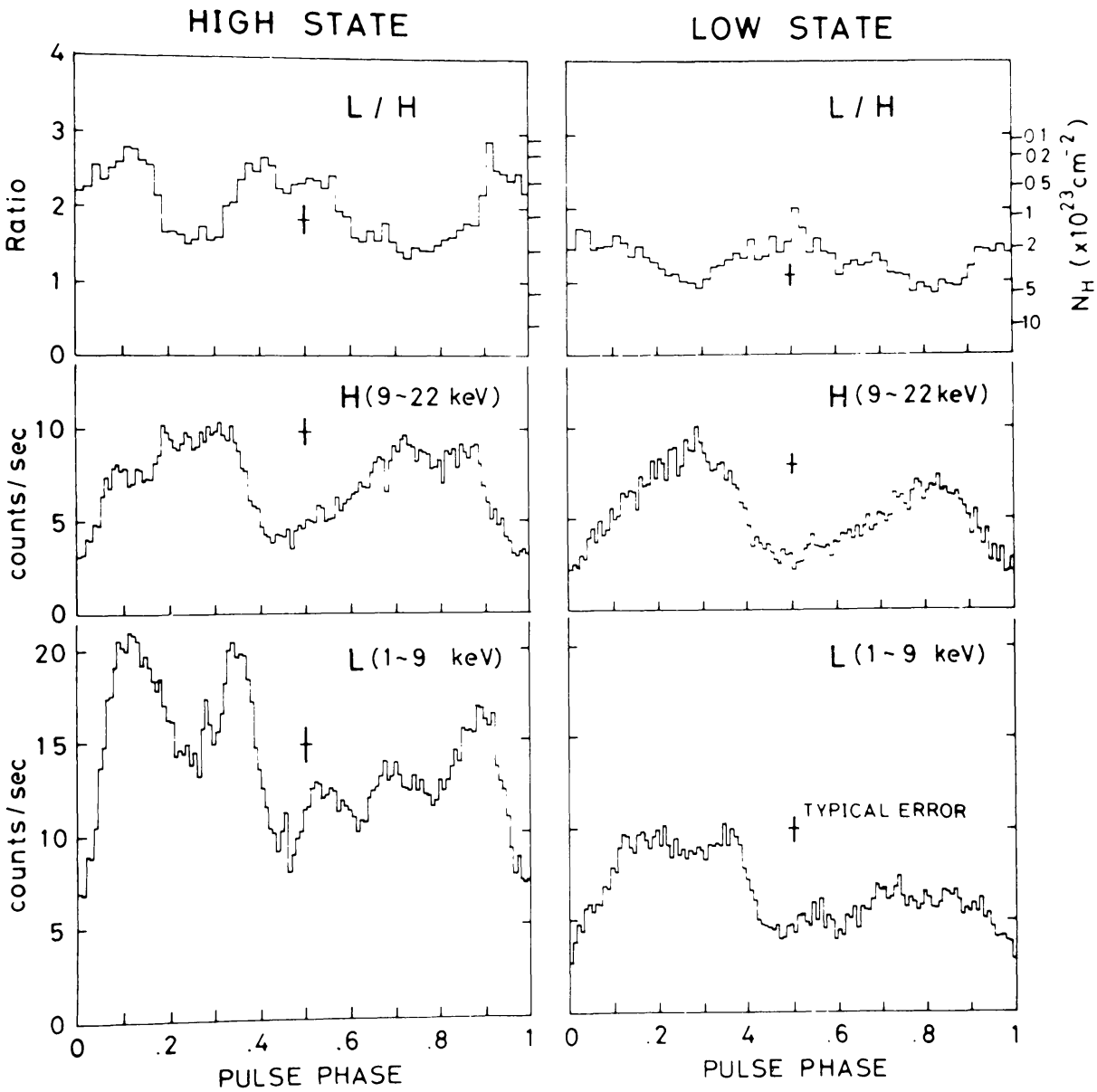

Fig. 36. The pulse profiles of Vela X-1 in two energy ranges averaged for the high and low states and the variations of the softness ratio which may represent the hydrogen column density N_H for absorption.

X-rays. The phase and magnitude of the absorption effect are found consistent with this flow pattern and the accretion rate required (Hayakawa and Nagase, 1981).

The other is attributed to absorbing matter attached to the X-ray source, so that the effect of absorption is in phase with the neutron star rotation which is considered to be the cause of pulsation. If X-rays are emitted from the accretion column formed on the magnetic pole, the height of X-ray emitting column is rather low for a small accretion rate; the absolute luminosity of about 7×10^{35} erg s^{-1} for the distance of 1.2 kpc is appreciably lower than the luminosities of most X-ray pulsars. Then X-rays are emitted over a wide cone with the beam axis nearly aligned with the magnetic axis. Near the axis the column density of infalling matter, estimated

from this luminosity, is high enough to absorb soft X-rays, but hard X-rays are not affected. Hence soft X-rays can come out only in the peripheral direction of the accretion column.

If the accretion rate is high, such as in the case of SMC X-1, the X-ray emitting column stands high above the stellar surface, and X-rays are mainly emitted from the side surface of the column, so that they are not subject to absorption. In fact, the pulse profile of SMC X-1 is simple, almost sinusoidal (Joss and Rappaport, 1980).

12.2. Pulsation period of Vela X-1

The pulsation period of Vela X-1 has been measured at 12 epochs as shown in Figure 37. This shows a general decrease at a rate of $\dot{P}/P \simeq -1.5 \times 10^{-4}\ \mathrm{yr}^{-1}$, except for an increase between late 1975 and early 1976.

Hakucho observed Vela X-1 during 8.1–12.8 March 1979 shortly after launch, although the observation was frequently interrupted by initial operations for testing various functions of the satellite. Hence the result was not accurate enough to

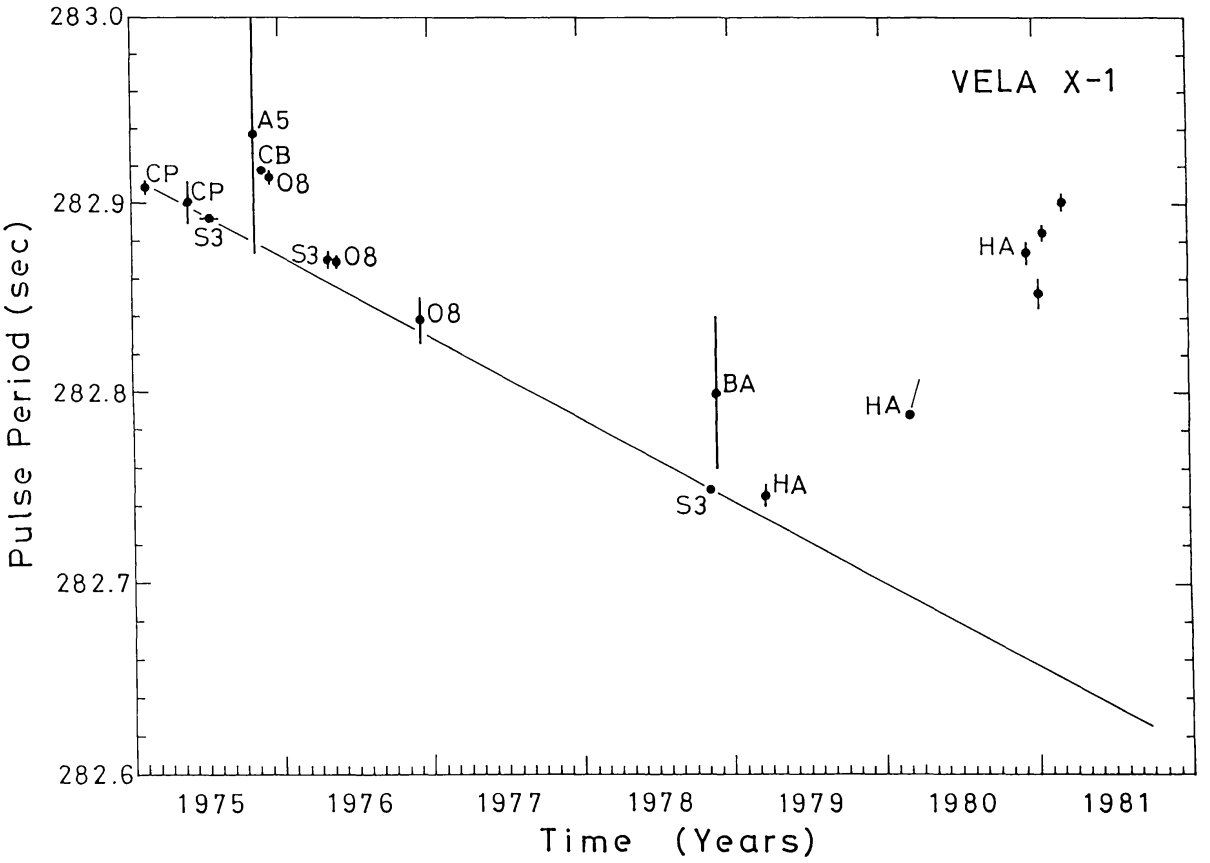

Fig. 37. The variation of pulse period of Vela X-1. The measurements were made with Copernicus (CP), SAS-3 (S3), Ariel-5 (A5), COS-B (CB), OSO-8 (O8), a balloon (BA), and *Hakucho* (HA); for references see Nagase *et al.* (1981a). The oblique bar to the second HA represents the rate of period change. The straight line shows a constant rate of period decrease with $\dot{P}/P = -1.5 \times 10^{-4}\ \mathrm{yr}^{-1}$.

derive some parameters related to apsidal motion, but the other parameters were consistent with those obtained by SAS-3 in November 1978 (Rappaport *et al.*, 1980).

The second observation was performed during 5.2–24.0 March 1980, covering a little more than two orbital periods for the first time. Thanks to a long coverage, we were able to obtain the rate of period change (Nagase *et al.*, 1981a).

Using 14 data points of X-ray eclipses, including one of us, we have derived orbital parameters (Nagase *et al.*, 1981b)

$$t_{e0} = 2\,441\,446.533 \pm 0.019 \text{ (JD)},$$
$$P_{orb} = 8.964\,11 + 0.000\,11 \text{ days},$$
$$\dot{P}_{orb} = (3.6 \pm 9.4) \times 10^{-8},$$

where t_{e0} is the epoch of the eclipse center, at the time of the first observation by *Uhuru* (Forman *et al.*, 1973). The orbital period is somewhat shorter than the previously adopted value, $P_{orb} = 8.9649 \pm 0.0002$ d (Rappaport *et al.*, 1980). For the present analysis of pulsation we fix $P_{orb} = 8.9641$ d.

The pulsation period is modulated by the Doppler shift associated with the orbital motion. The modulation is not purely sinusoidal so as to require a finite value of eccentricity e, the epoch of periastron passage τ, and the periastron longitude ω (Rappaport *et al.*, 1976). If we make a timing analysis taking these parameters into account, we find a systematic deviation as shown in Figure 38(a). The deviation vanishes if another parameter P is included, as shown in Figure 38(b). Thus we have, for the first time from a single observation, found the change of pulsation period

$$\dot{P}/P = (2.6 \pm 0.2) \times 10^{-3} \text{ yr}^{-1}.$$

This has an opposite sign compared with the general change and a much larger absolute value.

The best fit values of P, $\dot{P}$ and orbital parameters are given in Table VI for two of our observations. The orbital parameters are consistent with those obtained by SAS-3 in November 1978, also given for comparison in Table VI. The period in March 1979 agrees with that in November 1978, indicating an unappreciable change of period between them. However, the period in March 1980 is significantly longer than these two previous values, consistent with the positive value of $\dot{P}$.

In December 1980–March 1981 the values of period are, according to a preliminary result, found still higher, comparable to the value in early 1975, and show a zigzag change. These values of period are plotted in Figure 37.

An increase of period was observed in late 1976, but it is smaller and persists shorter. It may be questioned if the period generally decreases except for short, special intervals, since no data between late 1976 and late 1978 are available. The period may be changing erratically, as we can hardly draw a smooth line connecting our data points with gradients. Further observations are needed for answering this question.

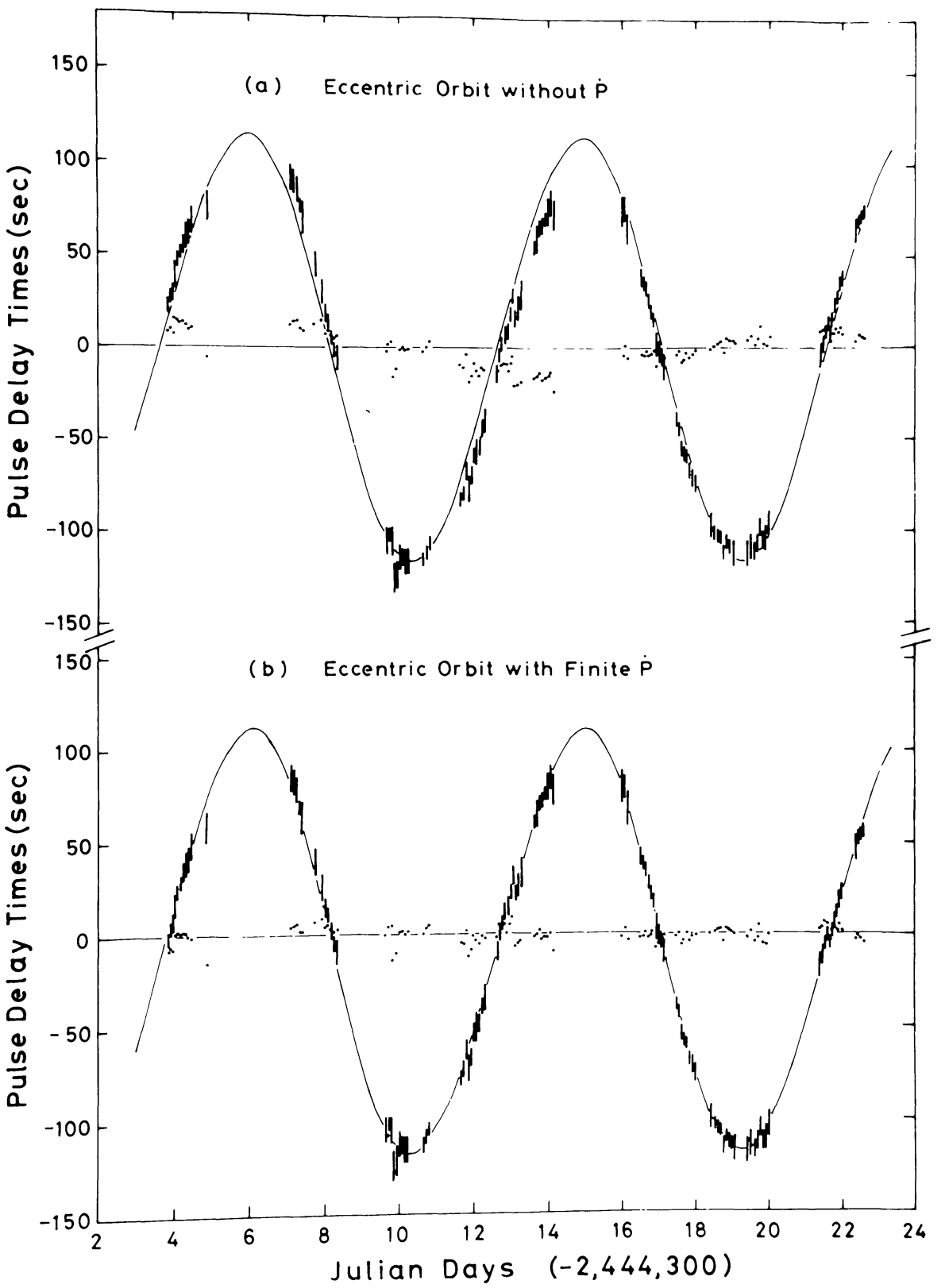

Fig. 38. The modulation of pulse period of Vela X-1 by the Doppler shift. The solid curves represent the calculated modulation curves (a) without $\dot{P}$ and (b) with $\dot{P}$. Dots near the horizontal lines are residuals after subtracting the calculated values.

TABLE VI

Best-fit orbital parameters for Vela X-1[a]

Parameters	SAS-3[b] Nov. 1978	Hakucho[c] March 1979	Hakucho March 1980
$a_x \sin i$ (1t–s)	112.3 ± 0.8	113.6 ± 2.6	113.8 ± 0.9
$f(M)$ ($M_\odot$)	19.0 ± 0.4	19.5 ± 1.5	19.9 ± 0.5
e	0.094 ± 0.005	–	0.089 ± 0.013
ω (degree)	158 ± 5	–	168 ± 5
P (s)	283.7468 ± 0.0004	282.746 ± 0.004	282.7875 ± 0.0010
$\dot{P}$ (s/s)	$(-9 \pm 18) \times 10^{-9}$ [d]	$(-21 \pm 8) \times 10^{-9}$	$(22.8 \pm 1.2) \times 10^{-9}$
τ(JD-2 440 000)	3823.53 ± 0.13	–	4307.89 ± 0.12
P_{orb} (days)	8.9643[e]	8.9641[e]	8.9641[e]

[a] All quoted uncertainties are single parameter 1σ confidence limits.
[b] After Table I of Rappaport *et al.* (1980).
[c] Best-fit circular orbit with $\dot{P}$.
[d] Corresponding to $\dot{P}/P = (-0.001 \pm 0.002)\ \mathrm{yr}^{-1}$.
[e] Orbital periods are fixed in the fitting.

The observation of pulsation period is of great astrophysical interest in the following respects. Since the orbital motion is eccentric, the periastron longitude is obtainable. This would change in time due to the interaction between the binary members, primarily due to the quadrupole moment of the primary star. Although the results available to date can hardly tell us such a variation, as seen in Table VI, further investigation will make us possible to obtain a periastron shift, if any.

The pulsation is believed to be due to the rotation of a neutron star. The spin-up observed for most X-ray pulsars is considered to be caused by the angular momentum transfer from the matter forming an accretion disk. Hence the spin-up rate is correlated with the accretion rate and accordingly with the luminosity approximately as $\dot{P}/P \propto -L^{6/7}$ (Rappaport and Joss, 1977). This predicts that the period variation is correlated with the luminosity variation. However, the luminosity of $7 \times 10^{35}\ \mathrm{erg\ s^{-1}}$ in the non-flaring high state is not appreciably different from that observed earlier. The spin-down may result if the corotation radius is smaller than the Alfvén radius, so that the accretion disk decelerates the stellar rotation (Gohsh and Lamb, 1979). However, the corotation radius of Vela X-1 is 7.5×10^9 cm, that is, Vela X-1 rotates too slowly, so that the spin deceleration mechanism as above is untenable. It should be noted that the spin-up rate of Vela X-1 generally claimed cannot be explained by the disk-fed model (Gohsh and Lamb, 1979).

Another possibility is the ejection of matter to take out the angular momentum of the star. The difference of period $\Delta P = 0.08$ s between March 1979 and March 1980 can be related to the ejected mass ΔM as $\Delta PI = \Delta M P r_{co}^2$, where $I \simeq 10^{45}\ \mathrm{g\ cm^2}$ is the moment of inertia of the star and $r_{co} = 7.5 \times 10^9$ cm is the corotation radius, at which the angular momentum is released. This requires $\Delta M \simeq 5 \times 10^{21}$ g and the corresponding energy $\Delta E = GM\Delta M/R \simeq 9 \times 10^{41}$ erg for $M = 1.4\,M_\odot$ and $R = 10^6$ cm. This amount of energy is compared with the flare energy of 10^{40} erg

observed in July 1979. A larger flare of 3×10^{41} erg was observed in August 1975 (Watson and Griffiths, 1977), and a period change of $\Delta P\simeq 0.02$ s occurred shortly thereafter. In this case the energy lost by mass ejection is comparable to the flare energy. During the spin-down episode in march 1980, however, the spin-down rate is far greater than that can be accounted in the above term, since only two small flares were observed. Hence the mass ejection theory is unlikely to hold.

We are therefore left with the possibility of internal origin. The rotation of a neutron star is disturbed by various modes of internal motion and can be modulated at a wide band of frequency (Lamb *et al.*, 1978). If the coupling between the solid crust and the fluid neutron core increases, the rotation of the crust is dragged by the core of large angular momentum. The angular velocity decreases until a new stationary state is reached, as was originally suggested for the spin-up of radio pulsars (Baym *et al.*, 1969). If the coupling is reduced, the crust spin is accelerated by an external torque. Although the stationary state thus reached gives the same spin rate as before, the time axis for the spin-up slope is shifted by the period, during which the coupling is strong. Our observation indicates that the rate of period change ranges from 10^{-9} to 10^{-6} s/s. Future observation will give the spectrum of period change which will enable us to see the internal structure of the neutron star.

12.3.. A0535+262

A transient X-ray source A0535+262 forms a binary with HDE 245770, a Be star, at a distance of 1.3–1.8 kpc (Stier and Liller, 1976). Since its discovery in April 1975 by Ariel V, X-ray enhancement seems to recur with a suspected period of about 110 days. *Hakucho* had been unable to detect this source until its flare-up was observed with a pair of counters SFX-V on 2 October 1980. Then the spin axis was directed to A0535+262 on 9 October, and the light curve was observed with FMC-1 for 25.6 days as shown in Figure 39.

At the time of discovery, a periodic pulsation of 104 s was found (Rosenberg *et al.*, 1975). The period seems to decrease as observed for other X-ray pulsars, but the rate of decrease is not constant (Li *et al.*, 1979). Although the pulse period is modulated probably by orbital motion, the orbital period has not yet been obtained, since the enhancement is shorter than the suspected orbital period.

According to the observation with FMC-2 in October 1980, the pulsation period was 103.67 s at the beginning of observation, gradually decreased to 103.61 s on the 14th day and fitted with a polynomial including up to $\ddot{P}$ as shown in Figure 40, where

$$P_0 = 103.67405\pm0.00016\ \text{s at JD } 2\,444\,521.465\,217\pm0.000\,004\,,$$
$$\dot{P} = (-8.428\pm0.023)\times10^{-8}\ \text{s/s},\quad \ddot{P} = (6.36\pm0.10)\times10^{-14}\ \text{s/s}^2\,,$$
$$\dddot{P} = (-1.51\pm0.12)\times10^{-20}\ \text{s/s}^3\,.$$

A set of orbital parameters to fit the time variation of period is sought, but no unique solution is obtainable. The orbital period shorter than 40 days can be

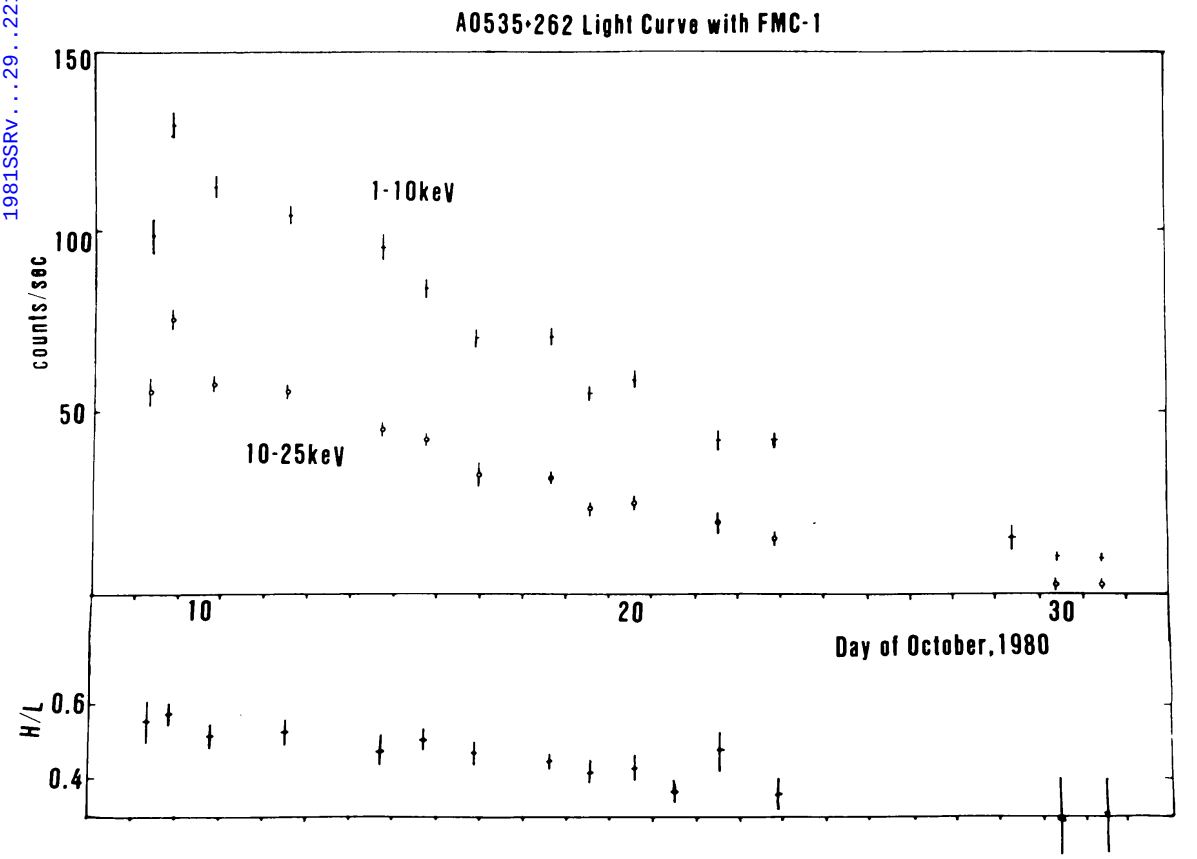

Fig. 39. Light curves of A0535+262 in two energy ranges in October 1980.

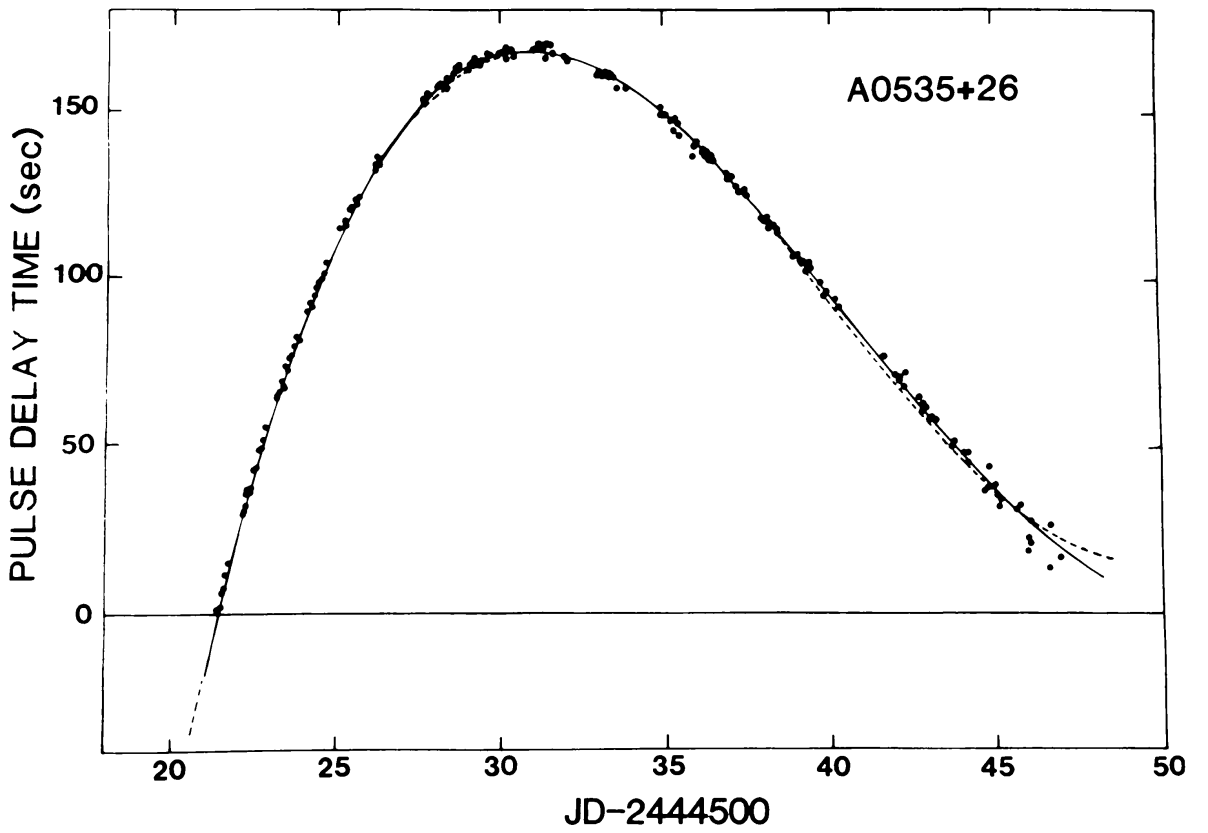

Fig. 40. The modulation of pulse period of A0535+262.

rejected at the 90% confidence level, and that longer than 120 days can be also rejected if the mass function

$$f(M) = \frac{M_*}{(1+q)^2} \sin^3 i < 20\, M_\odot ,$$

where $q = M_x/M_*$, M_* and M_x are the masses of the companion star, 5–20 $M_\odot$, and of the X-ray source, respectively, and i the inclination angle $>50°$. For a long period, say 110 days, a large eccentricity, $e \sim 0.4$, is required.

Hutchings *et al.* (1978) tried to obtain orbit solutions on the basis of spectral lines of HDE 245770. Three possible solutions with orbital periods of 28d, 48d, and 94d and with large eccentricities are not consistent with the X-ray pulse period change.

13. Summary

A small satellite such as *Hakucho* is proved to be useful for monitoring the X-ray sky, thanks to X-ray detectors of wide fields of view but capable to pin point source positions. Utilizing the spin with a period of about 10 s, X-ray detectors with view axes perpendicular to the spin axis monitor X-ray sources in a wide sky belt owing to their criss-crossed fields of view, while detectors with view axes parallel to the spin axis watch a specific source or sources in a selected sky region; modulation collimators incorporated with the latter are capable to pin point individual sources in a field of view even if they emit bursts as short as several seconds.

Two examples obtained with the vertical view axis detectors are:

(1) Cyg X-1 turned into high states in June and November 1979; in the former optical and UV observations were simultaneously performed, whereas in the latter the high state lasted only about a day.

(2) Vela X-1 flared up for about an hour in July 1979 and in October 1980 to the level of about four times the normal state level.

The parallel view detectors of wide fields of view (CMC and VSX-P) watch several transient and steady sources simultaneously owing to the sky chopping by spin. The main results thus far obtained are:

(3) Cir X-1 emitted an intense flare with a soft spectrum, but no detectable X-rays were observed at the next epoch suspected from the 16.6 days binary period.

(4) GX 349+2 = 1702–363 showed a bimodal behavior, quiescent and disturbed states. In the disturbed state the intensity is correlated with the hardness ratio. During an intense flare was observed a pulsation with 153 s period.

(5) GX 339-4 and NGC 6624 emit significant intensities of soft X-rays with energies down to 0.6 keV.

The parallel view axis detectors equipped with modulation collimators were very powerful for burst study. The following results may be worth while to mention.

(6) The activity of most burst sources is highly variable. There are two, 1728–337 and 1636–536, which are exceptionally stable, that is, they always emit bursts.

(7) Eight burst sources were newly discovered. Among them 1608–522 and 1702–429 had been suspected, because enhancements looking like bursts had been observed in rare occasions. Bursts from Cen X-4 and Aql X-1 were associated with their nova-like activities. Other four, 1715–321, Terzan-1, Terzan-5 and GX 3+1 are located with 5° from the galactic center. Two of them coincide with globular clusters studied by Terzan (1968).

(8) *Hakucho* missed bursts from six established bursters, 1658–298, Terzan 2, NGC 6441, NGC 6624, Ser X-1, and NGC 6712.

(9) The number of bursters within 5° from the galactic center is now doubled by the discovery, thus establishing a high concentration of bursters towards the galactic center. Nearly a half of X-ray sources in the close vicinity of the galactic center emit bursts.

(10) Cen X-4 and Aql X-1 bursted during the declining phase of nova activity. Their bursts are quite similar to bursts from other sources, despite that they are located far from the galactic center. Since they are binaries, the binary nature of bursters is observationally supported.

(11) Burst profiles are of great variety. The profile does not correlate with other parameters such as the flux of persistent emission, although 1608–522 showed a correlation only in 1979 such that bursts were sharp and of constant duration when the persistent emission was appreciable, while they were dull and of constant peak luminosity when the persistent emission was undetectable. In spite of a variety of profiles, the area of emission region stays constant.

(12) The ratio of energy for persistent emission to that for bursts fluctuates over a wide range, so that it is often smaller than the ratio of gravitational energy to nuclear energy.

(13) Double peaks were sometimes observed for bursts of high peak luminosities from 1608–522, 1636–536, 1728–337, Terzan-5 and 1906+000. An oscillation of 0.65 s period was observed for a double-peak burst from 1608–522. Adding four sources with double peak bursts, the total of nine bursters have emitted double peak bursts. Hence the double peak burst may be common to bursters.

(14) The time interval between two similar bursts is sometimes very short, for example, 10 min from 1608–522 and 8 min from Terzan-5. These bursts are neither associated with a change of persistent flux, nor with any variation of burst activity.

(15) Properties (11) through (14) are difficult to understand by the current model of nuclear flash. Further sophistication of the model or a different idea may be needed.

(16) The burst peak luminosity often exceeds the Eddington limit currently adopted, as proved for bursts from five sources in the galactic center region. Such a high luminosity can be accounted for only in terms of the reduction of opacity by a factor of two or more compared with the Thomson opacity.

(17) Ten simultaneous X-ray/optical bursts were observed from 1636–536. They show an essentially constant delay of optical burst with respect to X-ray burst, and there profiles are approximately related without appreciable smearing as $L_{\rm op} \propto L_x^{0.3}$

after correcting for the delay. The optical burst is probably emitted from an accretion disk whose periphery blows up by X-ray irradiation.

(18) The Rapid Burster was active in August 1979 but inactive half a year and one year later.

(19) The activity observed is different from that observed earlier. Shortly after the onset of the activity, all bursts were of trapezoidal profile with a flat top of duration ranging from 30 s to 700 s. The flat top luminosity for the bursts shorter than 150 s was nearly the same and significantly higher than the peak luminosities of ordinary triangular bursts and of longer trapezoidal bursts. The energy spectrum of the trapezoidal bursts is of blackbody type and becomes softer as the duration increases beyond 150 s.

(20) The finite flux of persistent emission was observed when bursts were exclusively trapezoidal, but it was stopped for about a minute before and after a burst.

(21) The burst activity seems to be controlled by the average burst luminosity, the burst energy divided by internal, which correlates with the persistent flux.

(22) No infrared burst was detected during a burst, and no X-ray burst was observed during a microwave burst.

A parallel view axis detector with a small field of view was suitable for observing X-ray pulsars over a considerable time length.

(23) Vela X-1 was observed for several separated periods. The pulsation period increased from March 1979 to January 1981, in contrast to the period decrease from 1976 to 1978.

(24) A positive derivative of pulsation period was obtained from the observation lasting for two orbital periods. Transitions between spin-up and spin-down states took place over a time length of about a week.

(25) The difference between pulse profiles in the high and low energy ranges and that between the light curves over a orbital period are due to the absorption probably of circumstellar origin.

A combination of detectors with two different directions worked nicely. A0535+262 was found to be active with the virtical view axis detectors, and then the source was continuously observed with the parallel view axis detectors.

(26) A recurrent transient source A0535+262 became active in October 1980. Its light curve and pulsation were observed for three weeks.

The results thus far obtained may be a small fraction of the whole results expected, since a considerable part of data already obtained are left unanalyzed and *Hakucho* will be active still more years. So far questions raised have been more than questions answered. Will this unbalance be upset by future results?

References

Basinska, E. M., Lewin, W. H. G., Cominsky, L., van Paradijs, J., and Marshall, F. J.: 1980, *Astrophys. J.* **241**, 787.

Baym, G., Pethick, C., Pines, D., and Ruderman, M.: 1969, *Nature* **224**, 872.

Bessell, M. S., Vidal, N, V., and Wickramasinghe, D. T.: 1975, *Astrophys. J. Letters* **195**, L117.

Calla, O. P. N., Bhandari, S. M., Deshpande, M. R., and Vats Hari, O. M.: 1979, IAU Circ. No. 3347.
Calla, O. P. N., Banathy, S., Snagal, A. K., Bhandari, S. M., Despande, M. R., and Vyas, H. O.: 1980, IAU Circ. Nos. 3458 and 3467.
Canizares, C. R. and Neighbours, J. E.: 1975, *Astrophys. J. Letters* **199**, L97.
Charles, P. A., Mason, K. O., White, N. E., Culhane, J. L., Sanford, P. W., and Moffat, A. F. J.: 1978, *Monthly Notices Roy. Astron. Soc.* **183**, 813.
Clark, G. W., Jernigan, J. G., Bradt, H., Canizares, C., Lewin, W. H. G., Li, F. K., Mayer, W., and McClintock, J.: 1976, *Astrophys. J. Letters* **207**, L105.
Dougherty, J. P. and Farley, D. T.: 1960, *Proc. Roy. Soc.* (*London*) **A259**, 79.
Fejer, J. A.: 1960, *Can. J. Phys.* **38**, 1114.
Forman, W., Jones, C., Tananbaum, H., Gursky, H., Kellogg, E., and Giacconi, R.: 1973, *Astrophys. J. Letters* **182**, L103.
Fujimoto, M. Y., Hanawa, T., and Miyaji, S.: 1981, *Astrophys. J.*, in press.
Gohsh, P. and Lamb, F. K.: 1979, *Astrophys. J.* **234**, 296.
Graham, J. A.: 1979, in W. B. Burton (ed.), 'The Large-Scale Characteristics of the Galaxy', *IAU Symp.* **84**, 195
Grindlay, J. E.: 1979, *Astrophys. J. Letters* **232**, L33.
Grindlay, J. E. and Gursky, H.: 1977, *Astrophys. J. Letters* **218**, L117.
Grindlay, J., Gurksy, H., Schnopper, H., Parsignoult, D. R., Heise, J., Brinkman, A. C., and Schrijver, J.: 1976, *Astrophys. J. Letters* **205**, L127.
Grindlay, J. E., McClintock, J. E., Canizares, C. R., van Paradijs, J., Cominsky, L., Li, F. K., and Lewin, W. H. G.: 1978, *Nature* **274**, 567.
Grindlay, J. E., Marshall, H. L., Hertz, P., Soltan, A., Weisskopf, M. C., Elsner, R. F., Gohsh, P., Darbro, W., and Sutherland, P. G.: 1980, *Astrophys. J. Letters* **240**, L121.
Hayakawa, S.: 1981, *Publ. Astron. Soc. Japan* **33**, 365.
Hayakawa, S. and Nagase, F.: 1981, *The 17th International Conference on Cosmic Rays.*
Hoffman, J. A., Lewin, W. H. G., and Doty, J.: 1977, *Monthly Notices Roy. Astron. Soc.* **179**, 57.
Hoffman, J. A., Cominsky, L., and Lewin, W. H. G.: 1980, *Astrophys. J. Letters* **240**, L27.
Hoffman, J. A., Marshall, H. L., and Lewin, W. H. G.: 1978, *Nature* **271**, 630.
Holt, S. S., Kaluzinski, L. J., Boldt, E. A., and Serlemitsos, P. J.: 1976, *Nature* **261**, 213.
Holt, S. S., Kaluzinski, L. J., Boldt, E. A., and Serlemitsos, P. J.: 1979, *Astrophys. J.* **233**, 344.
Hutchings, J. B., Bernard, J. E., Crampton, D., and Cowley, A. P.: 1978, *Astrophys. J.* **223**, 530.
Ilovaisky, S.A.: 1981, IAU Circular No. 3586.
Inoue, H. and Hakucho Team: 1979, *Proc. 16th International Cosmic Ray Conference* **1**, 5, 52, 55, 57; **12**, 7.
Inoue, H. and Hakucho Team: 1980, *Nature* **283**, 358.
Inoue, H. and Hakucho Team: 1981, *Astrophys. J. Letters*, in press.
Jones, A. W., Selby, M. J., Mountain, C. M., Wade, R., Sanchez, C. M., and Munoz, M. P.: 1980, *Nature* **283**, 550.
Joss, P. C.: 1977, *Nature* **270**, 310.
Joss, P. C.: 1978, *Astrophys. J. Letters* **225**, L123.
Joss, P. C. and Li, F. K.: 1980, *Astrophys. J.* **238**, 287.
Joss, P. C. and Rappaport, S.: 1980, *Proc. Symp. on Space Astrophysics*, Tokyo, p. 7.
Kamiya, A.: 1981, Master Thesis, Nagoya University.
Kemp, J. C., Barbour, M. S., and McBirney, R. E.: 1981, preprint.
Kleinmann, D. E., Kleinmann, S. G., and Wright, E. L.: 1976, *Astrophys. J. Letters* **210**, L83.
Kondo, I. and Hakucho Team: 1981, *Space Sci. Instr.* **5**, 211.
Koyama, K. and Hakucho Team: 1981, *Astrophys. J. Letters*, in press.
Kulkarni, P. V., Ashok, N. M., Apparao, K. M. V., and Chitre, S. M.: 1971, *Nature* **280**, 819.
Kunieda, H., Tawara, Y., and Hakucho Team: 1981, to be published.
Lamb, F. K., Pines, D., and Shaham, J.: 1978, *Astrophys. J.* **224**, 969; **225**, 582.
Lewin, W. H. G. and Clark, G. W.: 1979, *ISAS Symposium on X-ray Astronomy*, Tokyo, p. 3.
Lewin, W. H. G. and Joss, P. C.: 1981, *Space Sci. Rev.* **28**, 3.
Lewin, W. H. G., Doty, J., Clark, G. W., Rappaport, S. A., Bradt, H. V. D., Doxey, R., Hearn, D. R., Hoffman, J. A., Jernigan, J. G., Li, F. K., Mayer, W., McClintock, J., Primini, F., and Richardson, J.: 1976a, *Astrophys. J. Letters* **207**, L95.

Lewin, W. H. G., Hoffman, J. A., Doty, J., Hearn, D. R., Clark, G. W., Jernigan, J. G., Li, F. K., McClintock, J. E., and Richardson, J.: 1976b, *Monthly Notices Roy. Astron. Soc.* **177**, 83.
Lewin, W. H. G., van Paradijs, J., Cominsky, L., and Holgner, S.: 1980, *Monthly Notices Roy. Astron. Soc.* **193**, 15.
Li, F. K., Rappaport, S., Clark, G. W., and Jernigan, J. G.: 1979, *Astrophys. J.* **228**, 893.
Liller, W.: 1977, *Astrophys. J. Letters* **213**, L21.
Makishima, K. and Hakucho Team: 1981a, *Astrophys. J. Letters* **244**, L79.
Makishima, K. and Hakucho Team: 1981b, *Astrophys. J. Letters*, in press.
Markert, T. H., Canizares, C. R., Clark, G. W., Lewin, W. H. G., Schnopper, H. W., and Sprott, G. F.: 1973, *Astrophys. J. Letters* **184**, L67.
Matsuoka, M.: 1980, *Proc. Symp. on Space Astrophysics*, Tokyo, p. 88.
Matsuoka, M. and Hakucho Team: 1980, *Astrophys. J. Letters* **240**, L137.
McClintock, J. E., Grindlay, J. E., Canizares, C. R., Van Paradijs, J., Cominsky, L., Li, F. K., and Lewin, W. H. G.: 1979, *Nature* **279**, 47.
Mitsuda, K.: 1981, Master Thesis, University of Tokyo.
Murakami, T. and Hakucho Team: 1980a, *Astrophys. J. Letters* **240**, L143.
Murakami, T. and Hakucho Team: 1980b, *Publ. Astron. Soc. Japan* **32**, 543.
Nagase, F. and Hakucho Team: 1981a, *Nature* **290**, 572.
Nagase, F. and Hakucho Team: 1981b, to be published.
Oda, M.: 1977, *Space Sci. Rev.* **20**, 757.
Oda, M.: 1979, *Proc. Symp. on the Results and Future Prospects of X-Ray Astronomy*, Tokyo, p. 89.
Oda, M.: 1981, in R. Giacconi (ed.), *X-Ray Astronomy with Einstein Satellite*, D. Reidel Publ. Co., Dordrecht, Holland, p. 61.
Ogawara, Y.: 1980, *Proc. Symposium on Space Astrophysics*, Tokyo, p. 53.
Ohashi, T.: 1981, Ph.D. Thesis, University of Tokyo.
Ohashi, T. and Hakucho Team: 1981, *Astrophys. J.*, in press.
Rappaport, S. and Joss, P. C.: 1977, *Nature* **266**, 683.
Rappaport, S., Joss, P. C., and McClintock, J. E.: 1976, *Astrophys. J. Letters* **206**, L103.
Rappaport, S., Joss, P. C., and Stothers, R.: 1980, *Astrophys. J.* **235**, 570.
Rosenberg, F. D., Eyles, C. J., Skinner, G. K., and Willmore, A. P.: 1975, *Nature* **256**, 628.
Rosenbluth, M. N. and Rostoker, N.: 1962, *Phys. Fluids* **5**, 776.
Salpeter, E. E.: 1960, *Phys. Rev.* **120**, 1528.
Samimni, J., Share, G., Wood, K., Yentis, D., Meekins, J., Evans, W. D., Shulman, E. T., Chubb, T. A., and Friedman, H.: 1979, *Nature* **274**, 434.
Sato, S., Kawara, K., Kobayashi, Y., Maihara, T., Okuda, H., and Jugaku, J.: 1980, *Nature* **286**, 688.
Stier, M. and Liller, W.: 1976, *Astrophys. J.* **206**, 257.
Tanaka, Y.: 1979, *Proc. Symp. on the Results and Future Prospects of X-Ray Astronomy*, Tokyo, p. 61.
Tawara, Y.: 1980, Ph.D. Thesis, University of Tokyo.
Tawara, Y. and Hakucho Team: 1981, to be published.
Terzan, A. C. R.: 1968, *Acad. Sci. Paris* **267**, B-1245.
Tsunemi, H. and Hakucho Team: 1981, *Publ. Astron. Soc. Japan* **33**, 205.
van Paradijs, J.: 1978, *Nature* **274**, 650.
van Paradijs, J., Cominsky, L., and Lewin, W. H. G.: 1979, *Monthly Notices Roy. Astron. Soc.* **189**, 387.
Watson, M. G. and Griffiths, R. E.: 1977, *Monthly Notices Roy. Astron. Soc.* **173**, 513.